



Università
Ca'Foscari
Venezia

Master's Degree
in
Conservation Science and Technology
for cultural heritage

Final Thesis

**Development of functionalize
inorganic nanoparticles products for
the consolidation of sandstones and
concretes.**

Supervisor

Prof. Alvise Benedetti

Assistant supervisor

Dr. Elena Tesser

Graduand

Neva Maria Elisabetta Stucchi

Matricolation number

862411

Academic Year

2020 / 2021

A Venezia

*“Il pizzo verticale delle facciate veneziane
è il più bel disegno che il tempo -alias- acqua abbia lasciato sulla terraferma (...).
è come se lo spazio, consapevole - qui più che in qualsiasi altro luogo - della propria inferiorità rispetto al tempo,
gli rispondesse con l'unica proprietà che il tempo non possiede: la bellezza.”*

I. Brodskij “Fondamenta degli Incurabili”

Index

1 Aim	1
2 Introduction	3
2.1 Siliceous Consolidants	3
2.2 The beginning of the research	6
2.3 Functionalization, a promising step for the improvement of SNP	8
2.3.1 Functionalization with Calcium	9
2.3.2 Functionalization with siloxane	10
2.4 Concrete a new material to preserve and Co. Ri. La project	12
2.5 The new research	14
3 Experimental part	16
3.1 Consolidants	16
3.1.1 SNP100	16
3.1.2 Functionalization with $\text{Ca}(\text{NO}_3)_2$	16
3.1.3 Functionalization with Polymer	17
3.1.4 Evercrete Vetrofluid	19
3.2 Substrates	20
3.2.1 Lithotypes specimens	20
3.2.2 Concrete specimens	21
3.3 Methods	22
3.3.1 Characterisation of the particles and of consolidants	22
3.3.2 Test of application	26
3.3.3 Characterization of treated specimens	27
3.3.4 Decaying processes	28
3.3.5 Application of the consolidants	29
4 Results	30
4.1 Results of the analysis of the particles and of the consolidant	30
4.1.1 Chemical characterization of functionalized SNP	30
4.1.2 Analysis of degree of dispersion	33
4.1.3 FTIR analysis	34
4.1.4 Analysis of the structure of S2e by NMR	41
4.2 Results of preliminary tests of application	43
4.2.1 Application of SNP functionalised with $\text{Ca}(\text{NO}_3)_2$	43

4.2.2 Application of SNP functionalised with polymeric compound	45
4.3 Characterisation of the substrates	53
4.3.1 Characteristic of the texture and surface of the samples	53
4.3.2 Variation of the morphological aspect of specimens induced by the degradation	53
4.4 Evaluation of the consolidation treatments	63
4.4.1 SNP100	64
4.4.2 SNP-PDMS	66
4.4.3 Evercrete Vetrofluid	79
4.5 Comparison of different application methods	90
4.5.1 SNP100 via capillary absorption and spray	90
4.5.2 Evercrete Vetrofluid via brush and spray	91
5 Discussion	93
5.1 Preliminary analysis of functionalised particles	93
5.1.1 Functionalisation with Calcium Nitrates	93
5.1.2 Functionalisation with Polymeric compound	94
5.2 Characterisation of concrete materials and the effect of deterioration	95
5.3 SNP100	97
5.4 SNP-PDMS	98
5.5 Evercrete	100
6 Conclusions	102
7 Bibliography	104
8 Technical sheets	109
9 Index of figures	117
10 Acknowledgments	120

1 Aim

This research aims to synthesize and compare stone strengthening agents based on Silica Nano Particles (SNP) developing and improving the results obtained from NME Stucchi's bachelor's degree thesis named "*Sintesi e analisi di nano-prodotti a base di silice per il consolidamento di materiali lapidei naturali*"[1]. In the previous work two SNP products were synthesized in order to treat three siliceous lithotypes (two sandstones and *Pietra di Muggia* and a granite *Bianco Sardo*). Considering the pore size distribution and the pores dimensions of the selected stones, two dimensional ranges were chosen for the synthesis of SNP: 50 nm and 100 nm (SNP50 and SNP100 respectively). The results showed the total chemical compatibility of the treatment applied with the siliceous stones, even though the aggregation of the particles was observed due to chemical reaction between water and silica. This phenomenon reduced the penetration of the formulated consolidants in the stone substrates, causing secondary effects such as the colour alteration of the treated surfaces.

In order to avoid the aggregation of SNP and encourage their penetration into the stones porosity, the present work proposes to synthesize two functionalized SNP products and compare the results obtained from the treatment of siliceous substrates with the previous SNP100 product and a commercial one. For this reason, the same analytical and methodological approaches were used.

Several functionalization methods with different typologies of reagents were performed. In particular the functionalization with polysiloxanes and calcium ions were taken into account. In order to target the procedure of synthesis, the composition and nature of each SNP product was analysed by chemical and microscopic investigations (SEM-EDS, FTIR, NMR). Since the best results were obtained with the synthesized SNP functionalised with polydimethylsiloxane (*SNP-PDMS*), this new product was chosen for the treatment of stone and concrete materials.

Its strengthening effect and efficacy were evaluated by the comparison with a commercial silica consolidant named *Evercrete Vetrofluid* purchased by EcoBeton[®] and SNP100.

The three products were applied by spray method on five substrates: *Pietra di Firenzuola*, *Pietra di Muggia*, *Bianco Sardo*, *grey Portland concrete* and *Vicat concrete*.

In order to simulate real conservation conditions, before the application of the strengthening agents eight sound specimens for each kind of material were subjected to four different degradation procedures: thermal shock, salt crystallisation, frost and thaw and total immersion in water lagoon. Two specimens of each material were subjected to each degradation process.

Porosimetric analyses, ultrasound measurements and sponge test analysis were performed before and after the treatments in order to verify possible variations of textural and structural features of the specimens. Moreover, microscopic and colorimetric analyses were performed for evaluating the aesthetical changes of the surfaces. The results obtained allowed to select the best product useful for the consolidation of siliceous stones and concretes.

This research, as well as the previous one, has been developed in collaboration with LAMA-Lab-CoMaC laboratory of Iuav University. The study is partially part of Venezia 2021 research project aimed to the study of innovative solutions for the conservation of architectural materials in the Venetian lagoon.

2 Introduction

2.1 Siliceous Consolidants

The study of the methods relative to the conservation of natural and artificial lithotypes is of main importance in order to preserve structural and aesthetical components of buildings. Among the phases related to the process of conservation, consolidation is the most important. Thanks to the application of a suitable consolidant compound, it is possible to extend the preservation of materials to decay processes. Ideally, as reported in the book *Stone Conservation*, the effects induced by the same treatment must to be equal for all the types of decayed stones [2]. Study of the diversity of the composition of each stone materials has underline the importance of the application of selected compounds depending on chemical-physical composition of the substrates. Although the huge number of researches on the production of consolidants and the studies of new kind of treatments, the sector of consolidation still present some failings. Many materials were used without scientific support and the same procedures of application were followed also if applied on different substrates [3].

Among the widespread consolidants developed in the past and still used, silicone resins and ethyl silicate represent the main classes of materials of interest. Ethyl silicate, a silica-precursor consolidant, is reported in literature also as tetraethylorthosilicate (TEOS). Since 1926, formulation of consolidants based on TEOS were reported in literature and researches in this field increase greatly since the 70s [4]. Ethyl silicate was used intensively for the treatment of stone and mortars. Reaction of silanes with water induce process of hydrolyzation which form silanols. Then the process of condensation occurs with the polymerization reaction which gives a silicone polymer. This process can take place directly on the surface after the application, due to the interaction of the ethyl compound with water of the atmosphere or of the surface; in some case water is added intentionally [2]. The silicate component shows a low chemical compatibility with calcareous substrates [5], meanwhile it is fully compatible with siliceous substrates and is characterized by great stability [2]. As reported in different papers this family of consolidants shows a good penetration in porous matrix and a good distribution on the surface [6; 7]. However, the relative consolidation treatments show some tendency to form cracks and to increase the property of the surface to absorb water [7]. More recently some researches used TEOS not only for natural lithotypes but also for artificial one. The use of ethyl silicate, as consolidant agents for concrete materials, is increasing due to the positive results obtained. The products of the process of hydrolyzation and

condensation penetrate in the substrate with benevolent effects on the mechanical strength of concrete [8; 9].

TEOS is considered the basic species of alkoxy silanes (silicone resins), polymers composed by a repetition of siloxane groups (Si-O-Si). The durability of these materials is due to the bond strength of the siloxane groups. Nowadays, the most common silicone polymer is Polydimethylsiloxane (PDMS). Silicone are often used as main elements for the preparation of consolidants [10]. Siloxane based products in organic solvents were widely applied as protective and strengthening agents on monumental stones and architectural surfaces [7]. They found wide application as protective coatings since 1950 due to their good water repellence property. Siloxanes are based on alkoxy silanes mixed with ethyl silicate it was used for the first time as a consolidant for calcareous and dolomitic stones [4]. One of the most important paper concerning these systems is dated back 1970 and it is aimed to the development of siliceous consolidants based on methyltrimethoxy silane (MTMOS) for application on marble substrates [11]. Alkoxy silanes compounds revealed to be effective in reducing damage induced by weather for 5-20 years [12]. This finding underlined that silicone resins have a great resistance to thermal variation and to the radiations. After this initial success, many researches were focused on the development of silicone resins materials and on their applications on different substrates. Since TEOS has the properties to facilitate silanes to enter in the porous network [13], the use of alkoxy silanes was based on the mixture of the compound with TEOS [4]. Now, the largest number of consolidants commercially available are based on TEOS mixed with solvents.

Recent research has also evidenced the use of TEOS as precursor of reaction to achieve the production of nanomaterials.

TEOS is the main precursor for the Stöber reaction with the production of Silica nanoparticles (SNP) through the process of condensation and hydrolyzation. In the last decades, the use of SNP as consolidant of lime and concrete has been increased [14]. Compound of silica particles with nano dimensions show good preservation results [15; 16] and they were applied on architectural surfaces and monuments made of stone materials and cements. Nano dimensions help to envisage problems for example of cracks induced by the use of ethyl silicate [17]. As already reported for TEOS, also SNP induce the formation of a gel on the surface of the artefact that increase the strength of materials. The effect is better if SNP are mixed with TEOS. This mixture increases also the water repellence of the substrates [18]. Nevertheless, also these nano systems have some negative aspects such as chromatic alterations, formation of gel and powdering [19] due to a low penetration of SNP [20]. In fact, the product compacts on the surface of the material creating a

superficial layer. On the contrary, in porous substrates, the particles penetrate into the structures inducing increasing positive effects (i.e. reducing the migration of water) [21].

Consciousness about the promising effects of SNP for the consolidation of siliceous materials raised the interest in the development of research presented in §2.2. The study allows to understand the interaction of SNP and the drawbacks and the positive effects related to the use of these systems. Nowadays, new researches are focused on the process of functionalisation of SNP in one or two steps during the synthesis. The reduction of the interaction can be possible by changing some characteristics of SNP through the process of functionalisation (investigated in § 2.3).

2.2 The beginning of the research

A research entitled “*Sintesi e analisi di nano-prodotti a base di silice per il consolidamento di materiali lapidei naturali*” [1] was developed during my bachelor thesis. The aim was to synthesize a consolidant based on Silica Nanoparticles (SNP) for the preservation of sandstones *Pietra di Firenzuola*, *Pietra di Muggia* and a granite *Bianco Sardo*. SNP with two different dimensional ranges were synthesized and the relative consolidants were produced.

For each lithotypes, 6 cubic specimens of dimensions 5x5x5 were prepared. Three of the six specimens were subjected to degradation processes in order to simulate the real. All the processes were made following the procedures proposed in literature and the current regulations: (i) Thermal Shock (as reported by Pozo et al. [20]), (ii) Salt Crystallization (UNI EN 12370/1999 [22]), (iii) Frost and Thaw (UNI EN 12371/2003 [23]).

SNP system of 100 nm, synthetised by the Stöber method, was selected considering the pore structures of the analysed lithotypes. The results of the research showed that parameters such as humidity and temperature are strictly related to the sizes and to the agglomeration of the particles. When silica particles enter in contact with water (both in the liquid or vapour form) they aggregate and the size of the particles increase, reducing the penetration of the compound on the substrates. Moreover, was observed that the agglomeration process increases with the decreasing of the SNPs dimensions.

A deep analysis was performed in order to choose the more convenient concentration of the particles and the best solvent mixture. Ethanol was chosen as carrier for the application of the particles because of it performed a reduced process of aggregation respect to water dispersion. SNP were dispersed in Ethanol with a concentration of 10% w. The solution was diluted with water (EtOH: H₂O 75:25 w/w) just before the application. A final formulation of a silica based consolidant for the consolidation of stones, compatible with two sandstone and a granite called *SNP100* was proposed.

The application of *SNP100* on the lithotypes allowed to evaluate the compatibility and the efficiency of the product on the substrates. The product was applied by capillary absorption, for 5 hours, maintaining the surface in contact with the liquid. The evaluation of the efficiency of the consolidation was obtained by the comparison of the results obtained by several analytical techniques applied before and after the consolidation treatment. After the application, an increase of weight could be evidenced for all the samples. Microscopic observation made with different enlargements

showed a change of the aspect only on few specimens. Non colorimetric alterations were evaluated after the treatment on all the specimens, meanwhile ultrasonic analysis and water absorption analysis gave random results.

Finally, as already reported in literature [24], the agglomeration effect due to the high reactivity of the particles in environmental humidity that limits the penetration of the consolidant was confirmed. These negative aspects do not allow the consolidation to penetrate into the internal pore with the formation of translucent surface films that can alter the aesthetical aspect.

From these preliminary results, new steps based on the functionalisation of SNP are proposed in this new research. The new investigation (presented in §2.5) deals with the development of a system of functionalized particles with improved penetration properties into the porous network.

2.3 Functionalization, a promising step for the improvement of SNP

Process of functionalization can be applied during and after the process of synthesis in order to change the characteristic of the matrix of interest. It can be used in order to obtain specific characteristic of the particles, modifying some aspects as:

- Change in the precipitation reaction
- Degree of agglomeration and tendency to form aggregates (e.g. use of polyhydroxyalcohol prevent the binding with water molecules)
- Affect physicochemical properties
- Acquire organophilic properties
- Change of the size of the particles
- Change of hydrophobicity and hydrophilicity behaviour of the substance (e.g. use of glycol or of silanol, higher hydrophilicity to parity of higher silanol bond)

The commonest functionalisations concern the addition of organic solvents as alcohol (with long chain), surfactant, coupling agents as silane and titanium and alcanoic acids [25; 26].

The functionalization can be performed by a post modification or grafting process on pre-prepared SNP. *Grafting* functionalization, made right after the synthesis [27] involves the addition of surfactants or macromolecules. It can be made in two way [28]: *Grafting to* via covalent attachment of end functionalize polymers and *Grafting from* in situ monomer polymerisation with monomer growth of polymer chains. The specific properties of the nanocomposites can induce variation to the species of the grafting monomers, interfacial interaction between grafting polymer and matrix polymer [28].

In situ functionalization called *co-condensation*, involves a simultaneous synthesis and functionalization of colloidal silica nanoparticles using organofunctional silane agents, with incorporation of organic groups as bridging blocks on the pores of particles [29; 30]. In co-condensation process [27], molecules interact via noncovalent forces and they act changing the pore structure. Changes made via co-condensation is homogeneous and wide but does not induce excessive modifications into the matrix structure.

In literature is possible to find several methods to functionalize SNP. For example, the addition of solvents can change the pH of the solution giving higher control of SNP dimensions [31].

Surface modification of the charge of SNP can be made by the use of amine groups [28]. Electrolyte solution of can be mixed to TEOS [32] and added to enrich the surface of Si with silanol groups which became sites of functionalisation of SNP. The addition of Vinyl triethoxysilane during the synthesis can bring to the substitution of hydroxy group of Si by Vinyl groups, allowing the formation of super hydrophobic film characterised by a geometrical microstructure [33].

The use of coupling agents can also induce changes of the surface of SNP. The general structure of coupling agents is $RSiX_3$, where X is the group that reacts with the hydroxyl group on SiO_2 surface; the most used precursors are of the type $[(R'O) SiR]$ (alkoxysilane) and $[Cl SiR]$ (chlorosilane) [27]. A deep insight in the use of silane polymeric substances is presented in §2.3.2.

2.3.1 Functionalization with Calcium

Calcium Silicate Hydrate (C-S-H) is a compound formed during the process of hardening of hydrated Portland cements. C-S-H has a nano crystalline structure, where two silica are connected directly to the calcium oxide sheet, the third silica occupies a bridging position, and it is not directly linked to the calcium sheet [34]. Since C-S-H increases the resistance of the surface we have considered it for the consolidation process. Synthetic C-S-H can have different composition, structure and morphology. The amount of Ca^{2+} or SiO_2 , the pH value, the composition of the cements and the preparation method change the quality and the characteristics of C-S-H.

As reported in literature, formation of C-S-H can be obtained in different way as, for example, in presence of Nanolime with Silica Fume particles of small dimensions [35]. Camerini et al. [36], suggested a formulation of ternary composition, SiO_2 NP, $Ca(OH)_2$ NP, hydroxypropyl cellulose (HPC) in a solution 4:1 of EtOH:H₂O, for e the formation of C-S-H. The reaction proceeds with the dissolution of $Ca(OH)_2$. At the second step breaking of Si-O-Si bond occur and bring to the release of -OH. Then, Ca^{2+} bridge the depolymerised Si ions, forming basic units of C-S-H gel from the alkaline activation of nano silica [37]. In water the Silica NP have a negative potential while CaOH have a positive potential. CH formed by the hydration of Calcium Silicate react with Si fume particles forming C-S-H that precipitate in the pores of the substrates. The penetration depth of this system is affected by the type of dispersing solvent, the environmental condition and the aggregation of the particles. A large amount of Si on the concrete surface of treatment can increase the process of binding of Ca^{2+} , giving to the C-S-H structure the possibility to react. The amount of Ca^{2+} or SiO_2 on the surface change the features of C-S-H [38]. Thus, theoretically, if the stone substrate contains high amount of Si, the reaction between the dispersions and the stone might lead to the formation of a gel similar to CSH phases. Moreover, the interlayer of C-S-H and

its surface contains cations (H^+ , Ca^{2+}) which contribute to balance the negative charge of the deprotonated silanol groups [39].

Consolidants based on Ca^{2+} and SiO_2 can be suitable to increase the resistance of cements and stone. Theoretically, the presence of Calcium, Silica and water can bring to the formation of C-S-H allowing a consolidation process. As reported by Greasley et al. [40] addition of Calcium to SNP can be made by the use of Calcium Nitrate in aqueous dispersion. Functionalisation of Si with Ca^{2+} increase the properties of the particles [40] and the considered process allowed to maintain monodispersed particle with unchanged dimensions. The right ratio among $SiO_2:Ca(NO_3)_2$ is fundamental to have mono disperse particles, with controlled size [41]. Calcium Nitrate act as surface modifier, it precipitates on Si surface and diffuse in SiO_2 particles. The addition of Ca is made by a calcination process. Temperature of $400^\circ C$ is enough to allow the incorporation of Si particles, but T of $680^\circ C$ was considered the best for the process and the remotion of nitrates formed during calcination [42]. SNP functionalised with calcium can be dispersed in alcohol solution and then applied to the lithotypes in order to perform homogenous application of the compound on the surface [43].

2.3.2 Functionalization with siloxane

As mentioned in §2.2 silane and siloxane are widely used for the production of consolidants and protecting agents. Poly alkyl siloxane distributed with the commercial name of Rhodorsil or mix of siloxane and silane distributed with the commercial name Wacker 290, applied with white spirit, give a super hydrophobic behaviour to the surface, showing water repellent properties and reducing water permeability [44].

Introduction of SiO_2 in hybrid siloxane or silicone polymers, increase gel pore-size and reduce capillary pressure. Polymethylsilane (PMS) is frequently used as functionalization agent. Recent studies have shown that Polydimethylsiloxane (PDMS) can be considered complementary to PMS for the functionalization [45]. For example, PDMS/Silica Nanomaterials improve robustness and stain resistance of carbonate stone [46]. Application of modified epoxy SiO_2 with PMDS-OH 30% accelerate the curing process giving free cracking film, increase the viscosity of sol [47] and the hydrophobic properties. Furthermore, the ternary system composed of TEOS, PDMS and nano-hydroxyapatite (HA) reduces the surface tension and the capillary pressure and promotes the coursing of gel network [48].

PDMS and Poly(methylhydrosiloxane) (PMHS) are used to produced coatings (structure of the respective monomers are reported in Figure 1)[49]. For example, shells of PMHS are formed

around SiO₂ core [50]. PMHS is easy to handle, inexpensive and non-toxic [51], thus it can be suitable to be used. Poly(methylhydrosiloxane) (PMHS)/SiO₂ hybrid particles can be synthesised by mechanochemical ball milling. The presence of H group in the polymer allows the grafting of the monomers to the OH group present on the Si chain [52].

The functionalisation of the particles can be obtained by a condensation reaction of SNP added to PDMS-OH. The terminal OH group of the polymer allows the reaction between the polymer and Silica. Schematic reaction of the reagents and of the product is shown in Figure 2 [53]. All these methods of functionalisation can improve the specific characteristics of SNP.

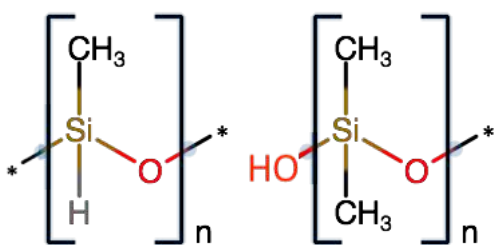


Figure 1. Monomers of the two polymers used respectively PMHS and PDMS-OH (from left to right).

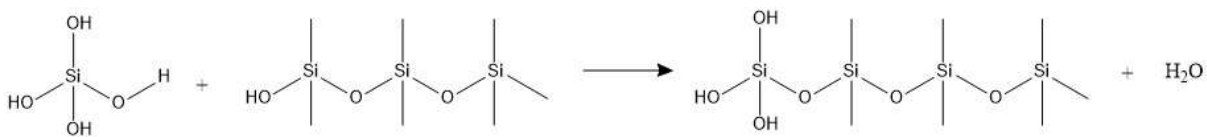


Figure 2. Schematic presentation of main reagents and final functionalized compound.

2.4 Concrete a new material to preserve and Co. Ri. La project

Conservation of concrete in contemporary architecture is commonly aimed to give structural strengthening but, architecture must be preserved also from an esthetical point of view. In Venice the highest example of different use of concrete are the architectural elements created by Carlo Scarpa. During the XX cen. also other architects demonstrate their interest in the use of new kind of materials applied in the construction of modern buildings or in the renovations of older ones. *Casa Torres* was designed by Giuseppe Torres and Edoardo Campese in the early year of XX cen. This architecture is one of the lagoonal examples where concrete wasn't used only as structural materials but also with decorative purposes. Torres was interested in the Middle Age decorative elements and decided to produce it not by using traditional material as stone but using concrete.

In Figure 3 are visible some of the concrete architectonic elements present in façade. The two masters were interested and focus their activity on the production and study of innovative materials for the architecture, trough the imitation of natural materials. Collaboration of artisans specialised in concrete production bring to the realisation of several decorative elements released in cements with different colour and granulometry.



Figure 3. Decorative elements visible in facade.

Co. Ri. La Project individuates the case study of Casa Torres as an example to evaluate the composition and the presence of deterioration phenomena that affect concrete present in the lagoon. Artificial stones, made of concrete as decorative elements, permit to simulate not only from an esthetical but also from a statical point the natural stone elements. Production of decoration can

be made working concrete in situ, directly on the surface, moulding it using a modine (e.g. creation of “bozzati”), or producing decorative elements in laboratory and subsequently applied on the surface. These cementers base elements showed good resistance and durability [54] and concrete can be considered a suitable material to be used as material for the production of aesthetical element. However, different textures and patterns of this material bring to the formation of different pathologies and of degeneration linked to concrete casting. Thus, since the last centuries its use has increased also in decoration and design sector bringing to the necessity to develop also strategies of analysis and methods of conservation.

Several studies are necessary to analyse and to fully know the building, characterising the material elements, defining properties and describing decay and alterations. Characterisation of pathologies, investigation of the time of decay process, evaluation of the resistance of materials must be performed in order to have a complete idea of the phenomena that affect concrete [55]. As for stone elements, black crust and run off water are common alteration processes. The presence of iron elements brings to corrosion phenomena which create *vaiolettura* and pitting with the consequent desegregation. Salt deterioration induces an increment of the depth of the carbonation process [56]. Depending on the texture and porosity, substrates are more subjected to aggressive agents due to the presence of micro cavity phenomenon of segregation. For the aim of conservation, it's important to evaluate decay phenomena related to the environmental condition of conservation to reduce it. Salt crystallisation phenomena induces the formation of ettringite, thenardite and gypsum. Soluble ions of Sulphates, Nitrates and Chlorites can induce alteration in the metal elements of the concrete. Frost and thaw phenomenon induce the production of *rustomite*, that is the first product and a mark of the degradation phase that induced an elimination of portlandite [55; 57]. The most dangerous kind of decay is the oxidation of iron reinforcing rods; this phenomenon could determine the cracking of conglomerates through their carbonation. Inspection of concrete elements present in situ allow to gain qualitative and quantitative information about the consistency of casting, the constructive techniques, the conservation elements and the laboratory survey.

Analysis of concrete samples obtained by different preparations and with different textures allow to characterise the material, correlating its decay state and its conservation to the specific conservation condition [55]. For these reasons the presented research takes in consideration the application of consolidants on concrete samples, in order to realise a survey model and to update data related to this material that is increasingly used in architecture.

2.5 The new research

On the basis of the previous results (§2.2) the aim of the presented research is: to produce a consolidant system based on functionalised nano silica and to compare the new results with the previous finding [58].

Processes of functionalization allow to maintain selected characteristic of SNP particles and to change some of the properties. Some positive aspects of the functionalization can summarize as follows:

1. avoid the interaction of particles with water
2. reduce the tendency of particles to the agglomeration
3. maintain constant particles size
4. induce a better penetration process
5. avoid aesthetic change of the surface induced by the no penetration of particles

The thesis is focused on two types of functionalisation:

- Functionalisation of the particles with calcium nitrates $\text{Ca}(\text{NO}_3)_2$.
- Functionalisation of the particles with Polymethylhydrosiloxane (PMHS) and Polydimethylsiloxane hydroxy terminated (PDMS-OH)

The functionalisation methods will be tested on samples in order to verify their performances. Morphological and dimensional analysis of the SNP will be performed using Scanning electron microscope (SEM) coupled with Energy Dispersive X-ray Spectrometry (EDS) that gives the elemental analysis of the sample. Fourier-transform infrared spectroscopy (FTIR) and Nuclear Magnetic Resonance Spectroscopy (NMR) will be used for the study of the composition. Investigation of the behavior of the particle in solution can give useful results in order to understand how particles will react in different solvents. This analysis will be made by Dispersion Analyser.

Changing some specific parameters of the reaction, it is possible to have a better knowledge of the process and to understand the final effects induced by each modification.

Nowadays, concrete is the second most used construction material after water [59] and for this reason is fundamental to understand its reaction if treated in specific conditions.

Two typologies of concretes, *Portland concrete* and *Vicat concrete*, will be investigated in addition to the natural lithotypes already used in the previous research. Natural and artificial lithotypes, with similar chemical composition, react differently so it could be very interesting to understand how they specifically react to degradation and to consolidation treatment.

Since, as presented in §2.4, the interest of *Co. Ri. La. Project* is to define the reaction of materials in lagoonal environment a process of deterioration simulating in laboratory, the real conditions present in situ has be performed. In this way it is possible to investigate the process with known parameters and monitored condition. In addition to the already studied degradation processes [1] (Thermal Shock, Slat Crystallisation and Frost and thaw), the water lagoon degradation process has been applied to all the materials. Thanks to this approach, it can be possible to understand how concrete interacts with different degradation phenomena and which of them affect much more the material. Moreover, the comparison of the reaction of natural and artificial material to processes allow to understand which is more resistant to environmental agents and so which can be more suitable to be used in new construction.

Comparison of the application of the synthesised consolidant with a commercial compound can be useful to understand the quality of the application. For the porpoise of the research, the protective and water repellent agent *Evercrete Vetrofluid* purchased by EcoBETON[®] was tested in order to satisfy the request of the *Co. Ri. La. Project*. The compound is specifically aimed to be applied to concrete, even though the application of the compound can be extended to natural lithotypes. Functionalised compounds have been compared with not functionalised particles (for example SNP100) systems applied in the first part of the research [1]. To this aim, stone specimens and concrete specimen were treated with SNP100. To allow the comparison of the results, it has been important to maintain the same procedure of application for all the specimens. As reported in the work of Ferreira Pinto et al. (2012) [60], the methodology of application is fundamental to obtain good treatments and it is strictly related to the typology of compound applied. It can be suitable to use the analytical methodology reported in thesis [1] in order to gain the same typology of information. Thus, it is possible to achieve a complete idea of how sound and degraded stone, granite and concrete specimens react to different treatments: SNP100, SNP functionalised with polymer and Evercrete Vetrofluid.

3 Experimental part

3.1 Consolidants

In the present work some synthesised and commercial strengthening agents were tested for the consolidation of silicate rocks and concrete.

3.1.1 SNP100

SNP with dimensional range of 100-120 nm were synthesised by Stöber method with reagents ratio H₂O: NH₃: TEOS¹ equal to 4,935 M: 0,826 M: 0,113 M. The synthesis details and the features of the analysed nanoparticles are reported in Stucchi et al. 2019[58]. Once synthesized, SNP were dispersed and store in ethanol in concentration of 5% in weight. Before the application, the consolidant was diluted in water with a concentration ratio of EtOH: H₂O of 75:25 w/w [1].

3.1.2 Functionalization with Ca(NO₃)₂

SNP100 were produced following the procedure described in 3.1.1, then grinded and dispersed in distilled water. As suggested by Greasley et al.[40], Ca(NO₃)₂² was added to the silica-water solution and the mixture was let to react for 20 minutes. The compound was divided in tubes and spin-dried for 10 minutes, in order to separate the pellet from the solvent; then the residual pellet was dried overnight at 60 °C. Finally, the compound was treated at 680°C in muffle for 3 hours with an increment of temperature of 3 °C/min. The so obtained particles were washed three times in EtOH and then dried overnight. Several SNP100:Ca(NO₃)₂ ratios and calcination temperatures were tested. All the information related to the experimentations performed are reported in Table 1.

¹ Technical sheet is reported in appendix §8 A

² Technical sheet is reported in appendix §8 B

Table 1. Details of the experimentations performed for functionalizing silica nanoparticles with calcium ions.

Labels	Notes about the composition
S1a	SiO ₂ : Ca(NO ₃) ₂ 70:30 (%m/m), T of calcination: 680°C
S1b	SiO ₂ : Ca(NO ₃) ₂ 50:50 (%m/m), T of calcination: 680°C
S1c	SiO ₂ : Ca(NO ₃) ₂ 30:70 (%m/m), T of calcination: 680°C
S1d	SiO ₂ : Ca(NO ₃) ₂ 70:30 (%m/m), T of calcination: 500°C
S1e	SiO ₂ : Ca(NO ₃) ₂ 70:30 (%m/m), T of calcination: 500°C. Change of the composition of the carrier.
S1f	SiO ₂ : Ca(NO ₃) ₂ 80:20 (%m/m), T of calcination: 500°C. Change of the composition of the carrier.

S1a, S1b, S1c were synthesized using the same procedure but different ratio SNP:Ca(NO₃)₂.

S1d, S1e S1f were subjected to a lower calcination temperature (500 °C). Moreover, S1e and S1f were synthesized storing SNP in a solution with a concentration 50:50 of water and ethanol.

3.1.3 Functionalization with Polymer

Two siloxanepolymers, polymethylhydrosiloxane (PMHS)³ and polydimethylsiloxane hydroxy terminated (PDMS-OH)⁴, both purchased by Sigma Aldrich, were used to functionalize silica nanoparticles.

In both cases, the synthesis procedure adopted was that suggested by Xu et al. [47] varying the type of polymer and using hexylamine⁵ as ammine. The functionalisation started by mixing EtOH with TEOS and SNP. The solution was kept under stirring and let to react for two hours. After that time, H₂O first and then the chosen polymer drop by drop were added, letting the reaction to go forward for 15 minutes. Finally, hexylamine was added leaving the reaction to continue under

³ Technical sheet is reported in appendix §8 C

⁴ Technical sheet is reported in appendix §8 D

⁵ Technical sheet is reported in appendix §8 E

stirring for 20 minutes. In order to improve the final product, several changes were made to the procedure, such as the type of polymer or the concentration of polymer and ammine.

In Table 2 are described the tests performed for the functionalization of SNP with polysiloxane polymers.

Table 2. Details of the experimentations performed for functionalizing silica nanoparticles by the use of a polymer.

Labels	Notes about the composition	
S2a	SNP (2 w/v %), with PMHS and TEOS	
S2b	SNP (2 w/v %), with PMHS, without TEOS	
S2b1	SNP (2 w/v %), with PMHS [0,001 mol], without TEOS	
S2c	S2c1	Achieved sol phase of the simultaneous synthesis and functionalization of SNP with PMHS
	S2c2	Dried product of the simultaneous synthesis and functionalization of SNP with PMHS
S2d	Dissolution of S2A in EtOH	
S2e	SNP (2 w/v %), with PDMS-OH [0,004 mol], without TEOS	

S2a was synthesised following the procedure and the concentration reported by Xu et al. [47], but using polymethylhydrosiloxane (PMHS) [61] as polymer. The final product was a gel.

S2b and S2b1 differ from S2a, since TEOS was not added. S2b1 has half of the concentration of both the two reactants than S2b.

The synthesis and functionalization of S2c was made in one step. The reaction starts with the production of SNP by Stöber method. After two hours of reaction, PMHS and esylamine were added to the solution. The mole ratio of the reagents used is H₂O: NH₃: TEOS: PMHS: esylamine 4,935 M: 0,826 M: 0,113 M: 0,004 M: 0,0004 M. The product was divided in two parts:

one part was preserved as liquid and used as consolidant, whereas the second part was subjected to the process of separation and cleaning of the particles, as expected by Stöber method.

S2d was produced for evaluating the possibility to convert the S2a gel back into solution. For this reason, 2 gr of S2a gel were dissolved in 30 ml of EtOH and kept under vigorous stirring for at least 2 hours, then the compound was subjected to 10 minutes of ultrasonic bath and again 2 hours of stirring.

S2e was produced as S2b but using polydimethylsiloxane hydroxy terminated (PDMS-OH) [62] as polymer. The achieved compound was stored in liquid form in closed vials.

3.1.4 Evercrete Vetrofluid

Evercrete Vetrofluid compound is a commercial product purchased by EcoBETON®⁶ [63]. It is a water base product with waterglass and catalyst. Thanks to its chemical composition, theoretically it can penetrate for 10-40 mm in concrete substrates. It is a colourless and odourless compound that should not change the superficial aspect of treated surfaces. It is a non-toxic component, stable and permanent, compatible with other products.

It is a water-proof, protective, consolidant, anti-decay agent useful for the conservation of concrete substrates. It acts as barrier closing the porosity of the substrates and showing a good water-proof action.

⁶ Technical sheet is reported in appendix §8 F

3.2 Substrates

3.2.1 Lithotypes specimens

The consolidants were applied on three silicate stones. *Pietra di Firenzuola*, *Pietra di Muggia* and *Bianco Sardo*. The stones were characterized in the previous work [1, 58] and proposed as test systems because of their chemical compatibility with the conservative products.

For each lithotype 11 specimens having cubic shape of 5 x 5 x 5 cm were used (Figure 4).

Pietra di Firenzuola is a sandstone with a mainly felspathic composition. The matrix is composed of clay with a low amount of calcitic elements. The quarries where this material is extracted are located in the central part of Italy, in the area around the city of Perugia.

The stone is characterized by a blue grey colour as visible in Figure 4a. If subjected to natural weathering the colour veers to yellow-grey tonality. Interactions of the material with air-pollution and salts are considered the main causes of deterioration of the material. Due to the low resistance of the stone to natural environmental condition it was used for internal covering [64].

Pietra di Muggia is a sandstone that is extracted in the Peninsula of Muggia in the North-East of Italy. The stone is characterized mainly by siliceous components. Quartz and feldspar crystals, volcanic rock fragments and carbonate cement are nested in a fine clay matrix [65]. The composition gives to the material a zoned coloring, with alternance of orange and grey area (see Figure 4b). The good stability of the stone to atmospheric agents (also in extreme condition) let the material to be suitable for the use in external covering.

Bianco Sardo is a typical granite that is extracted from the area of Buddusò (Olbia Tempio) located in the northern part of Sardinia. The material is characterized by a white/grey colour due to the huge presence of quartz and feldspars. It presents small black grains of biotite crystals that are nested in the matrix as visible in Figure 4c. The material is easily available and has good physical-mechanical characteristics, for these reasons it is suitable to be used to cover both internal or external surfaces of private and public buildings [64].

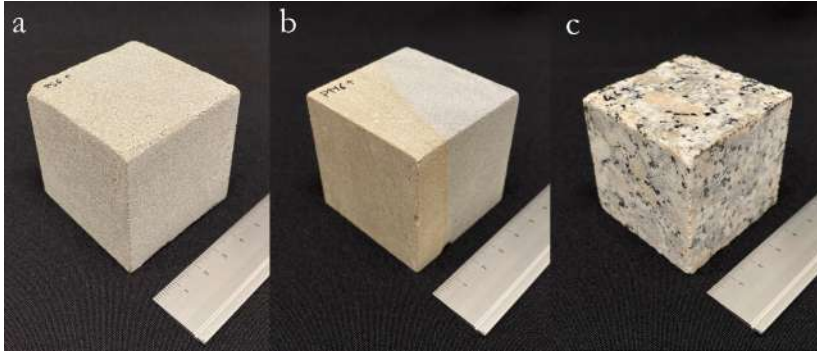


Figure 4. The three lithotypes studied in the present work: a) *Pietra di Firenzuola*, b) *Pietra di Muggia*, C) *Bianco Sardo*.

3.2.2 Concrete specimens

For the purpose of the research two kind of concrete were used as substrates: *grey Portland* and *Vicat* (Figure 5). Eleven specimens for each typology of material with dimensions of 4 x 16 x 4 cm were prepared.

Grey Portland concrete 42,5: is a typical material used in construction and building sector. For the 75% of its composition, it is made of sands of different type, whereas the 22% is composed by water. The 20% of sand is of alluvial type, a siliceous kind of sand with grains with an average dimension of 1-2,5 mm, the 40% is made of quartz, with grains of an average dimension of 0,7-1,2 mm, and the remaining 40% of sand is based on quartz with grains of average dimension 0,3-0,9 mm.

VICAT concrete: is a new innovative material purchased by Vicat[®]. The composition of this material is equal to the composition of grey Portland concrete, but it differs in the amount of water equal to 19%. It is composed of sand for the 75%, of which the 20% is of alluvial type, the 40% is made of quartz with grains of dimension between 0,7-1,2 mm, and the residual 40% is of quartz characterized by grains of dimension between 0,3-0,9 mm.

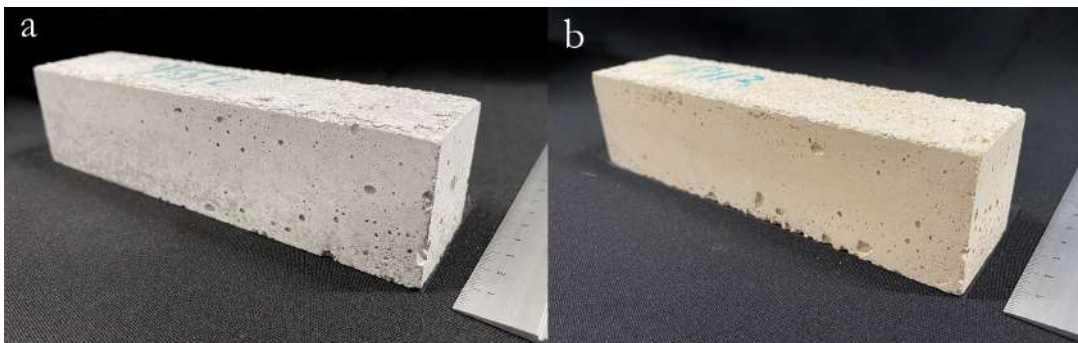


Figure 5. Artificial lithotypes (concrete) used in the research: a) Grey Portland concrete, b) Vicat concrete.

3.3 Methods

3.3.1 Characterisation of the particles and of consolidants

Microscopic observations and chemical analyses were performed in order to evaluate the morphology and chemical composition of SNP and to verify the effectiveness of the functionalization process.

SEM – EDS analysis

In order to monitor the morphology and the dimensions of synthesized SNP, a *Philips XL 30 SERIES SEM* Scanning Electron Microscope (for short SEM) was applied. As reported in the literature [66], SEM observation gives morphological information of small regions of the sample and allow to obtain images at high magnifications. The comparison between the images achieved by the analysis of different compounds helps to evaluate change in morphology of the particles induced by changes in the process of synthesis. Sample can be both organic or inorganic, with the dimensional limit due to the dimension of the space of the chamber of analysis of the instrument and the detection limit of the instrument related to the quantity of the sample.

Technically, an electron beam is produced in a vacuum system and focused by electromagnetic lenses to the sample. The sample is excited with the incident beam, that causes the dislocation of the electrons of the sample. The excitation produces the release of three different kind of signals and each of them allow to reveal: (i) the topography of the sample and the presence of different elements through the different molecular weight, (ii) to construct images of the morphology, (iii) to identify the elements that composed the sample. The secondary beam generated by the interaction with the sample is collected by a detector (the most common is an Everhart–Thornley detector) and transferred to a computer, which elaborates the data and decodes them into black and white images. The grayscale effect in the image is due to the different molecular weight of the elements in the sample.

If coupled with an EDX microprobe the SEM analysis gives elemental information of the composition of the sample in a specific analysed point/area. EDX microprobe allows the detection of X-ray emitted from the sample, giving back a spectra where the peaks, that fall at specific wavelengths, correspond to chemical elements that composed the sample [10]. SEM-EDX could be a mapping technique that use the electron beam in order to reconstruct through false colours the elemental distribution in a portion of the sample.

For the aim of the research, this technique was applied in order to estimate the nature of functionalized particles. SNP functionalized with Calcium nitrates (S1n type) were analyzed to evaluate the effective presence of Ca on the SNP structure. EDX analysis allowed to assess the presence of the Ca^{2+} element on SiO_2 particles, as results the analyses give back a report of the concentration of the elements detected on the sample. Information present on the report are about the concentration of three different type: (i) the unnormalised concentration in weight percent of the element (unn. Ca [wt.%]), (ii) the normalised concentration in weight percent of the element (norm. Ca [wt.%]), (iii) the atomic weight percent (Ca Atom. [at.%]). The atomic weight percent gives information about the ratio between one kind of atom and the total number of atoms [67] and estimate the error related to the evaluation of the atomic percent. The comparison of the reports of different specimens allow to evaluate different elemental concentration. Comparisons of the images achieved by SEM analysis allow to understand which functionalisation process gave best results. Moreover, the comparison with image of SNP100 underline the change induced by the functionalisation to the SNP.

FT-IR analysis

It is a qualitative method that enables to analyse functional groups in organic and inorganic samples [66]. Nowadays, it is the most used technique for the investigation of unknown samples composition. It identifies chemical bonds through the study of vibrational movements in the molecules of the sample caused by the interaction with an IR beam. Technically, the source emits radiations in the mid-infrared or far-infrared region that passing trough an interferometer (the commonest is Michelson interferometer) are split in two different part. The beam splitter allows the passage of ray and its partial reflection and transmission. The two splitted beams converge in the detector creating the interferogram. The sample, hitted by the IR radiation, emits energy at specific range of interference depending on its composition. Distances and frequencies of the signals are recorded by the converter that collects the data and transferred it to a computer, where are put in relation trough to Fourier transformation function [68]. The analysis gives back spectra with a signal composed by different peaks. The spectra obtained reports all the absorptions of each functional group at specific wavelengths. Each functional group has one or more characteristic bands of absorption linked by the movements that happened along the bonds of the molecule. Spectra can be interpreted thanks to the comparison of spectra collected in the library [10].

Depending on the kind of FTIR instrument used, low amount of sample of different kind can be examine in liquid or solid form: (i) powders are analysed in the form of standard KBr pellets (at least 0,1 mg of sample powder); (ii) flakes of polychrome part; (iii) planar surfaces of polymeric, natural, synthetic film; (iv) stratigraphic or thin sections; (v) pure or obtained from extraction liquid samples; (vi) fibers [10].

For the analysis of SNP and SNP functionalised with $\text{Ca}(\text{NO}_3)_2$ a *Nicolet iS10 (Thermo Fisher Scientific)* was used to determine the composition of solid sample. A small quantity of dried powder of functionalised nanoparticles was mixed and grinded with KBr, that is transparent in the range of investigation of the UV/ NIR, and then press to form platelets. Platelets of SNP functionalise with calcium nitrates in different ratio were analysed and the spectra were compared to evaluate the presence of different amount of functionalized molecules.

For the analysis of SiO_2 functionalised with polymeric substances *Nicolet iS5 (Thermo Fisher Scientific)* instrumentation was used in ATR mode. A drop of substance was put on the stage, directly in contact with the diamond and the analysis was recorded. Thanks to this instrument was possible to analyse all the compounds functionalised by the use of polymer, both in liquid and in gel form, by the application of a small part of gel sample.

Dispersion analysis

LUMiSizer Dispersion Analyser is a microprocessor controlled analytical photocentrifuge. It investigates the degree of dispersion of particles in solvents and phenomena as sedimentation and flotation. It calculates the velocity distribution in the centrifugal field and the size of the particles. The system uses a *SEPView Software* in order to display the results achieved by the analysis. The technology is based on *the Space and Time resolved Extinction Profiles (for short STEP) Technology* and is based on the use of near infrared or blue light to illuminates the cell and records the transmitted light. The transmission of light is converted into light extinction. The instrumentation records the variation of extinction caused by centrifugal segregation over the entire sample length at any time of the centrifugation. The analyses of 12 different samples can be recorded simultaneously [69].

This analysis was used to investigate samples of SNP functionalised with calcium nitrates (S1n) and SNP not functionalised. The interest was to investigate the different velocities of precipitation of the compounds. Differences in the behaviour of precipitation of the compounds were expected because of the changing of the parameters of synthesis. Theoretically, an increasing time of sedi-

mentation must be related to particles with smaller dimensions and well dispersed. On the contrary, particles with bigger dimensions or aggregates should be characterized by a greater velocity of precipitation because of the higher weight.

The samples were prepared with a concentration of 5 mg/ml of powder in solution. Ethanol and a mixture of H₂O and EtOH in concentration 75:25 was used as solvents. The solution was sonicated right before the analysis in order to have the best dispersion of the solid phase in solution. Vials were put in the locations and the measurements were taken. Laser chosen for the analyses is characterized by a wavelength equal to 410 nm. Once the analysis was acquired data achieved must be read starting settings parameters. The kind of analysis of interest for the research is set to sedimentation of velocity, the last profile acquired was set as profile of reference for the analysis. Then number of nodes were set equal to 3 and positioned in the point of interest near the flexus, settings constant time and constant position and settings the number of profile equal to 300. Thanks to the set parameters resulting documents for each sample with graph of the sedimentation and tables reporting information about the sedimentation were achieved.

Nuclear Magnetic Resonance spectroscopy (NMR)

NMR analysis can be used to investigate the chemical species that interact with the SNPs surface. The technique allows to obtain structural data and to investigate the presence of interactions on the particle interface. Moreover, NMR analysis allows to collect details about both kinetics and thermodynamics of sorption processes. Thus, NMR spectroscopy is largely exploited to investigate particles interfaces and to assess the effect of functionalization procedures [70] for example, in the case of polymeric substances. Furthermore, liquid state NMR (used in this research) allows to investigate the dynamics of colloidal systems.

This technique is based on the observation of nuclear spin transitions stimulated by the absorption of a radiofrequency that properly matches the resonance conditions. The sample is located in a static magnetic field that reduce the degeneration of the nuclear spin levels for NMR active nuclei. The transition between the non-degenerate energy levels is induced by a radio wave pulse that hits the sample causing a tilting in the total magnetization of the nuclear magnetic spins, this process induce electric currents on the detection coils and an analogical signal can be recorded.

Since the resonance frequency depends both by the properties of the nuclei (defined by the gyromagnetic ratio) and by the chemical environment (that affect the local magnetic field expressed by the shielding parameter), the analysis of the resonance frequency allows to investigate the chemical nature of the probed atoms. Furthermore, in the case of the 1D proton NMR (¹H-NMR), the

intensity of a peak depends on the number of protons excited and the analysis of the integrated area of the peak can be performed to extract relative concentration data. Finally, the analysis of the peak fine structure reveals critical details on the connectivity that links the probed atoms.

In the present thesis, this kind of analysis was used in order to investigate the functionalization of silica NPs with the polymer PDMS-OH. Thanks to NMR analysis it is possible to evaluate the presence of interactions between polymeric substances and SNP in a colloidal solution. The analysis was conducted using SiO₂ NPs dispersed in ethanol:D₂O solution at the concentration around 1 mg/ml. The presence of ethanol cause interference in the analysis, however, this requirement is mandatory to ensure a good colloidal stability of the nanoparticles and the signals that are related to ethanol protons do not overlap with the signals of the PDMS-OH protons. The spectroscopic results were interpreted by comparison with spectra reported in literature and standard.

3.3.2 Test of application

Preliminary tests of SNP application were made to evaluate the effect of the synthesized consolidants on stone surfaces. Thanks to these applications, it was possible to chemically evaluate the compounds, to define how to improve the synthesis process and to verify the performance of the compounds.

Vicenza white limestone and *Carrara marble* (respectively materials with high and low porosity) were selected as substrates for the application for their different porosity and similar composition.

SNP functionalised with Calcium Nitrate (S1n) were applied on the surfaces following the same parameter of dispersion and dilution already used in the previous research [1; 58]. Particles were dispersed in ethanol with a concentration of 5 % in weight. The solution was stirred for an hour and diluted in water with a concentration of 75:25 Solution: H₂O in weight.

SNP functionalised with polymers (S2n) were dispersed in ethanol with different concentration and then applied on the surfaces.

The application of the consolidants was made by brushing method, repeating the process a total of three times every 24 h. After each application, samples were weighted for evaluating the effective absorption of the consolidants.

Properties of the treated specimens were analysed after each drafting of the product and after 15 days since the last application.

Analysis of the morphology of the substrates were made using optical microscope *Leitz LABOR-LUX 12 POLS* (enlargement 40x - 100x) with *Leica CLS150E camera*. Images at different enlargement (6,5 x, 16x, 25x) were gained during the analysis and changes of characteristics of the surface were evaluated.

Colorimetric evaluations were made using spectrophotometer *Konica Minolta CM-2600d* and system *CIE L*a*b**.

Orthogonal photos of drop applied on the surface were taken and the evaluation of the contact angle of the drop was made. Thanks to this analysis was possible to evaluate the change in hydrophobic behaviour of the surfaces after the application of the products.

3.3.3 Characterization of treated specimens

Sixteen specimens of each kind of stone and 11 specimens of concrete were characterized. All the treated specimens were analyzed during each steps of the research by the use of physical analysis and by microscopic observation of the substrates.

The same methodology used for the characterisation of stones made in the previews research was repeated for the characterisation of untreated concrete specimens and for the evaluation of the change in characteristics of all the treated specimens. Analytical methods were the same used in the previous research [1].

In order to achieve information about the textural characteristics of the samples, porosimetric analyses were applied on three fragments of each kind of material. The evaluations were made following NORMAL – 4/80 [71] using a *Thermo Scientific Pascal 140 series* and a *Thermo Scientific Pascal 240 series* porosimeters for meso and micro porosity. Data were evaluated using *SO. L. I. D Software for Pascal series Mercury Porosimeter*.

Change in weight and volume was evaluated and recorded before and after deterioration and consolidation processes.

Microscopic investigations were taken by the use of optical microscope *Leica F12I* (with enlargement 0,75x, 2x, 4x). The observation allowed to evaluate textural and morphological characteristic of the surfaces, detecting eventual modification trough the comparison of images taken at different moments.

As described in §3.3.2 colorimetric analysis were taken in order to evaluate chromatic variations of the substrates not visible to naked eye.

Sponge test was made in order to evaluate the change in the quantity of water absorbed by the surfaces following the procedure described in UNI 11432 [72].

Ultrasound velocity was measured following normal UNI EN 14579 [73] by the use of a *Matest* portable instrument.

3.3.4 Decaying processes

Decay processes were performed to simulate real condition of stone materials in real case studies. Three of four decay processes applied (Thermal Shock, Frost and Thaw, Salt Crystallization) were already described in Stucchi et al. 2019 [58]. The methodology used was applied respecting norms and recommendations in literature. In particular, thermal shock process was applied following the indication reported in Pozo-Antonio et al. [20], frost and thaw was made following UNI EN 1237/2003 [23], while salt crystallization decay procedure was applied respecting UNI EN 12370/1999 [22].

The subsequent evaluation of the resistance of the material to decay was made using the analytical techniques reported in §3.3.3.

For implementing the knowledge of the aggressiveness of Venetian environment, a new decay process was introduced in order to simulate lagoonal conditions.

Simulation of Lagoon condition

The procedure used for the degradation of samples simulating the condition of the lagoon was made following the same procedure used for degradation with salt crystallization but using water lagoon as saline.

Samples were subjected to wet dry cycles composed of 2 hours of time of immersion in water taken from the channel, followed by 20 hours of dry process in oven at 80°C in humid condition and 2 hours of cooling in air. The process was repeated 15 times.

Then, desalinization in distilled water was made. During desalinization water was changed repeatedly monitoring the conductivity every time. The process was considered finished when the parameter of conductivity was equal to that of pure water. In order to increase the fastness of the process, samples were periodically gently brushed in order to remove the salt crystallized on the surface.

3.3.5 Application of the consolidants

Three different consolidants were tested by application on one selected face of each specimens.

As reported in the technical sheet (present in the appendix of the book § 8), Evercrete Vetrofluid® must be applied via spray method. In order to respect the given procedure, a spray application method was developed and standardized for all the products and samples, with a total of two application two hours apart. The application was made through a low-pressure spray bottle with the nozzle directed to the center of the surface. The specimen was located on a stand, at a distance of 30 cm from the dispenser. In Figure 6 is possible to see the application conditions. The consolidant was sprayed for 5 seconds for each application. From the first to the second application, the orientation of the surface of the specimens was flipped to achieve the complete covering of the surface. The chosen distance between the spray bottle and the specimens, the height of the specimens and the height of the nozzle, the application time were defined after some tests. The adopted conditions allow to apply the consolidants without having an excess of product on the surface.

In the same way, SNP-PDMS was applied on both deteriorated and sound specimens.

For concrete specimens the first application was made in the same way as for other samples, whereas the second one was made moving the specimens along the horizontal axes every one second, thus the complete covering of the surface was achieved.

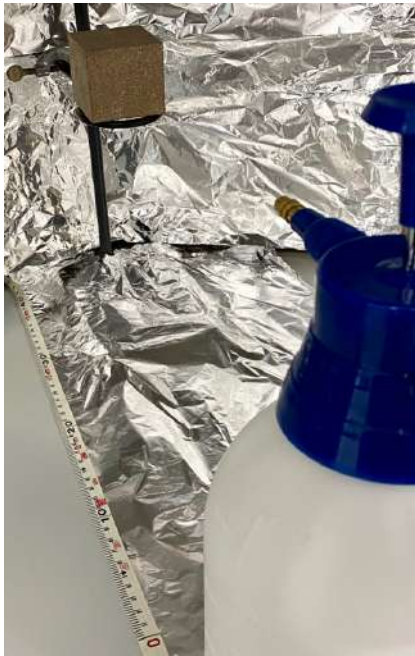


Figure 6. Application method used to apply the compounds.

4 Results

4.1 Results of the analysis of the particles and of the consolidant

4.1.1 Chemical characterization of functionalized SNP

SEM-EDX analyses of SNP revealed the effectiveness of functionalization reactions using $\text{Ca}(\text{NO}_3)_2$.

The comparison among S1a, S1b and S1c (see table §3.1.2 for the explanation of the labels used) evidence the differences of morphology of the particles caused by different reagents ratio. SEM images show the aggregation of the functionalized SNP due to the high temperature used in the process of calcination (680°C) (Figure 7). Figure 7b and 7c, related to S1B and S1C samples, show that the higher is the amount of calcium, the higher is the degree of fusion and aggregation of SNP. S1a, (Si:Ca equal to 70:30) sample with a low quantity of calcium, does not show the same degree of agglomeration and for this reason, was considered the best. For all the functionalised compounds a dimensional analysis of the particles was made. The resulting graphs of the size distribution function show a peak maximum at about 100 nm (Figure 8). This is the same values obtained for the bare SNP.

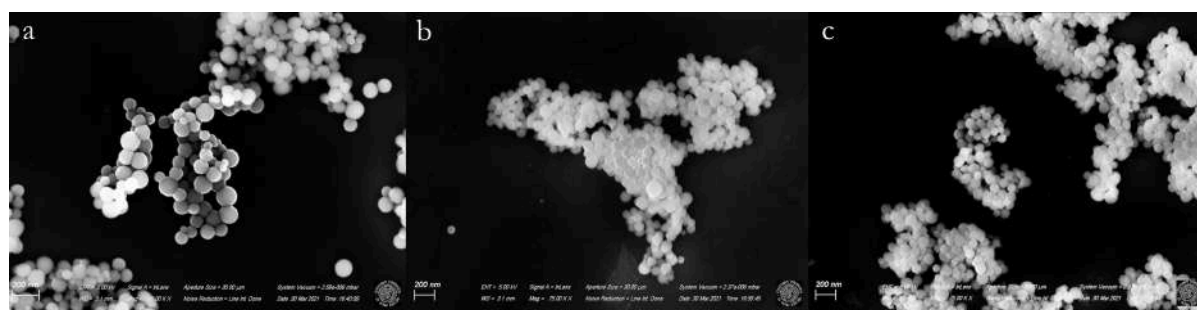


Figure 7. SEM analysis: a) S1a, b) S1b, c) S1c.

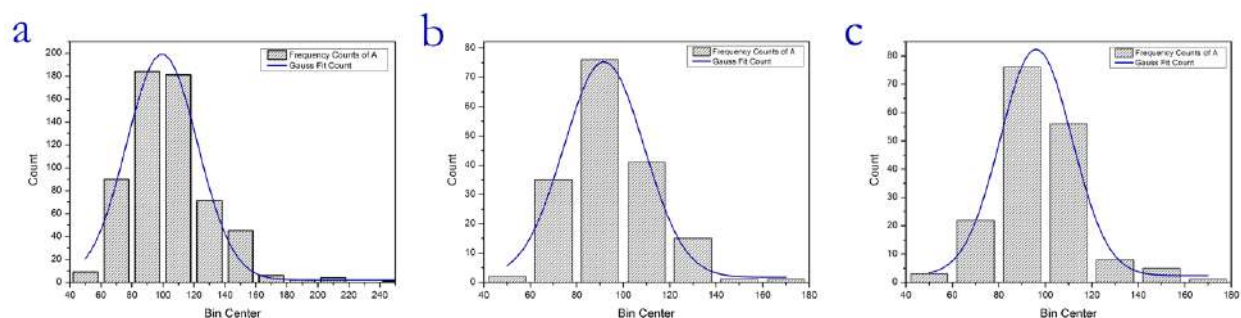


Figure 8. Results of the analysis of the sizes of the functionalized particles: a) S1a, b) S1b, c) S1c.

EDX elemental analysis revealed the presence of Ca suggesting the effectiveness of functionalization process (Figure 9). The map of elemental investigation is reported in Figure 9b. In the figure, the elements are distinguishable thanks to different colours: red for Silicon, green for Oxygen and blue for Calcium. An overlap of SEM image (Figure 9a) and EDX map, highlight the distribution of the elements in the particles (Figure 9c).

Quantitative analysis of the elements is reported in Table 3. The results show a correlation between the amount of Si and Ca determined after functionalization and their theoretical concentration before the functionalization.

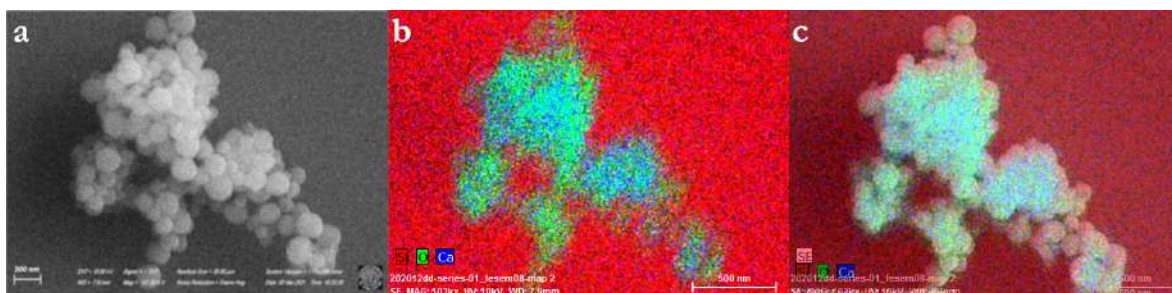


Figure 9. SEM-EDS analysis of S1A: a) SEM images of the particles, b) EDS analysis of the composition, c) overlap of previews images.

Table 3. Elemental analysis of SNP functionalized with $\text{Ca}(\text{NO}_3)_2$.

	S1A		S1B		S1C	
Element	Atom. C [at.%]	Error [wt.%]	Atom. C [at.%]	Error [wt.%]	Atom. C [at.%]	Error [wt.%]
Si	94,0	2,0	90,0,	2,2	86,0	2,0
Ca	6,0	0,2	10,5	0,3	14,0	0,4

In order to reduce the drawback of partial fusion of SNP, a lower calcination temperature during functionalization process was tested. As reported in literature [42], temperature of 680° is required to remove all the nitrates formed during the synthesis. However, we have verified that a decrease of the calcination temperature can be still effective: a decrement of the temperature at 500°C can be sufficient to remove nitrates and to obtain particles with a higher degree of separation.

For this reason, the synthesis was improved maintaining the proportion of Si:Ca 70:30 and reducing the temperature of calcination at 500°C (synthesis S1d). Moreover, aware of the water effect

on SNP particles [1], a new synthesis was followed dispersing SNP in a mixture 50:50 of EtOH:H₂O (synthesis S1e and S1f).

A last consideration was made in order to evaluate if a lower amount of calcium could vary the properties of the particles. S1f was synthesised with a concentration of 80:20 of SiO₂:Ca(NO₃)₂, using a calcination temperature of 500°C . No significant changes were found.

No particular changes were achieved by the analysis of S1d, differently as possible to see in Figure 10, particles S1e show an increasing dispersion of the particles if compared with S1a. Concentration of calcium in compound S1F is too low and particles don't show to be affected by the functionalisation. Finally, functionalisation relative to S1e sample can be considered the best.

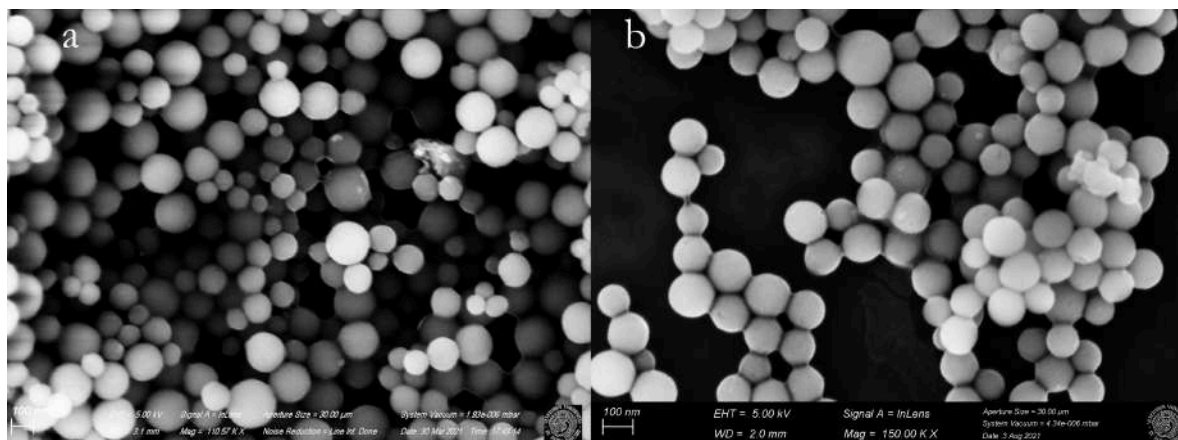


Figure 10. SEM analysis of functionalised particles: a)S1a, b)S1e.

4.1.2 Analysis of degree of dispersion

The use of dispersion analyser allowed to investigate the precipitation velocity of particles dispersed in a carrier. All the analyses were performed keeping constant the parameters and the ratio of concentration of pellet and solvent. Thanks to process of functionalization, particles were expected to be characterised by a grater dispersion in solvent, a reduced tendency to agglomeration and a high retention time in suspension. This, theoretically, from the analysis of functionalized particles, corresponds to a low sedimentation velocity.

The values, obtained by the analysis of the resulting graph of the profiles of precipitation, are reported, with the related standard deviation, in Table 4. Sample S1a has the lowest mean value of velocity ($31.47 \mu\text{m/s}$) if compared with all the other samples, but it has a value of standard deviation too large. Samples S1b and S1c show greater values of sedimentation velocity equal to $347 \mu\text{m/s}$ and $430.6 \mu\text{m/s}$ respectively.

Table 4. Evaluation of precipitation velocities of the compounds (expressed in $\mu\text{m/min}$).

Sample	Mean in $\mu\text{m/s} \pm \text{Std. Dev. in } \mu\text{m/s}$
SNP	90 ± 314
S1a	31 ± 243
S1b	347 ± 348
S1c	430 ± 440

Comparing the results of S1a with pure SNP, it is possible to observe the reduction of the precipitation velocity of functionalized particles. It is possible to assume that in case of S1a, the lower precipitation velocity is due to a higher degree of dispersion of the particles in the suspension, confirming the good effect of functionalization process in maintaining particles dispersed.

From the values obtained for S1b and S1c it is not possible to make the same consideration. Particles shows a high degree of agglomeration, which negatively affects the precipitation velocity. The formation of big aggregates was confirmed by SEM (§4.1.1). Since S1a, S1b, S1b differ in $\text{SiO}_2: \text{Ca}(\text{NO}_3)_2$ ratio, it is possible to relate the aggregation phenomenon with the amount of the reagents. It should also be remembered that calcination temperature and water promote the formation of aggregates influencing the degree of dispersion. On the basis of these results changing in functionalisation process were made.

4.1.3 FTIR analysis

FTIR analysis was performed to evaluate the composition of all the synthesised consolidants.

As reported in Figure 11 the spectra of all the compounds S1n and SNP show similar pattern. The presence of silanol groups were confirmed by a band at about 3435-3440 cm^{-1} related to ν Si-OH, due to the hydration of silica [74]. The presence of O-H bond is related to the band at 1635 cm^{-1} . All the spectra show characteristic peaks of Si bonds, with primary absorption band at 1100 cm^{-1} and the shoulder at 950 cm^{-1} due to ν Si-O-Si of the linear chain structure and the related bending vibration at about 790 cm^{-1} . The band at 950 cm^{-1} appears in pure SiO_2 and S1c spectra, in which the calcium content is null or minimal [75].

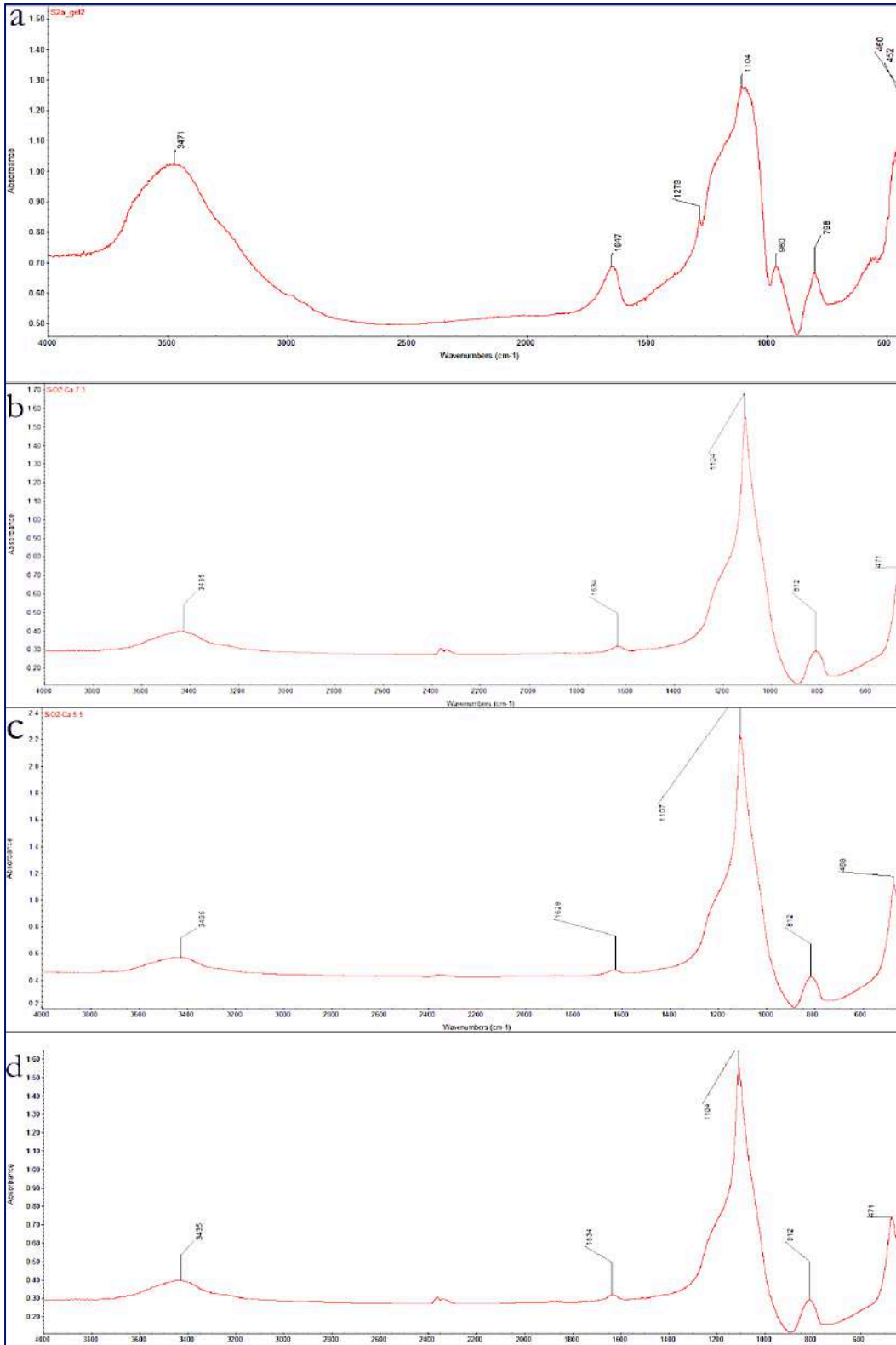


Figure 11. Spectra of SNP and of SNP functionalized with $\text{Ca}(\text{NO}_3)_2$: a) SNP; b) S1a; c) S1b; d) S1c.

The Analysis of SNP functionalized with PMHS were made both in liquid and gel phases (see Figure 12 and Figure 13). The spectra obtained in liquid phase shows several similarities. The peaks at 3435 cm^{-1} and at about 1635 cm^{-1} corresponds to the vibrational motions of O-H bond in silanol groups and water, the last used in part as carrier of the treatment solution. Symmetrical stretching of C-H chemical bonds corresponds to the signal in the range $2880\text{-}2975\text{ cm}^{-1}$ related to ethanol [76], used as career and PMHS polymer [77]. Regarding asymmetrical and symmetrical bending of C-H, these correspond to the peaks in the range $1450\text{-}1330\text{ cm}^{-1}$. The presence of polymer in the chemical structure of the product is confirmed by the peak at about 1273 cm^{-1} , which is characteristic of the symmetrical stretching of Si-CH₃ bond. The doublet at 1086 cm^{-1} and 1044 cm^{-1} are related to Si-O-Si stretching bond in a cycle structure. Presence of silica groups was revealed also by the characteristic vibration of Si-O-Si at $879\text{-}803\text{ cm}^{-1}$ [76].

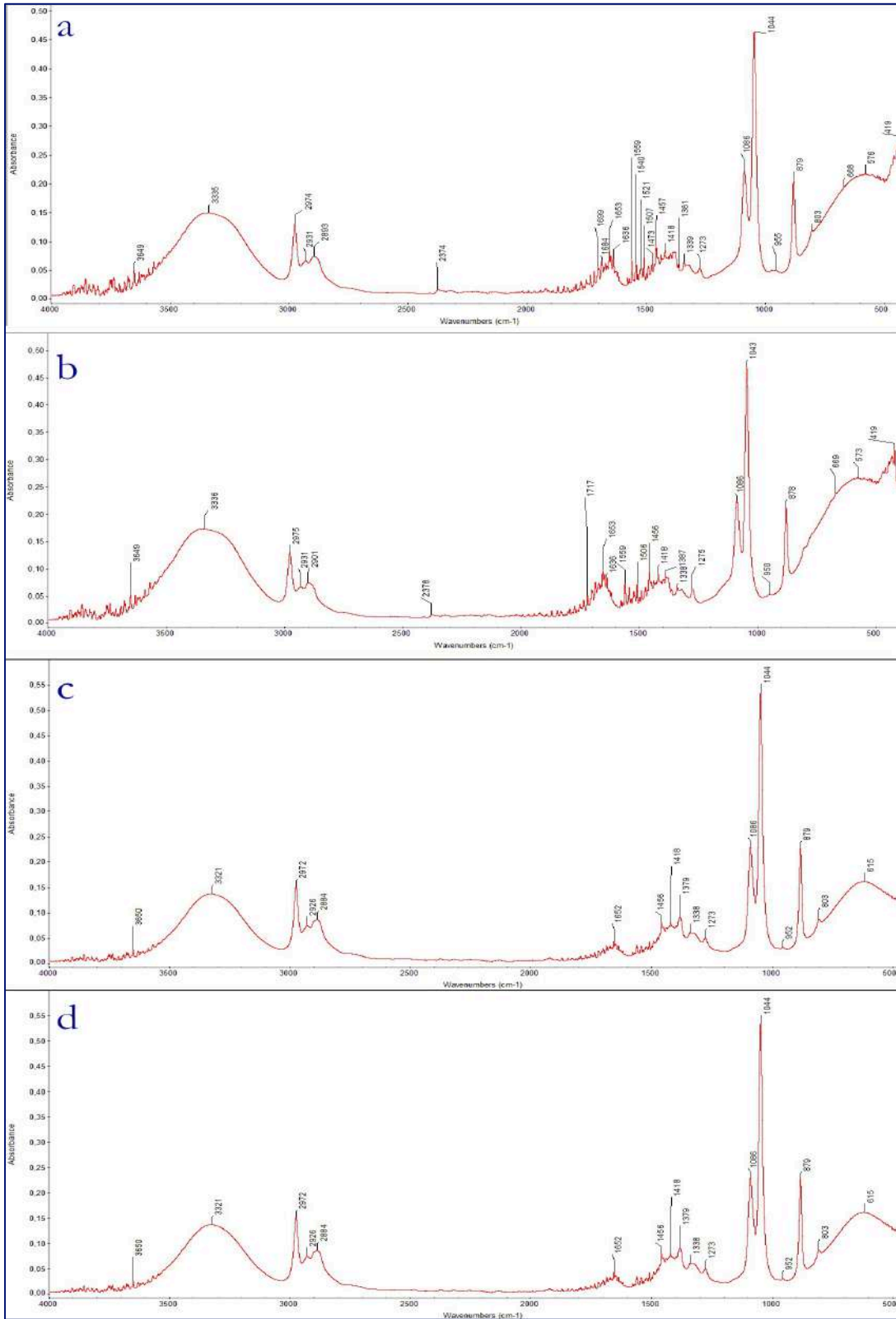


Figure 12. Spectra of SNP functionalized with PMHS (sol phase): a) S2a; b) S2b; c) S2c; d) S2d.

The analyses of gel phases show (Figure 13) some differences among the spectra. All the compounds report a certain number of O-H groups (3450 cm^{-1} and 1640 cm^{-1}), index of non-complete condensation reaction or water evaporation. Peaks related to C-H chemical bond in the range $2880\text{-}2975\text{ cm}^{-1}$ are really weak [77] whereas the peak at $\sim 780\text{ cm}^{-1}$ represents δ_s Si-O-Si in the siloxane chain. The peak at 1280 cm^{-1} is characteristic of $\nu\text{Si-CH}_3$. The wide peaks at $\sim 1050/1080$ and $\sim 790\text{ cm}^{-1}$ corresponds to the Si-O-Si symmetrical stretching and bending confirming the polymerization reaction [78].

The bumps at 1420 cm^{-1} are related to C-H bond of the polymer. Even though, S2c and S2d were synthesised in a completely different way, S2c by a one pot synthesis while S2d by a dissolution of polymeric compound in ethanol, they show a similar pattern.

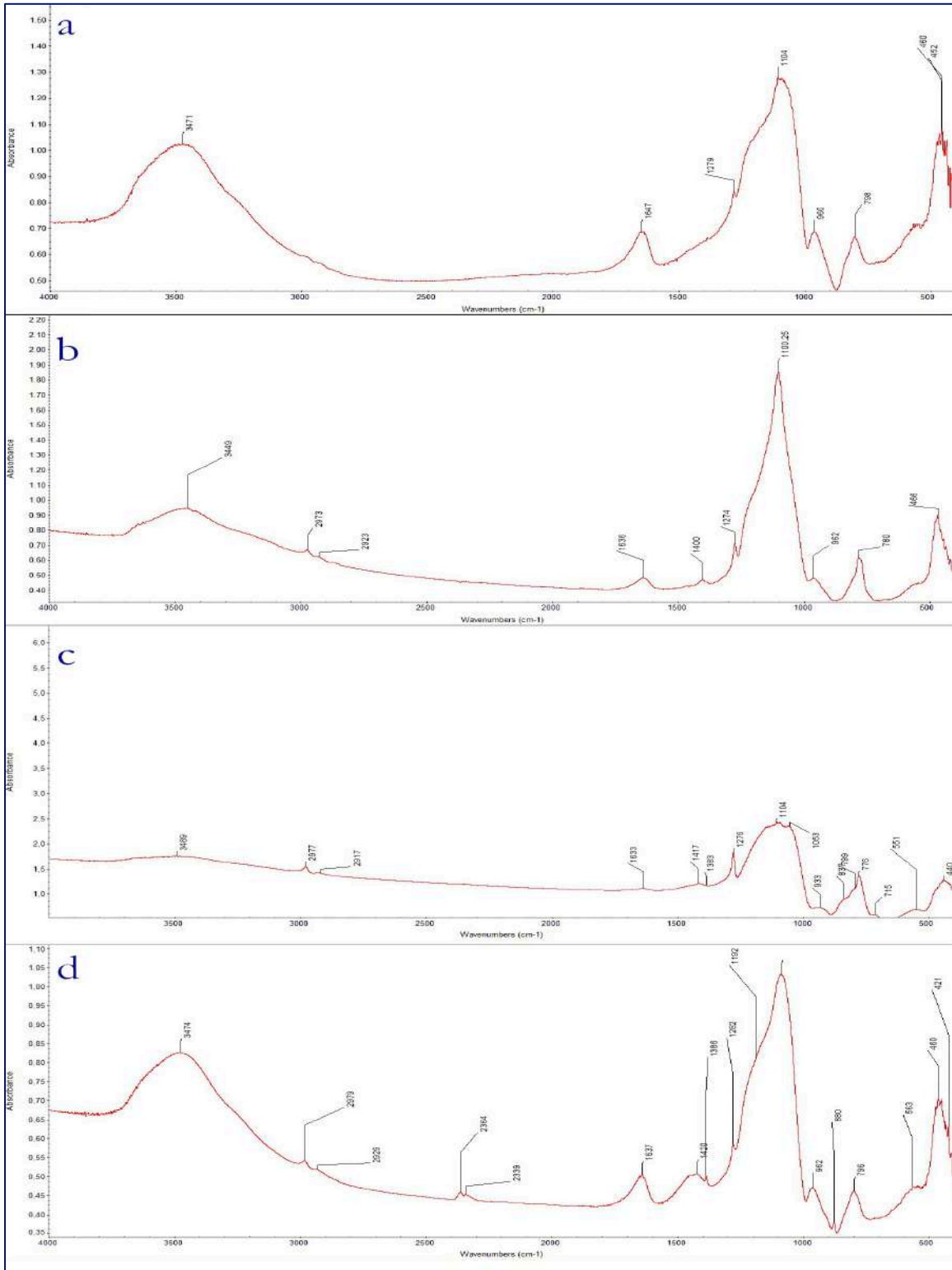


Figure 13. Spectra of SNP functionalized with PMHS (gel phase): a) S2a; b) S2b; c) S2c; d) S2d.

S2e and S2b1 spectra show similar FTIR signals (Figure 14). This result is due to the similar chemical composition of the polymers used in the functionalization. Peaks at about 2973 cm^{-1} and 2928 cm^{-1} are due to stretching vibrations of C–H [77]. In the same range can be found also peaks that correspond to the ethyl group due to TEOS hydrolyzation [76]. The absorption bands at 1450 cm^{-1} and 1261 cm^{-1} are associated with the asymmetric and symmetric deformation of CH_3 , respectively [79]. Peaks at 1272 cm^{-1} is attributed to the $-\text{CH}_3$ bending [78]. Si–O–Si bonds are related to absorption present at 1043 cm^{-1} and 800 cm^{-1} . The two spectra present only a difference related to the band at 952 cm^{-1} in S2e, this peak belong to Si–OH [80] or to the terminal group of the polymer PDMS-OH. Also absorption at 878 cm^{-1} are evidence of the presence of Si–OH hydrogen bond and are meaning that the hydrolysis process of TEOS had taken place [76] The Hump at 785 cm^{-1} is related to Si–C stretching [78]. Wide band after 800 cm^{-1} corresponds to the absorption due to the vibrations of OH. Smaller peaks at about 420 cm^{-1} are related to the presence of Si element.

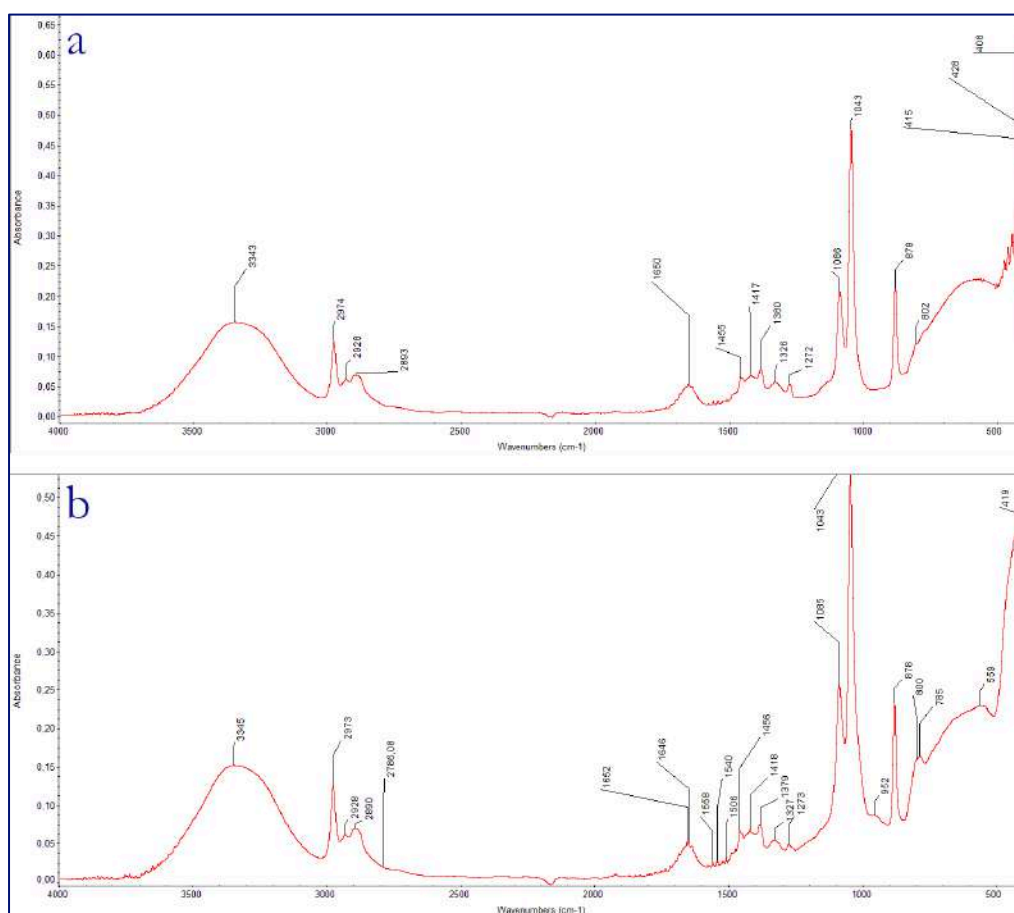


Figure 14. Spectra of S2b1 (a) and S2e (b) synthesis.

4.1.4 Analysis of the structure of S2e by NMR

The NMR analysis in liquid phase was performed in order to investigate the colloidal solution of S2e sample. PMHS presents a termination made by trimethylsilyl groups (-SiMe₃) and for this reason it cannot give the formation of covalent bond with the SiO₂ surface via basic catalysed condensation reaction. Differently, PDMS-OH, thanks to its hydroxide terminations is able to covalently link the SiO₂ surface by the formation of covalent Si-O-Si bridges. The structure of the polymer in its pristine and bounded forms is shown in Figure 15. The green letters near the protons are used to facilitate the reading of the spectra.

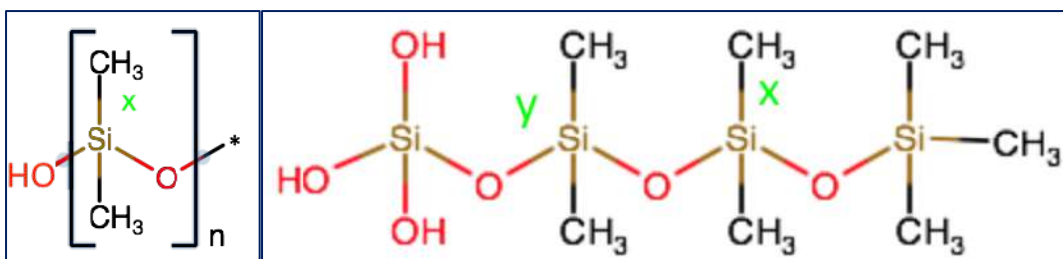


Figure 15. Structure of the compounds analyzed (from left to right) S2e and PDMS-OH.

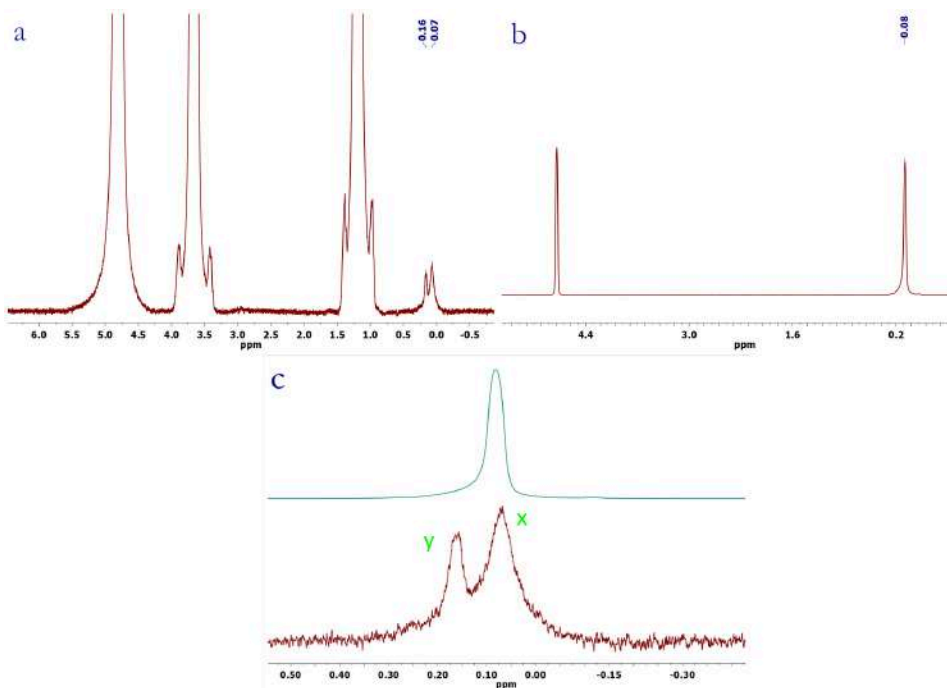


Figure 16. NMR spectra of: a) S2e; b) PDMS.OH; c) comparison of the main peaks blue line PDMS-OH, red line S2e.

The spectra resulting from NMR analysis of S2e are reported in Figure 16a. The peak that falls at 4,79 ppm is ascribed to the isotopic residual of deuterate water (D_2O) used as main solvent for the analysis [81]. The peak at 3.66 ppm and 1.19 ppm are related to presence of ethanol and can be ascribed to $-CH_2-$ and $-CH_3$ respectively by the analysis of the integrals 2H and 3H and fine structure as well. As expected, the $-OH$ proton of ethanol is not visible due to its rapid exchange with the water protons. The peak at 0.16 and 0.08 ppm can be ascribed to the methylic ($-CH_3$) protons of the polymer.

The analysis of the pristine polymer was performed to allow a direct comparison with the spectra of the functionalised particle (Figure 16b). This analysis shows only one peak at 0.08 ppm that can be related to the methylic protons.

A magnified image of the characteristic peaks of PDMS-OH and the sample S2e is reported in Figure 16c. The peak at 0,08 ppm, that can be attributed to methylic protons of the polymer, is observed in both the spectra and it can be related to methylic protons that are mainly surrounded by solvent, moreover, a new peak appears in the S2e spectra around 0.16 ppm that can be related to the effect of the proximity of the particle surface that affect the local magnetic field of the methylic protons in a potentially bonded condition. The observation of a distinct signal at 0.16 ppm in S2e supports the presence of some interactions between the particles surface and the polymer, however, more detailed analyses via solid state ^{29}Si -NMR are needed in order to collect direct evidence on a covalent interaction between PDMS-OH and the SiO_2 surface.


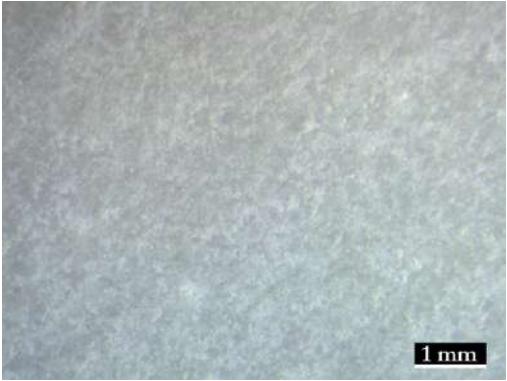
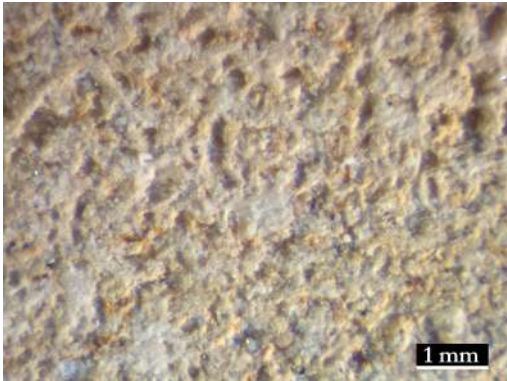
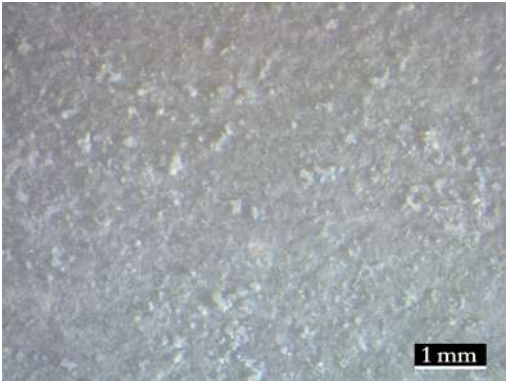
4.2 Results of preliminary tests of application

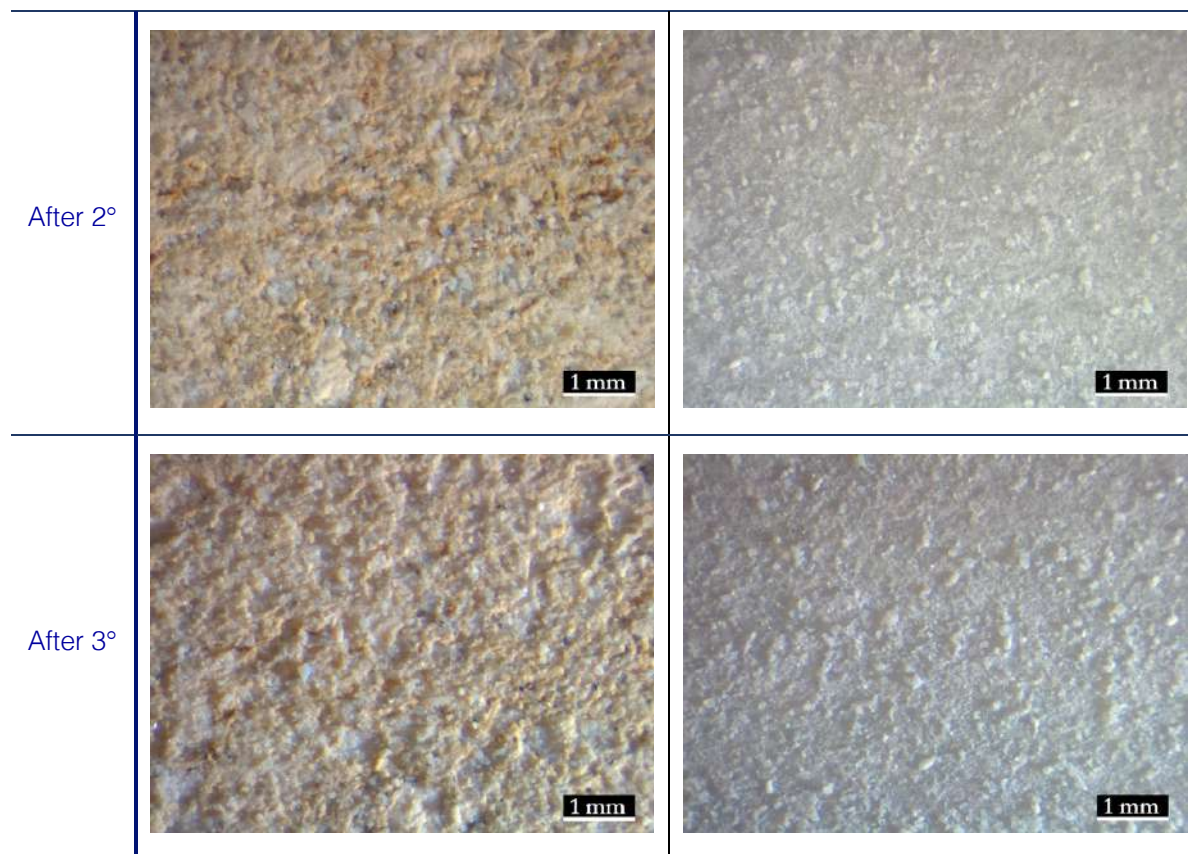
4.2.1 Application of SNP functionalised with $\text{Ca}(\text{NO}_3)_2$

Consolidant S1e, composed of SNP functionalised with calcium nitrate applied to Carrara marble (C9), show an increment of the sample weight during the treatment process, the application was repeated three times. This effect did not occur on Vicenza limestone (V9), which no longer showed any weight variation after the third application, probably due to the complete saturation of the superficial pores that did not allow the absorption of additional amount of compound.

In Table 5 are reported the images acquired from the microscopic investigation of the treated surfaces, before and after the 3 applications of the treatment. After the first application, the stone substrates showed the presence of a white opalescent patina consisting of small grains, which caused bleaching effect altering the typical aspect of the substrates.

Table 5. Microscopic investigation of the substrates before and after the treatment, Vicenza limestone (V9) and Carrara marble (C9).

	V9	C9
Before		
After 1°		



The whitening effect induced by the treatment was confirmed by colorimetric analysis. Table 6 reports L^* values (brightness), which shows the gradual increase of the whiteness of the surfaces. No significant variation was recorded for parameter a^* (value referred to green-red tones) on both the specimens, whereas a decrement of parameter b^* (value referred to yellow-blue tones), slight on Carrara marble and marked on Vicenza stone, showed a certain yellowing of the treated surfaces.

Table 6. Values of L^* measured before the treatment, after the 1° and the 3° application, on the samples C9 and V9

Sample	L^*	Sample	L^*
C9_before	77,19	V9_before	79,43
C9_after1°	77,6	V9_after1°	80,42
C9_after3°	77,89	V9_after3°	82,37

Contact angle test resulted completely useless since the treatment applied gradually promoted the spread of the drop increasing the number of applications.

From the results, S1e cannot be considered a good consolidant. As main drawbacks, the tendency of aggregation of SNP prevent the penetration of the compound in the porous network, although theoretically the functionalisation must decrease this phenomenon.

4.2.2 Application of SNP functionalised with polymeric compound

Due to the xerogel nature, S2a was applied by a palette knife. During drying gel created a cracked white layer visible also to naked eye (as visible in Figure 17). Due to these results, no further analyses were made on S2a compound and it was immediately discarded.

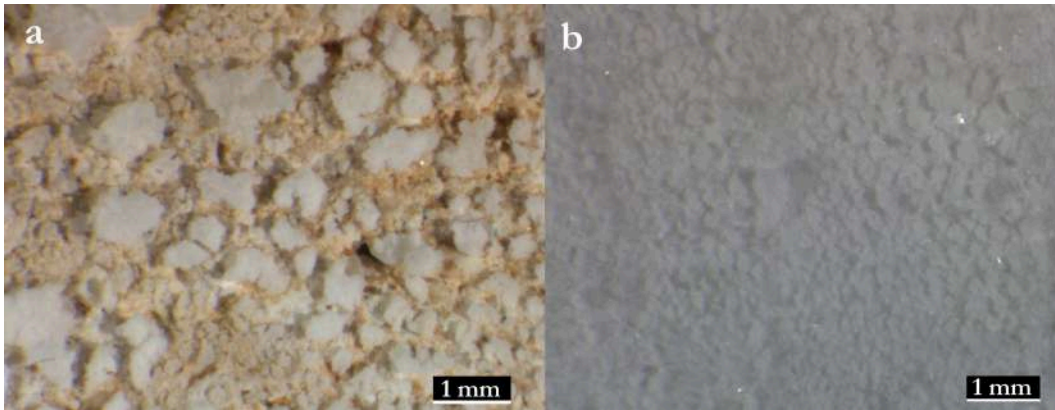


Figure 17. Microscopic images of specimens after the treatment of S2A compound: a) Vicenza, b) Carrara.

To avoid gel composition, S2b was synthesised excluding further TEOS addition to SNP. The differences between the two compounds (S2a and S2b) let to state that the gel nature is linked to the further addition of TEOS to SNP, that probably increased the condensation reaction. Table 7 reports some micrographs of Vicenza white limestone and Carrara marble surfaces treated both with S2b and S2c. Surfaces treated with S2b show a homogenous white patina, which completely filled the superficial porosity of Vicenza white limestone and an opaque effect on Carrara marble, due to the covering of the calcite minerals by a superficial patina, both visible also at naked eye.

After the treatment application, the colorimetric parameters L^* value decreased for both the materials, demonstrating a decrement of the brightness and a dulling of the surfaces. Evaluation of ΔE express a great change in colour, perceptible also ate naked eye, on both Vicenza limestone, with a value equal to 9, and Carrara limestone, equal to 8. Table reports the results of the tests of

hydrophobic behaviour of the treated surface. Vicenza specimens treated with S2b shows an increment of hydrophobicity after the first application, from 0° to 50° . The surface became heavily hydrophobic after the third application with an angle of 97° .

The application of S2c1 on the surface of both stone materials it's visible to microscopic observation and confirmed by weight variations. As observable in Table 7, only a slight white opacity is induced by the application of the compound on marble, whereas on the limestone is possible to see a stronger opaque layer on all the surfaces. Contact angle test on Vicenza limestone treated with S2c1 showed a strong increase after the first application (80°) remaining stable during the following applications.

The stone surfaces absorbed quickly the S2d compound. The absence of change in the weight values of the specimens after the treatment, demonstrates that the compound applied is mainly composed by EtOH that saturated the porosity and evaporated quickly after the application. The minimal presence of compound on the material induced neither colour changes nor differences in hydrophobicity on Vicenza limestone (Table 8). On Carrara marble specimen the treatment induced a decrement of the contact angle. This behaviour was similar to that of SNP- $\text{Ca}(\text{NO}_3)_2$ applied on marble and reported in §4.2.1. Most likely, an excess of compound on the surface brings water to react with SNP directly on stone surface. The absence of any variation in the investigated parameters are probably due to the low concentration of S2d functionalized compound in the carrier solution.

Table 7. Microscopic images of the materials before and after the treatments with S2b and S2c1 compounds.

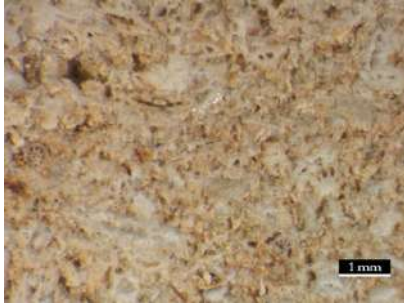
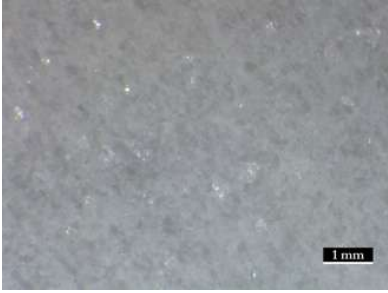
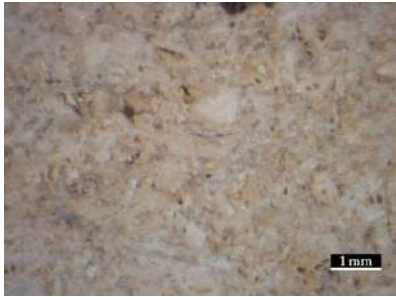

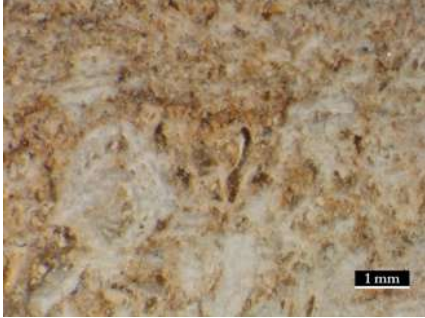
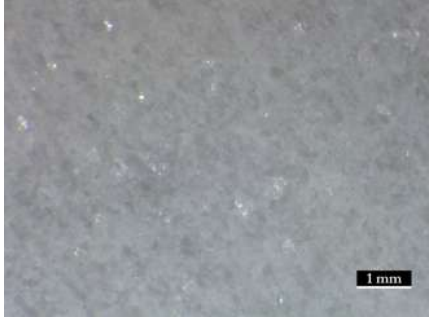
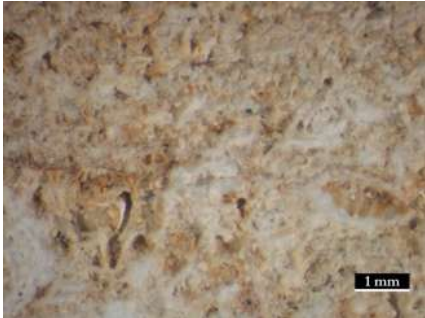

	Vicenza, S2b	Carrara, S2b
Before		
After		
	Vicenza, S2c1	Carrara, S2c1
Before		
After		

Table 8. Measurements of the contact angle before the treatment, after the 1° and the 3° application of S2b, S2c1, S2d on Vicenza limestone and Carrara marble.

	Vicenza, S2b	Vicenza, S2c1	Vicenza, S2d
Before	0°	0°	0°
After 1°	50°	80°	0°
After 3°	97°	78°	0°
	Carrara, S2b	Carrara, S2c1	Carrara, S2d
Before	67°	64°	48°
After 1°	90°	114°	21°
After 3°	128°	124°	13°

Comparing S2b and S2c1, the first alters more the macro morphologies of the lithotypes than the second one (Table 7). On the contrary, S2c1 shows a stronger increment of the contact angle value than S2b. S2b effects may be related to a high concentration of the compound; this can be reduced decreasing the number of application or diluting SNP-PMHS solution. From these results, S2b was chosen as the best compound synthesised among the four consolidants analysed, however some improvements have been made and a second test of application was done.

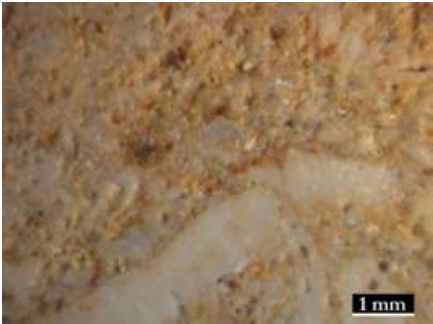



S2b was dispersed in a solution of EtOH:H₂O 50:50 with a concentration of 10% and 20% in weight (compounds were called respectively S2b10% and S2b20%). Moreover, a second compound named S2e was synthesised using the same concentration of S2b solution (10% and 20%) but using PDMS-OH instead of PMHS. As for S2b, S2e10% and S2e20% they were applied on both Carrara marble and Vicenza white limestone specimens.

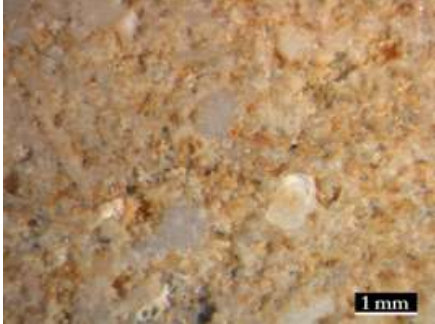



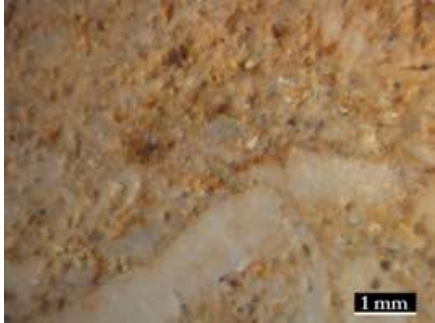



Absorption of treatments was confirmed by the continuous increment of weight values for all the samples.

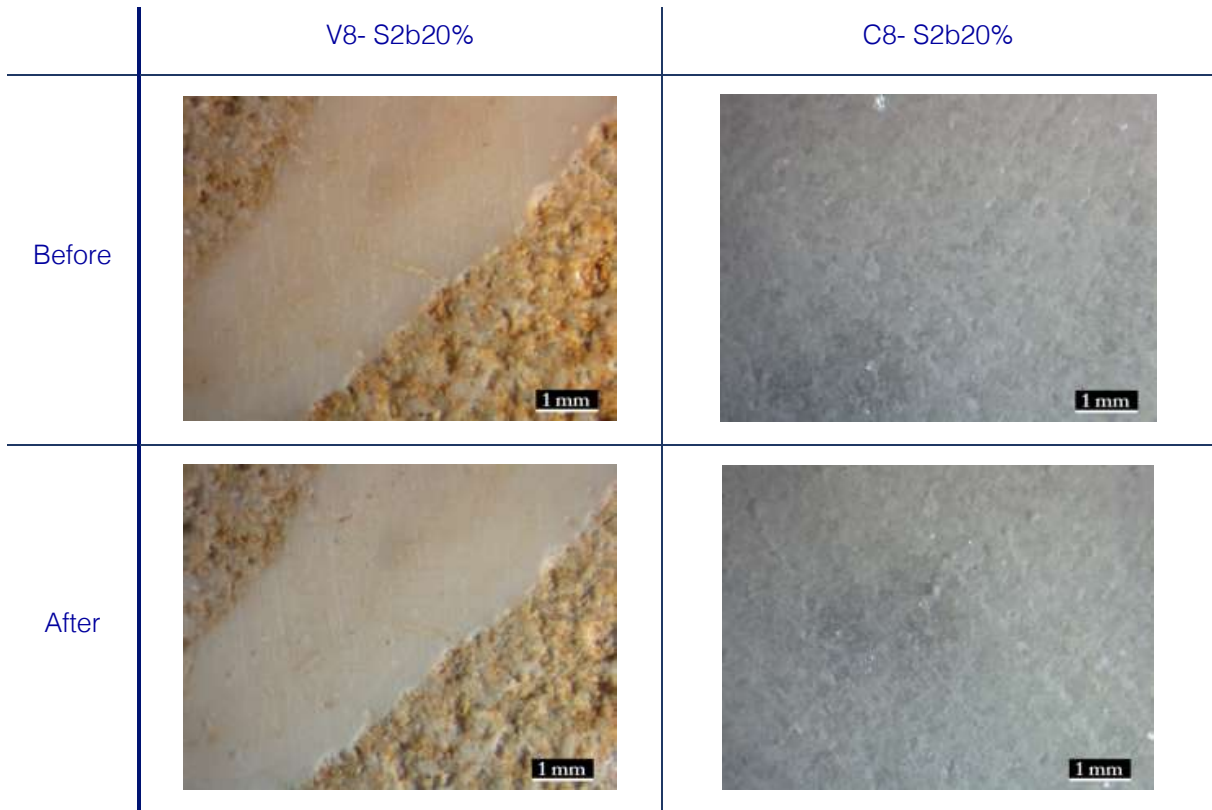
Table 9 shows the comparisons among micrographs before and after the application of the treatments for all the considered specimens. Comparing all the specimens treated with S2e and S2b with different concentration it is possible to conclude that the first typology of treatment show less impact from an aesthetic point of view. Veers of colour of the surface is reduced and no presence of compound in excess on the surface is recorded. On the other hand, S2B treatments confirmed the presence of grains of material on the surface.

Colorimetric analysis ascertained the colour change of Vicenza specimens treated with all the compounds, particularly for the decrement of b^* (value referred to yellow-blue variation), that veers to blue tonality with the application of S2e20%. Carrara specimens treated with all the compounds show more or less stable values of a^* and b^* but great variance in the value of L^* , less marked with the application of S2e10%.

Table 9. Microscopic observations of the surfaces treated with different concentration of S2b and S2e.

	V5- S2e10%	C5- S2e10%
Before		
After		

	V6- S2e20%	C6- S2e20%
Before		
After		
	V5- S2e10%	C5- S2e10%
Before		
After		



The results of the contact angle test are reported in Table 10. S2e showed an increment of the angle considering all the different concentrations. S2b showed a marked increment. Clearly the great increment induced by S2b is too large, indeed a good consolidant must increase the hydrophobicity of the surface without inducing the complete closing of the pores of the material.

Table 10. Results of the measurement of the contact angle for all the specimens before and after the treatment.

	V5- S2e10%	C5- S2e10%	V6- S2e20%	C6- S2e20%
Before	0°	10°	2°	12°
After	39°	49°	36°	50°
	V7- S2b10%	C7- S2b10%	V8- S2b20%	C8- S2b20%
Before	0°	22°	0°	23°
After	102°	135°	84°	150°

The system functionalized with Polydimethylsiloxane hydroxy terminated (PDMS-OH) called S2e gave the best results. Similar results were obtained using solutions with concentration 10% and 20% respectively, however the less aesthetic variation obtained with S2e10% bring to choose this treatment solution as one applied for the porpoise of the research.

4.3 Characterisation of the substrates

4.3.1 Characteristic of the texture and surface of the samples

Concerning the Porosimetric analysis of the stones the results of the previous research [1] were taken as reference. *Pietra di Firenzuola* is characterized by the highest medium values of open porosity (6.02%) and so it is the most porous stone of the three investigated. The dimensions of its pores (15 nm e 200 nm) are similar to the *Bianco Sardo* 15 nm e 300 nm. The granite results to be the least porous structure. *Pietra di Muggia* is characterized by pores with the smallest dimensions 8 - 70 nm but its porosity depends on the zone that characterized the material due to the heterogeneity of the material.

In order to have a better knowledge of the porous matrix of the typology of concrete, porosimetric evaluation were made on three sample of Portland and Vicat concrete. The results are the average of the three measurements. Portland concrete is characterized by an accessible porosity of 13,66% and a total pore volume of 62,63 mm³/g. The average of the pore radius is equal to 33,8 nm. Vicat concrete is characterised by an accessible porosity of 22,47%, the total pore volume is equal to 112,28 mm³/g and an average pore radius equal to 37,2 nm. Comparing the two materials, Portland is less porous than Vicat concrete, its total pore volume is lower of a half and it is characterized also by smaller pore radius.

4.3.2 Variation of the morphological aspect of specimens induced by the degradation

The same methodology of investigation previously used was repeated to evaluate physical- aesthetic changes in stone and concrete specimens induced by decay. The selected degradation process was the same of those applied in Stucchi et al. 2019 [1; 58], adding water lagoon as innovative degradation process for this research. In the following paragraphs the results collected will be presented.

In this research, water lagoon process of degradation was applied for the first time to stone specimens, while concretes were subjected to all the cited decay processes. In the following paragraphs the collected results will be presented.

Stones

Consideration about the reaction of sandstones and granite to thermal shock, salt crystallisation and frost and thaw are reported in the previews research. *Pietra di Firenzuola* resulted to be much more affected by salt crystallisation that caused the complete detachments of the faces of the specimens. *Bianco Sardo* resisted well to all the process of degradation. *Pietra di Muggia* showed pronounced changes of colour induced by degradation with thermal shock and salt crystallisation.

The effect of water lagoon on stone samples was not relevant.

Ultrasound analysis did not show significant variation after degradation process (Table 11). All the samples showed an increment in the values, more or less marked. Increment of values of anisotropy indicates an increment of voids inside the materials. In some cases, the increment is really low that values can be considered unchanged, as for example in PM16. The value of anisotropy of BS18 suffered the greatest rise, but this change was not equal to the other sample of the same material (BS16), which value was practically unchanged. *Pietra di Firenzuola* and *Pietra di Muggia* showed a similar increment of the values.

Table 11. Values of anisotropy before and after the treatment process of deterioration of sandstones *Pietra di Firenzuola* e *Pietra di Muggia* and a granite *Bianco Sardo*.

Sample	Before	After
PF16	7,11	8,83
PF18	6,43	8,28
PM16	5,38	5,39
PM18	4,63	5,69
BS16	5,58	5,44
BS18	2	7,33

All the specimens increased their values of water absorption.

Colorimetric change ΔE was for all the specimens lower than 5, so undetectable to the naked eye. In particular, *Bianco Sardo* showed the greatest variation with ΔE values in the range between 3,5 and 4. In contrast, *Pietra di Muggia* showed the lowest change with values equal to 2,07 and 1,47

respectively for PM16 and PM18. *Pietra di Firenzuola* values were equal to 2,49 for PF16 and 3,49 for PF18.

The inhomogeneity of results achieved by these simulations stress the difficulties to assess the effects induced by weathering and to set parameters and conditions useful for the conservation of stone materials.

Concrete

Thermal Shock

No evident morphological or colour changes of the surfaces were detected. Nevertheless, from a microscopic point of view some changes induced by the process of degradation were visible. Portland concrete specimens CSTP3 and CSTP4 showed an increment in the number of holes on the surface (Figure 18). In CSTV4 a fracture on the surface appeared after the decay process (Figure 19).

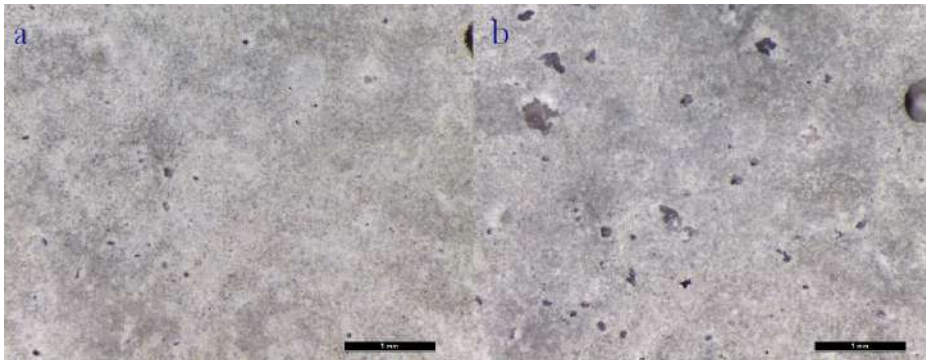


Figure 18. Microscopic observation of the surface of specimen CSTP4 before (a) and after (b) the degradation process.

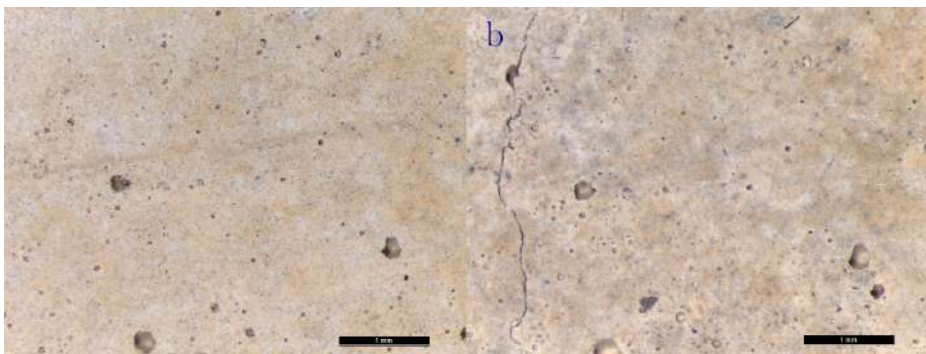


Figure 19. Microscopic observation of the surface of specimen CSTV4 before (a) and after (b) the degradation process.

Differently from what expected, values of ultrasonic analysis of CSTP3 showed a decrement of anisotropy and an increment of ultrasound velocity. These results are typically index of a decrement of voids. CSTP4 showed a decrement of anisotropy to parity of a stable value of velocity. Analysis of Vicat Concrete showed that the process induced a strong decay of the samples. CSTV3 result to be so deteriorated that was impossible to perform any measurement. CSTV4 was characterised by a decrement of ultrasound velocity that mean an increment of voids and empty spaces into the sample.

Evaluations of Water Absorption (WA) made via sponge test, before and after the decay, gave different results for the two types of concretes. The process of degradation strongly affected the water absorption capacity of Vicat specimens, which showed the greatest increment of WA value. On the other hand, Portland concrete showed a tendency to reduce the quantity of water absorbed by the degraded surfaces.

Evaluation of colorimetric change (ΔE) of the samples underlined the low change in colour induced by the thermal process on Vicat concrete ($\Delta E \sim 3$). On the contrary, Portland concrete was characterised for both the specimens by a change of colour equal to 7,29 and 7,9 respectively for CSTP3 and CSTP4. Values of ΔE greater than 5 underlines that the change of colour was visible also to the naked eye. Figure 19 reports the image of the surface of specimens CSTP4. As one can see, the change of colour was visible and the sample became darker, effect confirmed by the decrement of the value of L^* .

This kind of degradation affects more Portland than Vicat concrete in terms of ultrasonic and colorimetric evaluation. Vicat concrete was affected only for the change in capacity to absorb water.

Salt Crystallization

In Figure 20 are reported images of one of the specimens of Vicat concrete (CSTV5). This specimen was visibly more affected by salt crystallization than others (Figure 21 and Figure 22). As possible to see a big number of holes appeared on the surface and the hedges of the specimens resulted rounded.

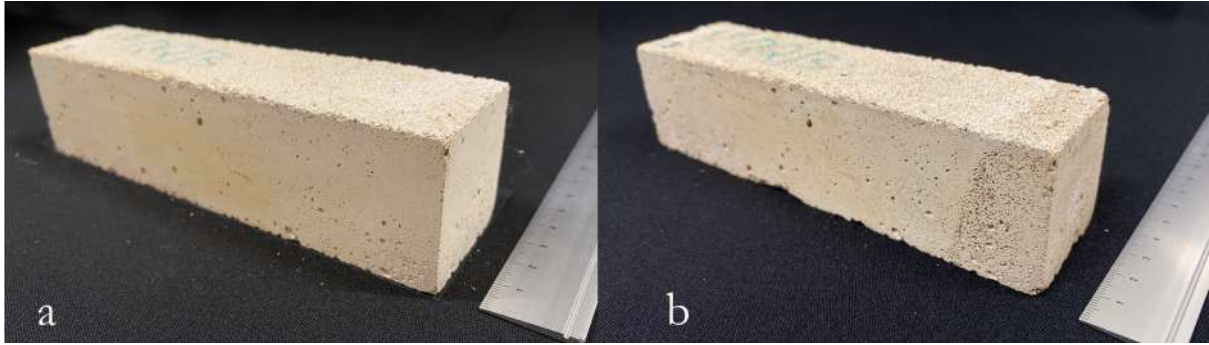


Figure 20. Change of the aspect of sample CSTV5 induced by salt crystallisation degradation.

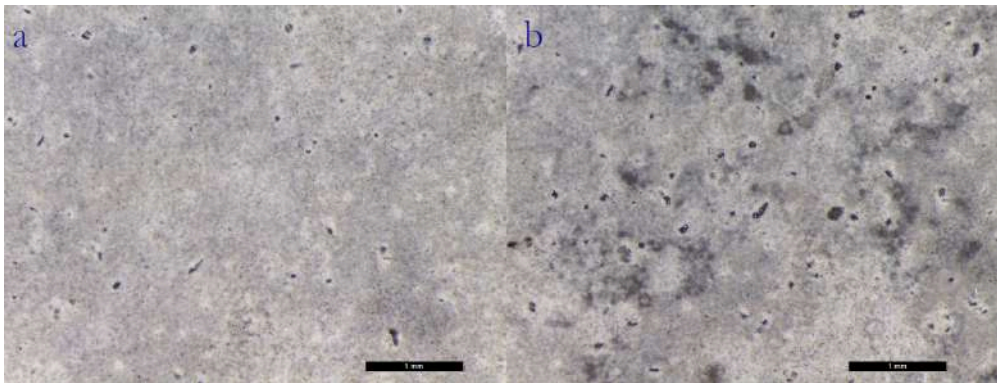


Figure 21. Microscopic observation of the surface of specimen CSTP5 before (a) and after (b) salt crystallization.

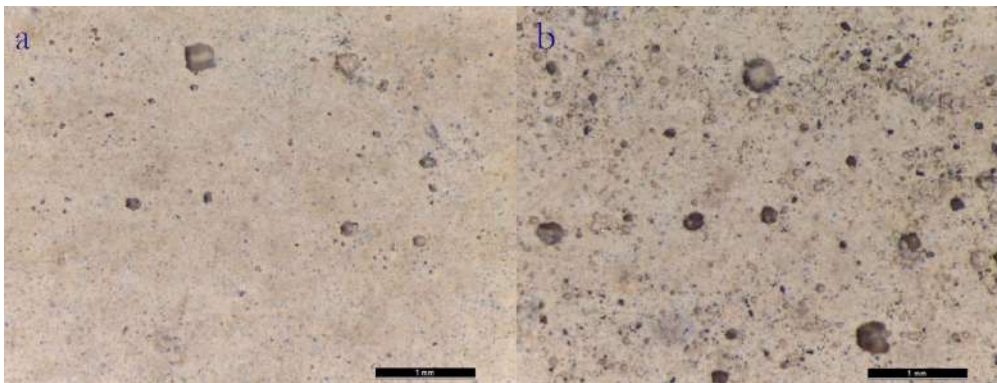


Figure 22. Microscopic observation of the surface of specimen CSTV6 before (a) and after (b) salt crystallization.

Measurement of ultrasound velocity showed a high decrement of anisotropy values, particularly for CSTP6 (from 70,86 to 2,18), while sample CSTP5 showed unchanged value. Values of anisotropy related to Vicat concrete decreased. Decrement of anisotropy mean a decrement of quantity of voids inside the structure. But looking to values of ultrasound velocity the reduction of the values indicates an increment of voids. Because of the achieved results, thanks to the low variation of ΔM of CSTP5 and CSTV5 the increment of voids can be assessed only for these two specimens.

The decrement of voids indicated by the results achieved for sample CSTV6 and CSTP6 can be related to the presence of salts inside the pores.

Sal crystallization process determined a reduction of water absorption for Portland concrete, whereas Vicat samples increased the WA values.

Colorimetric analyses of the surface showed an acceptable change of colour for all the Portland specimens (ΔE values equal to 3,63 for CSTP5 and 2,72 for CSTP6). Also sample CSTV5 showed an acceptable value of the change of colour with ΔE equal to 3,49. Differently, sample CSTV6 is characterised by a value equal to 5,23, which means that the change of colour was visible to naked eye (Figure 26).

Frost and thaw

Portland specimens showed a different aesthetical behaviour after frost and thaw cycles. CSTP7 and CSTV7 seemed unaltered after degradation. CSTP8 (Figure 23) showed the formation of superficial holes and disaggregation among the edges CSTV8 (Figure 24) showed rounded edges but no significant macroscopic variation was visible on the surface. The increment of superficial porosity was detected by microscopic investigation (Figure 25) on sample CSTV7.

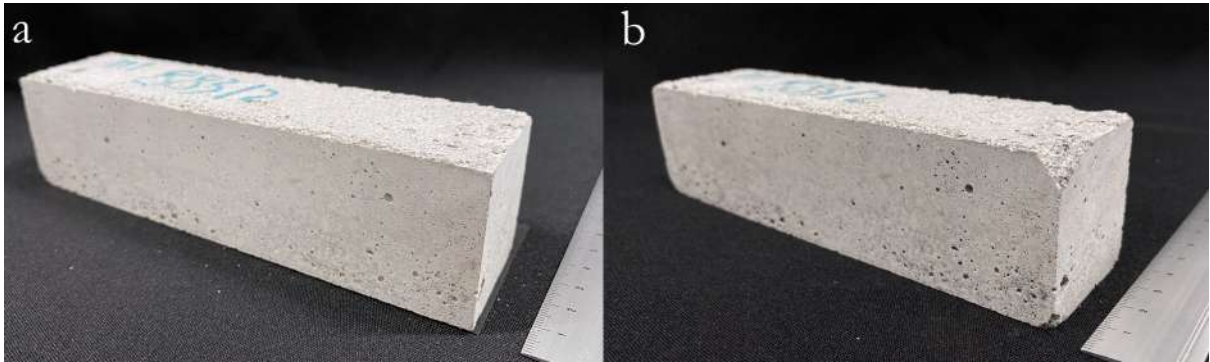


Figure 23. Change of the aspect of sample CSTP8 induced by frost and thaw degradation.

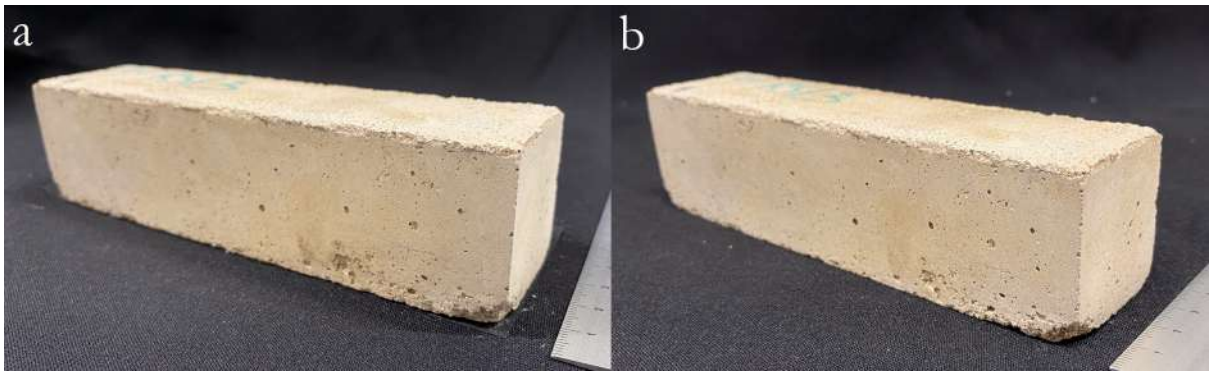


Figure 24. Change of the aspect of sample CSTV8 induced by frost and thaw degradation.

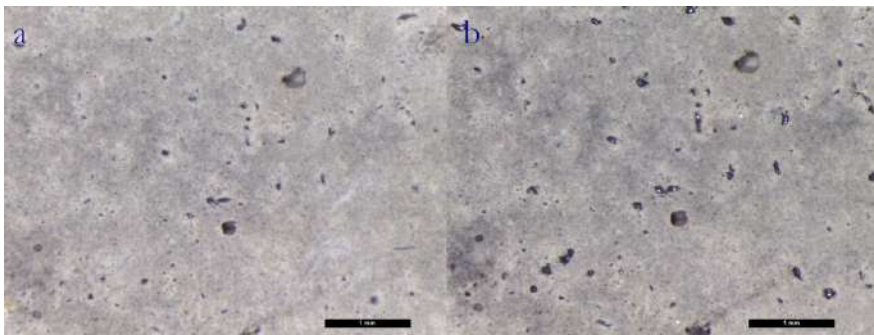


Figure 25. Microscopic observation of the surface of specimen CSTP8 before (a) and after (b) the degradation process.

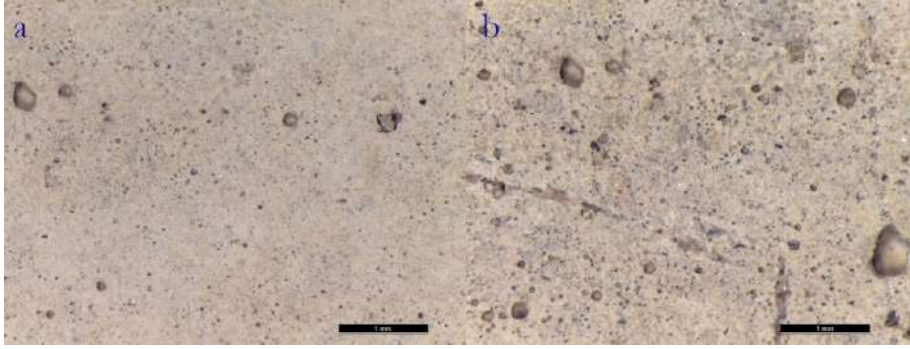


Figure 26. Microscopic observation of the surface of specimen CSTV7 before (a) and after (b) the degradation process.

Frost and thaw induced a different change in terms of anisotropy for the two types of concrete. Vicat concrete reduced equally the proper values from ~ 71 to $\sim 9,7$. On the contrary Portland concrete resulted practically unchanged (CSTP7 from 70,82 to 70,74 and CSTP8 from 70,52 to 69,83).

Water absorption capacity was strongly reduced after degradation for all concrete specimens.

Portland concrete affected by frost and thaw revealed a low chromatic variation. ΔE Values were equal to 3,88 and 3,45 for CSTP7 and CSTP8 respectively. Differently, Vicat concrete showed a higher change of superficial colour: CSTV7 value is equal to 12,86. ΔE values greater than 12 mean that the change was so high that the two colours, before and after degradation, can be considered two different colours. The effect of colour variation was visible also in sample CSTV7 (Figure 26) and it was probably due to the diffuse appearance of holes that change completely the pattern of the surfaces and its interaction with incident light. Colorimetric value of CSTV8 was equal to 4,87.

The results assessed that Vicat concrete suffer much more than Portland to deterioration by frost and thaw process.

Water lagoon

The only change visible on the surface of all the specimens was a grey patina, clearly visible on the rough side of the specimens (Figure 27). Nevertheless, specimens didn't show any other significant change from a macroscopic point of view.

Colour variation was confirmed for all the specimens through spectrophotometer. ΔE equal to 6,98 was recorded for CSTP9 (Figure 28). Differently CSTP10 was characterized by a lower ΔE value equal to 3,76. In the same way, CSTV9 ΔE value was equal to 5,11, while in CSTP10 was 4,76.

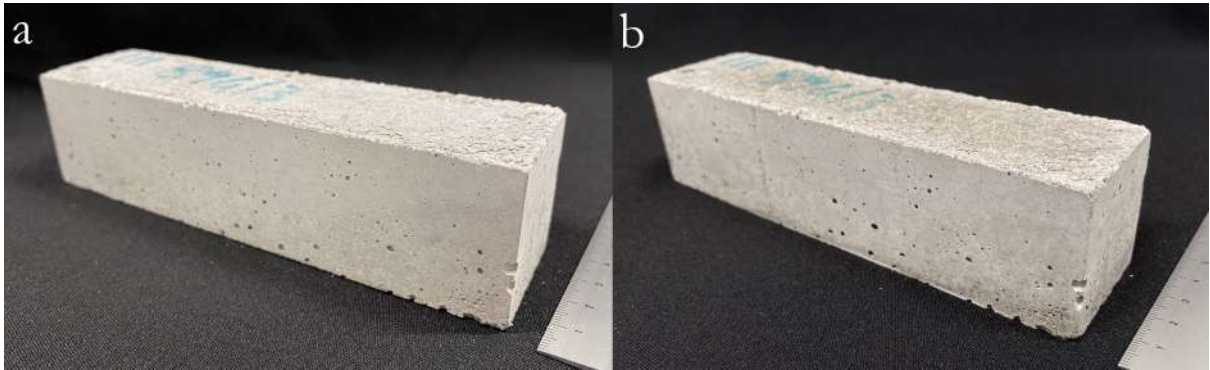


Figure 27. Change of the aspect of sample CSTP10 induced by water lagoon degradation.

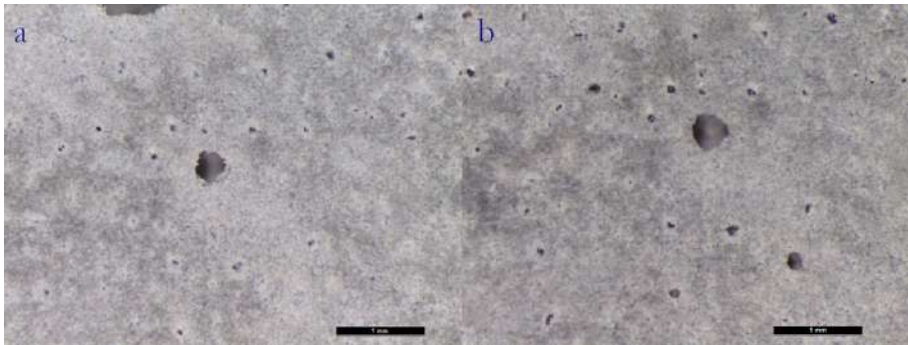


Figure 28. Microscopic observation of the surface of specimen CSTP9 before (a) and after (b) the degradation process.

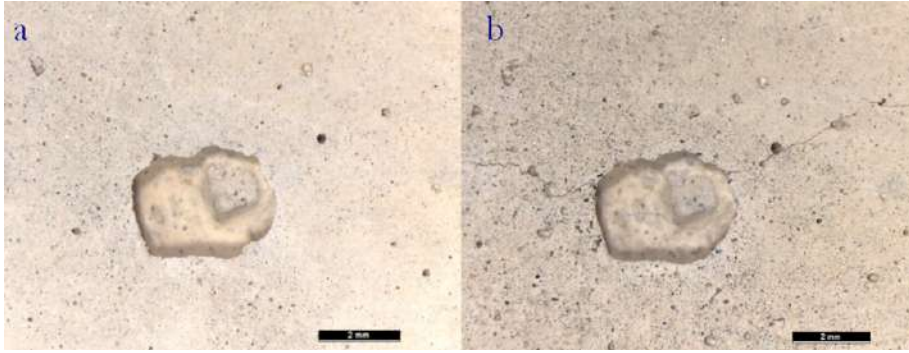


Figure 29. Microscopic observation of the surface of specimen CSTV9 before (a) and after (b) the degradation process.

CSTP9 appeared quite stable, from 70,72 to 71,24. CSTP10 showed a decrement of the value of anisotropy from 96,97 to 70,89 and a stable value of velocity. Also data achieved by the measurement of anisotropy of Vicat specimens showed a different behavior: CSTV9 value of anisotropy became unmeasurable, while value of CSTV10 reduce greatly from 72,64 to 8,32 to parity of a null change of value of velocity. Comparison with measurement of ultrasound velocity was made in order to have a greater understanding of the possible increment of voids induced by degradation, that can't be assessed for any specimens.

Sponge test results showed no significant variation of the values of water absorption coefficient after degradation for Vicat specimens, in contrast Portland samples showed a reduction of WA.

4.4 Evaluation of the consolidation treatments

Results obtained from treated specimens are grouped depending on strengthening agent tested. All the consolidants were applied by spray method using the same parameters (time, distance, dispenser). To facilitate the comprehension of the results in Table 12 are reported labels and numbers referred to each specimen. The absence in table of some samples is due to choices made during the research. A remind of each type of consolidants is reported at the beginning of each paragraph and in references.

Table 12. Schematic table of the information about samples, with specific methods of deterioration and treatments for each sample.

Material	Labels	Number	Decay	Consolidant
<i>Pietra di Firenzuola</i> <i>Pietra di Muggia</i> Bianco Sardo	PF PM BS	6	-	SNP100
		7	Thermal Shock	Evercrete Vetrofluid
		9	Thermal Shock	SNP-PDMS
		10	Salt crystallization	Evercrete Vetrofluid
		12	Salt crystallization	SNP-PDMS
		13	Frost and thaw	Evercrete Vetrofluid
		15	Frost and thaw	SNP-PDMS
		16	Water lagoon	Evercrete Vetrofluid
		18	Water Lagoon	SNP-PDMS
		19	-	Evercrete Vetrofluid
		21	-	SNP-PDMS
Portland Concrete Vicat Concrete	CSTP CSTV	2	-	SNP100
		3	Thermal Shock	Evercrete Vetrofluid
		4	Thermal Shock	SNP-PDMS
		5	Salt crystallization	Evercrete Vetrofluid
		6	Salt crystallization	SNP-PDMS

		7	Frost and thaw	Evercrete Vetrofluid
		8	Frost and thaw	SNP-PDMS
		9	Water lagoon	Evercrete Vetrofluid
		10	Water Lagoon	SNP-PDMS
		11	-	Evercrete Vetrofluid
		12	-	SNP-PDMS

4.4.1 SNP100

*SNP100*⁷ was applied in this research in order to evaluate the performance of silica nanoparticles on concrete specimens. Moreover, spray method was tested for comparing a different application method with capillary absorption on stone material used in the previews research [1]. In this case, the application of the consolidant was made on sound sample not subjected to deterioration treatment.

Microscopic observation of treated surfaces did not show any changes on Portland and Vicat specimens (CSTP2 and CSTV2), as well as on sandstones and granite samples.

Table 13 reports ΔE values, which express the color variation caused by the application of the treatment. All the measurements revealed a value lower than 1, so change in color can be considered null. CSTV2 was the only sample that showed a ΔE value between 1 and 3, which is in any case an acceptable variation.

Table 13. Values of colorimetric variations for specimens treated with SNP100.

SNP100	
Specimen	ΔE
CSTP2	0,9
CSTV2	2,31
PF6	0,27

⁷ SNP100: SNP of 100 nm (not functionalized) dispersed in EtOH:H₂O solution 70:30 already studied in the previews research.

PM6	0,3
BS6	0,48

Results of variation of ultrasound analysis before and after the application of the treatment are reported in Figure 30. Values of anisotropy and ultrasound velocity are compared in order to evaluate possible changes. To lower values of velocity correspond increasing value of anisotropy, which correspond to the increasing quantity of voids in the matrix [82]. High velocity is index of amorphous structure, while high anisotropy is index of organized structure [83].

Calculated values of anisotropy (see Figure 30a) increased for all the samples, however it cannot be considered since the increment is in the error range of untreated samples. Ultrasound velocity decreased in case of CSTP2 sample, indicating an increment of voids, while increased for CSTV2. As for concrete also sandstones acted inconsistently: PF6 showed a low decrement of the calculated values of velocity, meanwhile the velocity value of PM6 increased. Since both the values are in the range of error of untreated samples, they can be considered unchanged. The values of anisotropy and ultrasound velocity of BS6 increased.

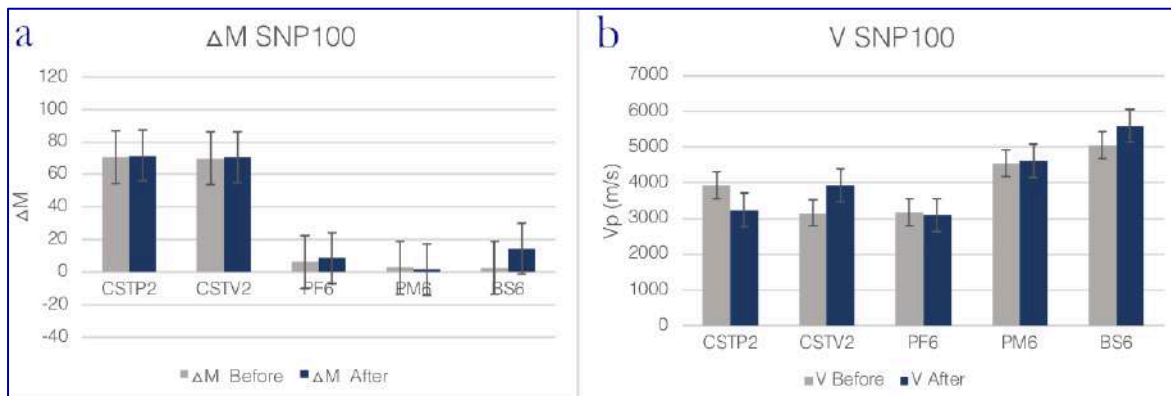


Figure 30. Graphs of changes of values of anisotropy (a) and velocities for samples treated with SNP100.

In Figure 31 are reported the changes in water absorptions capacity (WA) before and after the application of the treatment. The mean value of the amount of water absorbed increased for all the specimens, except for CSTV2 which showed a great decrement of the value. Increment of WA for CSTP2 and PM6 can be considered acceptable since it falls in the range of error. PF6 and BS6 showed a strong increment of the quantity of water absorbed.

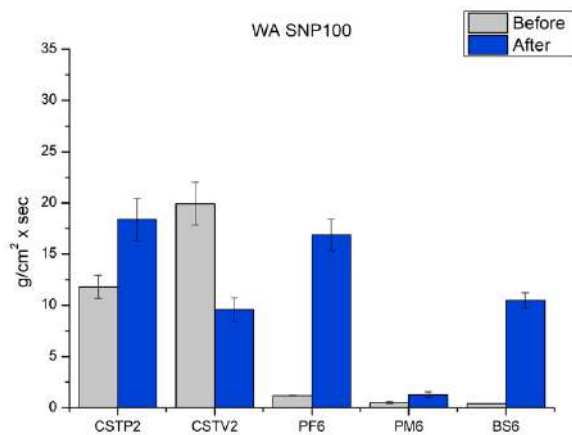


Figure 31. Graph of the evaluations of changes of water absorption for samples treated with SNP100.

4.4.2 SNP-PDMS

Consolidant *SNP-PDMS*⁸ (previously named S1e) was diluted before the application at 10% in a 75:25 EtOH:H₂O solution (Figure 32) under stirring for preventing partial precipitation of the compound. The concentration was assessed as the best in order to be applied avoiding excess of compound on the surface. The consolidant was kept under stirring till the application of the treatment.

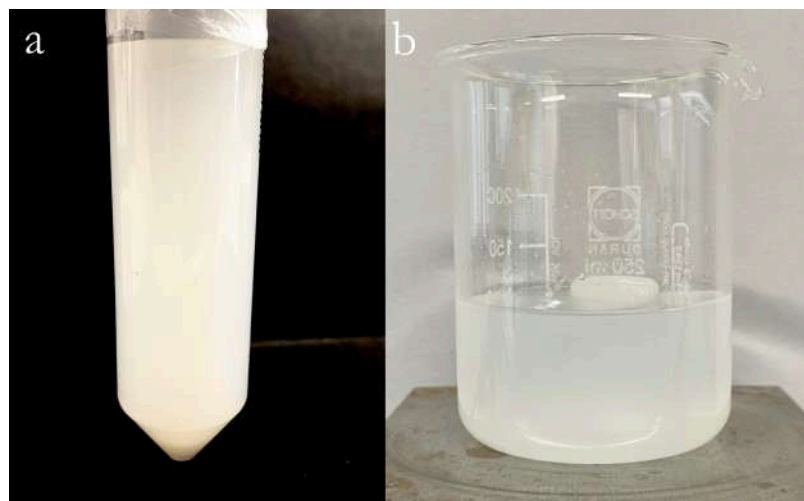


Figure 32. Production of SNP-PDMS: a) after the functionalization, b) after the dilution.

⁸ SNP-PDMS: compound S1e prepared by the functionalization process of SNP with PDMS-OH diluted before the application.

Pietra di Firenzuola (PF)

The consolidation of *Pietra di Firenzuola* with SNP-PDMS did not cause any perceptible variation of the surface, confirmed by colorimetric analysis. ΔE was lower than 1 for all the specimens, except for PF12 that showed a value larger than 3 slightly larger than the range of acceptance of change (that is between 1 and 3). However, as shown in Figure 33, no particular variation was observable in this sample by microscopic investigation.

Table 14. Values of colorimetric variations for *Pietra di Firenzuola* specimens treated with SNP-PDMS.

SNP-PDMS	
Speci-	ΔE
PF9	0,82
PF12	3,15
PF15	0,36
PF18	0,41
PF21	0,7

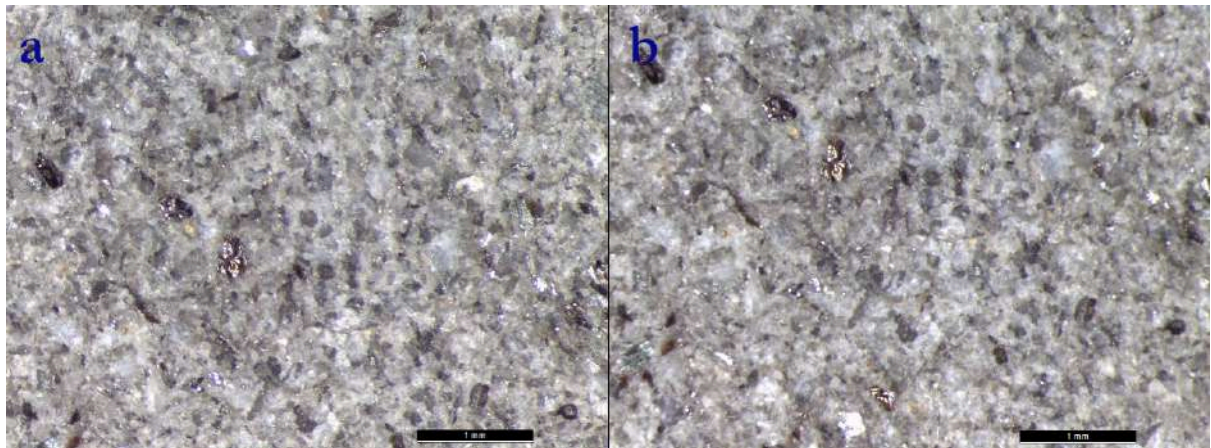


Figure 33. Microscopic investigation of the specimen PF12 before (a) and after (b) the treatment (enlargement 2x).

The ultrasound analysis results are reported in Figure 34. Anisotropy value decreased particularly for PF9, which was also characterized by an increment of ultrasound velocity that, thanks to the consolidation, returned to sound specimen value. The decrease in ΔM and increase in ΔV were

also found for PF15. PF18 showed a discrepancy since for this sample both ΔM and ΔV decreased. In contrast, increment of anisotropy and ultrasound velocity were recorded for PF12 and PF21, even if in case of PF12 the increment was slight and falls in the range of error. The reduction of voids is related to ΔM decreases or V increases. Theoretically when ΔM increases V decreases and vice versa. From these analysis it was possible to state that only PF9, PF15 respect the concept at the base of ultrasound analysis and showed a decrement of voids.

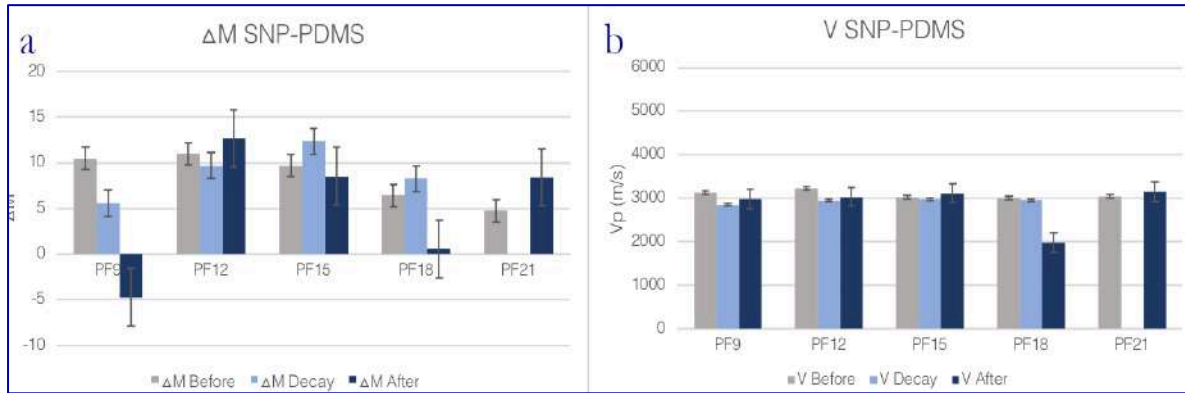


Figure 34. Graphs of changes of values of anisotropy (a) and velocities (b) for *Pietra di Firenzuola* samples treated with SNP-PDMS.

Values of water absorption increased for PF9, PF12, PF15 and PF21. Only, PF18 (water lagoon) evidenced a marked decrease of WA coefficient achieving a value similar to that of sound specimen (

Figure 35).

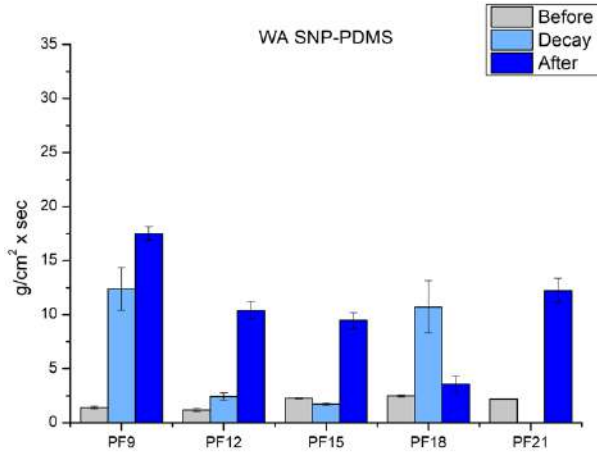


Figure 35. Graph of the evaluations of changes of water absorption for *Pietra di Firenzuola* samples treated with SNP-PDMS.

Pietra di Muggia (PM)

Application of SNP-PDMS on *Pietra di Muggia* did not seem to induce any change to the surface sample. This was confirmed by colorimetric analysis (Table 15). PM12 was the specimen which showed the greatest value of ΔE , but this value was in the range of acceptance between 1 and 3. Also by microscopic analysis it was not possible to see any variation of the superficial aspect (Figure 36).

Table 15. Values of colorimetric variations for *Pietra di Muggia* specimens treated with SNP-PDMS.

SNP-PDMS	
Specimen	ΔE
PM9	0,67
PM12	2,64
PM15	0,11
PM18	0,35
PM21	1,15

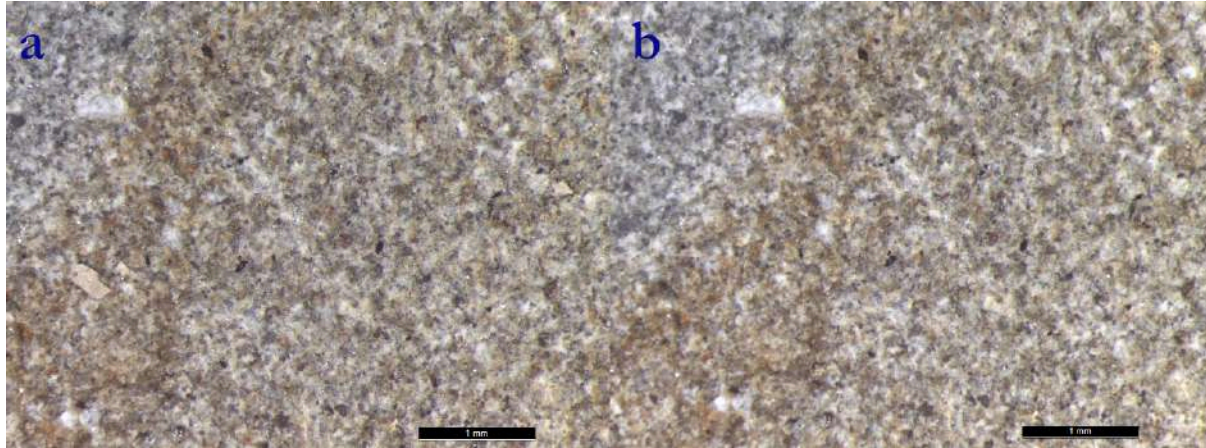


Figure 36. Microscopic investigation of the specimen PM12 before (a) and after (b) the treatment (enlargement 2x).

Concerning PM9 ultrasound analysis (Figure 37) showed the increase of anisotropy value for specimen PM9 and increase of ultrasound velocity in the range of error. PM12 showed an increase of ΔM value and the decrease of ultrasound velocity. The results obtained for PM15, PM18, PM21 samples were satisfying, to parity of decrement of anisotropy, velocity increased or stay equal, demonstrating a reduction of voids.

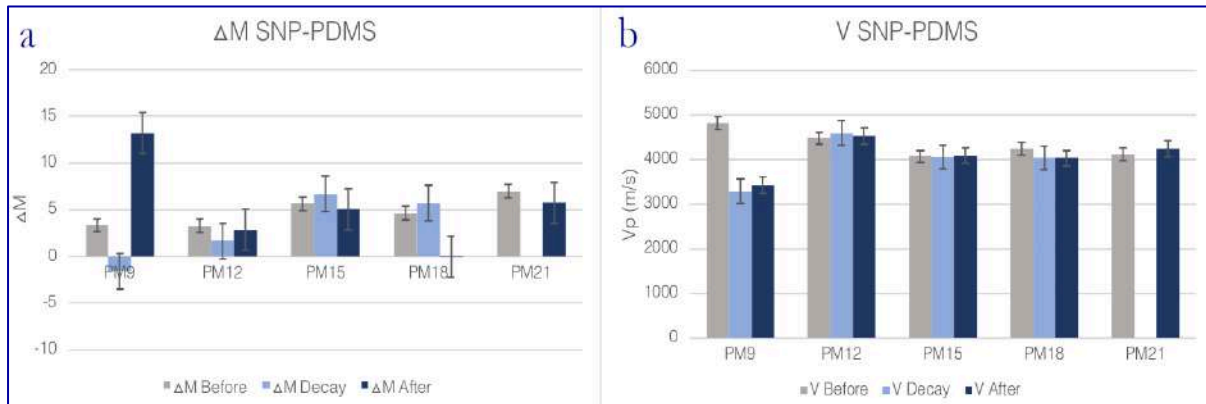


Figure 37. Graphs of changes of values of anisotropy (a) and velocities (b) for *Pietra di Muggia* samples treated with SNP-PDMS.

Significant variation of WA values were recorded only for PM12 and PM18 (Figure 38), which decreased returning almost to sound material values. All the other samples remained practically unchanged.

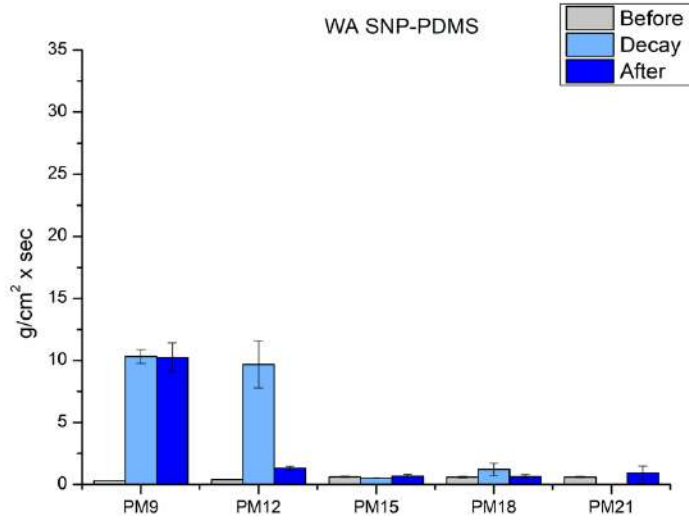


Figure 38. Graph of the evaluations of changes of water absorption for *Pietra di Muggia* samples treated with SNP-PDMS.

Bianco Sardo (BS)

Microscopic investigation showed no variation of the aspect of specimen surfaces after the application of the treatment, also using high magnification (Figure 39). Only BS9 showed a ΔE value lower than 1, while all the other specimens were characterized by values which fell in the range between 1 and 3 (Table 16).

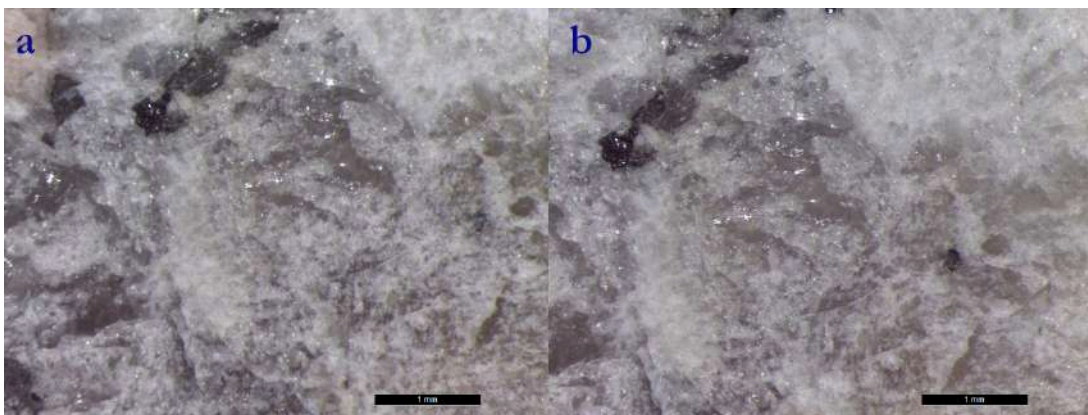


Figure 39. Microscopic investigation of the specimen BS12 before (a) and after (b) the treatment.

Table 16. Values of colorimetric variations for *Bianco Sardo* specimens treated with SNP-PDMS.

SNP-PDMS	
Specimen	ΔE
BS9	0,42
BS12	2,64
BS15	1,7
BS18	1,91
BS21	2,11

Both anisotropy and ultrasound velocity values increased for all the samples (Figure 40). However, all the collected values (except for BS9 and BS12) were in the range of error, so evaluations can be considered unchanged from the previews.

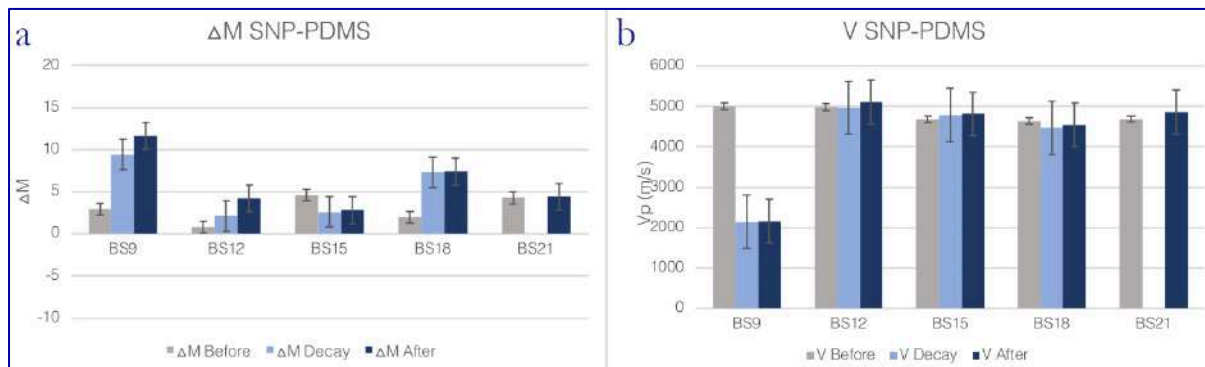


Figure 40. Graphs of changes of values of anisotropy (a) and velocities (b) for *Bianco Sardo* samples treated with SNP-PDMS.

Water absorption analysis (Figure 41) demonstrated that BS15 and BS18 were the only samples that showed a decrement of WA.

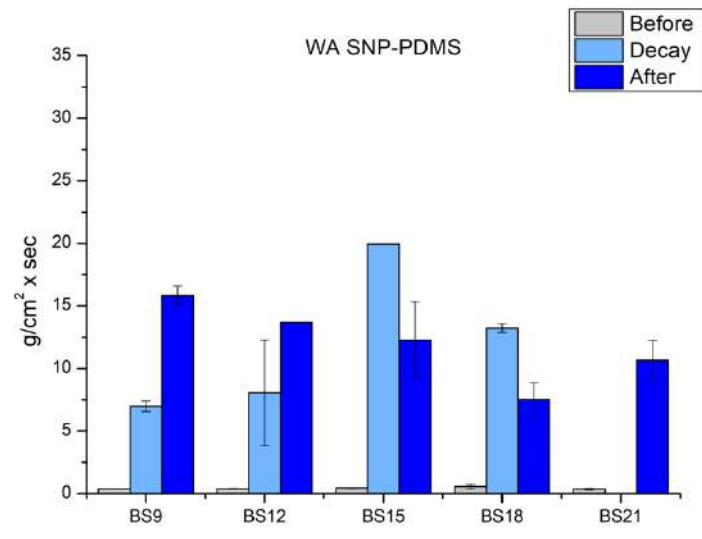


Figure 41. Graph of the evaluations of changes of water absorption for *Bianco Sardo* samples treated with SNP-PDMS.

Portland Concrete (CSTP)

CSTP8 was the only sample that showed a slight aesthetic variation (Figure 42). On the surface was possible to see the reflection of light induced by the presence of a compound on the surface. Except of this, no other particular change was detected by microscopic investigation. ΔE (Table 17) was similar for all the samples (mean value 1,34) and was in the range of acceptable variation ($1 < \Delta E < 3$).

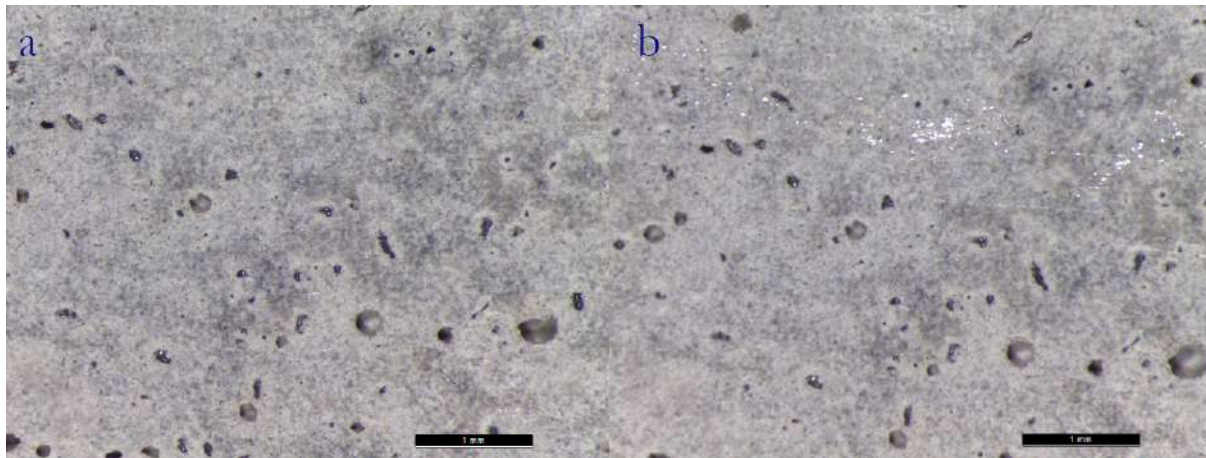


Figure 42. Microscopic investigation of the specimen CSTP8 before (a) and after (b) the treatment.

Table 17. Values of colorimetric variations for Portland Concrete specimens treated with SNP-PDMS.

SNP-PDMS	
Specimen	ΔE
CSTP4	1,39
CSTP6	1,59
CSTP8	1,09
CSTP10	1,42
CSTP12	2,46

The samples showed a different behaviour of the parameters obtained by ultrasound analysis (Figure 43). Evaluation failed for CSTP4 since during the acquisition the measure was unstable. CSTP6 and CSTP12 showed a decrement of both anisotropy and velocity, meanwhile CSTP8 showed an increment of both the values. Strong decrement of ΔM was recorded for CSTP10 to parity of a value of velocity that stay unchanged.

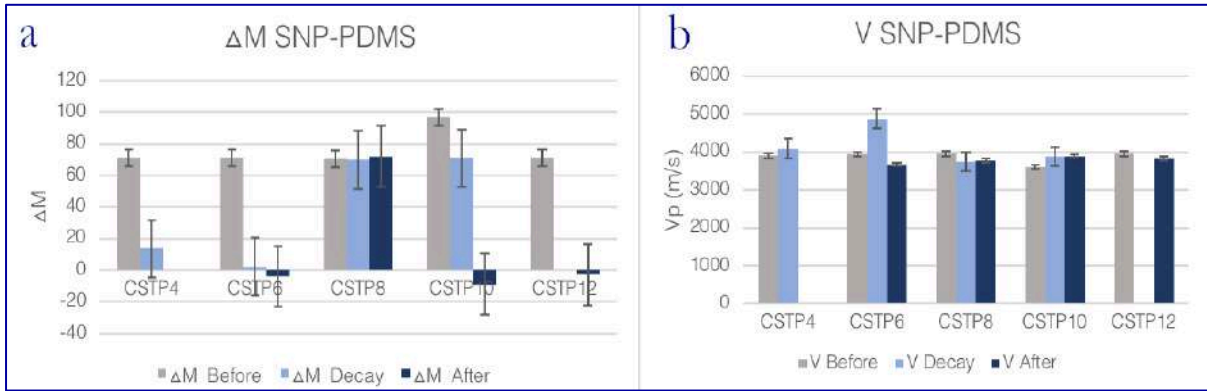


Figure 43. Graphs of changes of values of anisotropy (a) and velocities (b) for Portland Concrete samples treated with SNP-PDMS.

From the analysis of water absorption (Figure 44) was possible to evaluate an increment of WA coefficient for all the samples, except for CSTP8 and CSTP10 for which the values remained almost unchanged.

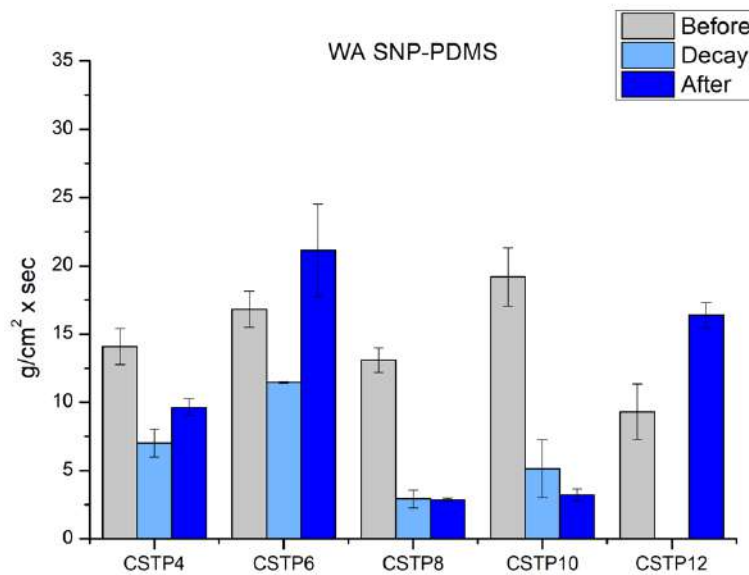


Figure 44. Graph of the evaluations of changes of water absorption for Portland Concrete samples treated with SNP-PDMS.

Vicat Concrete (CSTV)

Microscopic analyses of specimens showed particular changes for sample CSTV4, CSTV8, CSTV10. On sample CSTV4, high magnification revealed the presence of a compound filling the crack (Figure 45), whereas for sample CSTV8 a slight variation of lightness was visible (Figure 46), also confirmed by the colorimetric analysis ($\Delta E > 3$, Table 18). Sample CSTV10 showed a thin white patina on all the surface observable in Figure 47.

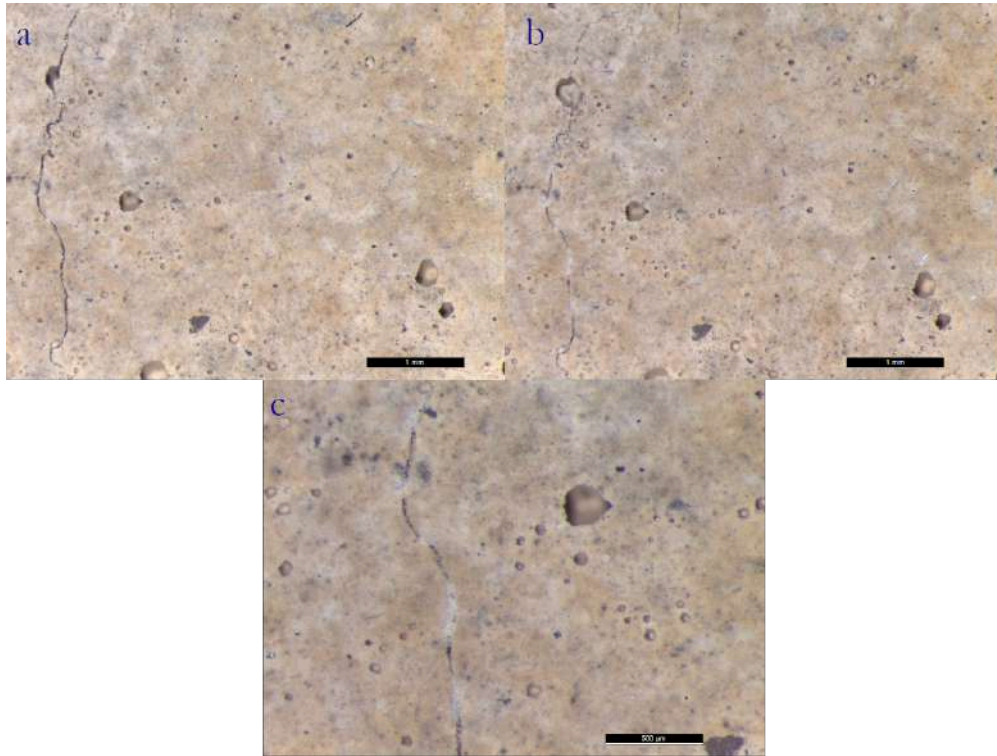


Figure 45. Microscopic investigation of specimen CSTV4 before (a) and after (b) the treatment (enlargement 2x), (c) detail of the crack (enlargement 4x).

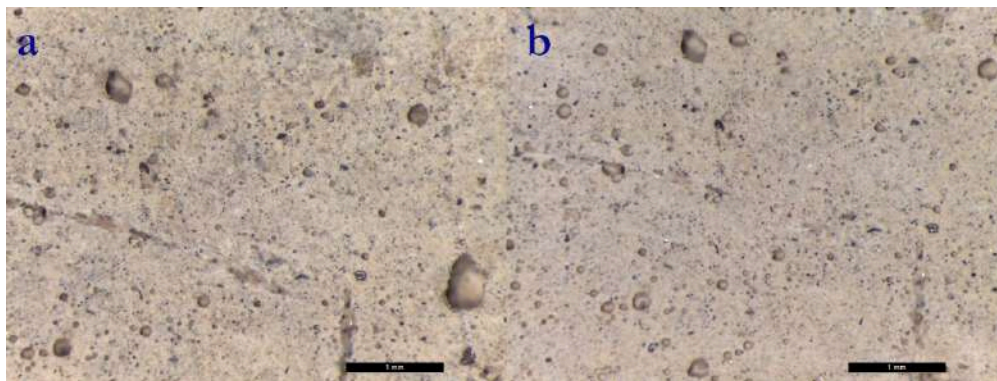


Figure 46. Microscopic investigation of specimen CSTV8 before (a) and after (b) the treatment.

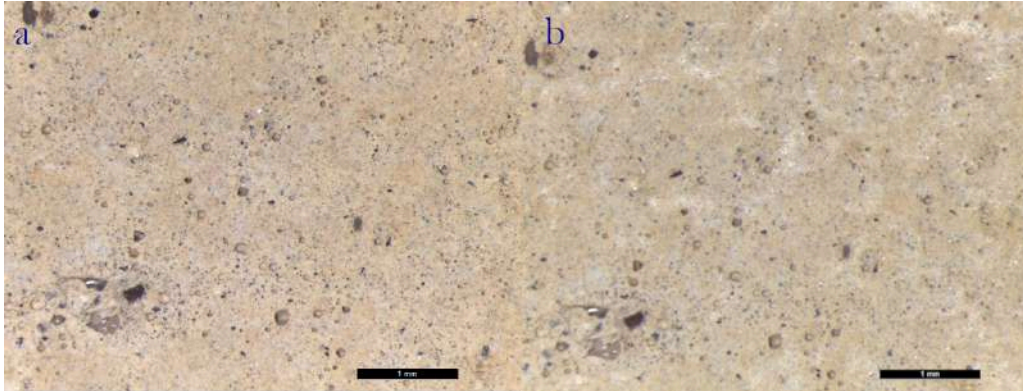


Figure 47. Microscopic investigation of specimen CSTV10 before (a) and after (b) the treatment.

Table 18. Values of colorimetric variations for Vicat Concrete specimens treated with SNP-PDMS.

SNP-PDMS	
Specimen	ΔE
CSTV4	0,64
CSTV6	0,97
CSTV8	3,54
CSTV10	1,59
CSTV12	2,24

Anisotropy decreased for all the specimen and for specimens CSTV4 and CSTV8 an increment of values of velocity was recorded. In contrast CSTV10, CSTV12 showed a strange decrement of V (Figure 48) and the analysis of CSTV6 sample failed.

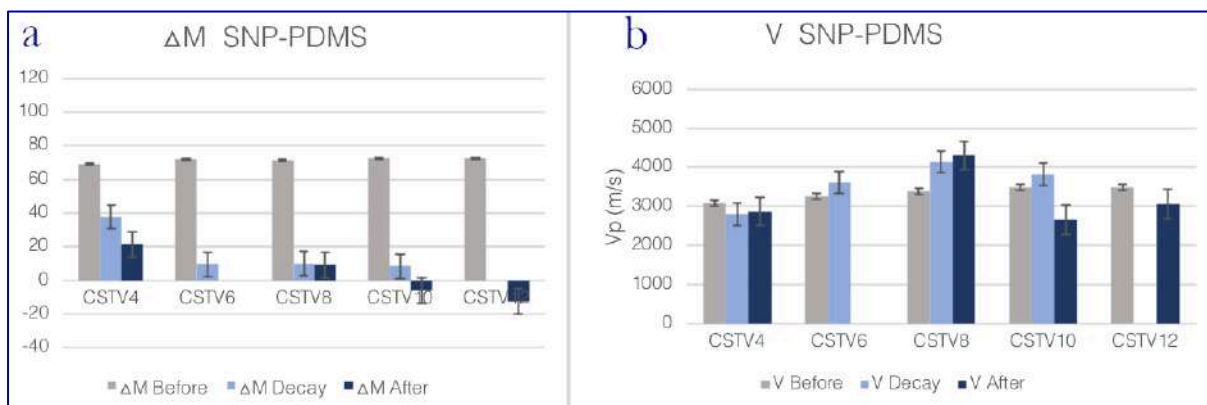


Figure 48. Graphs of changes of values of anisotropy (a) and velocities (b) for Vicat Concrete samples treated with SNP-PDMS.

The treatment showed to strongly decrease the value of water absorption for samples CSTV4 (Figure 49). Specimens CSTV6, CSTV10, CSTV12 showed a less mean value of WA than untreated specimens, however they are within the error range. Only sample CSTV8 absorbed after the application of the treatment a greater amount of water.

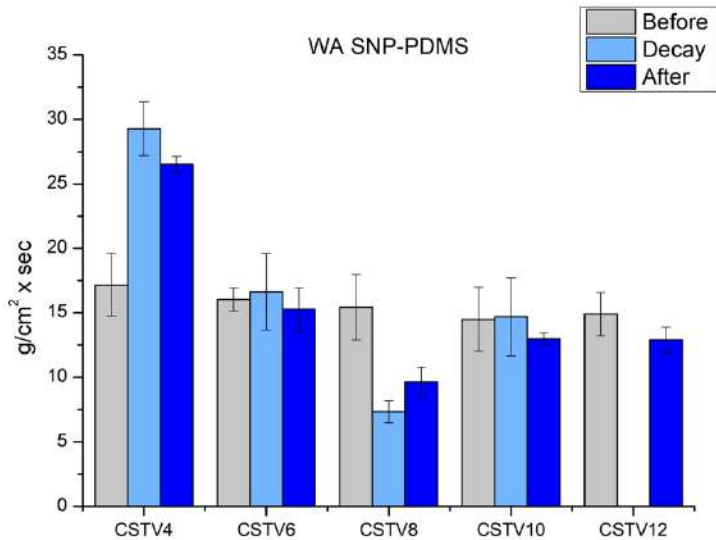


Figure 49. Graph of the evaluations of changes of water absorption for Vicat Concrete samples treated with SNP-PDMS.

4.4.3 Evercrete Vetrofluid

Pietra di Firenzuola (PF)

Microscopic investigations of the treated samples did not reveal particular variation. Figure 50 reports microscopic images of PF16 sample, which showed the greatest colorimetric variation among the *Pietra di Firenzuola* specimens (Table 19). ΔE value was greater than 5 corresponding to a change in color visible also with naked eye. A detailed analysis of the results showed the decrease of L^* value from 57,618 to 52,154, resulting in a darkening of the surface.

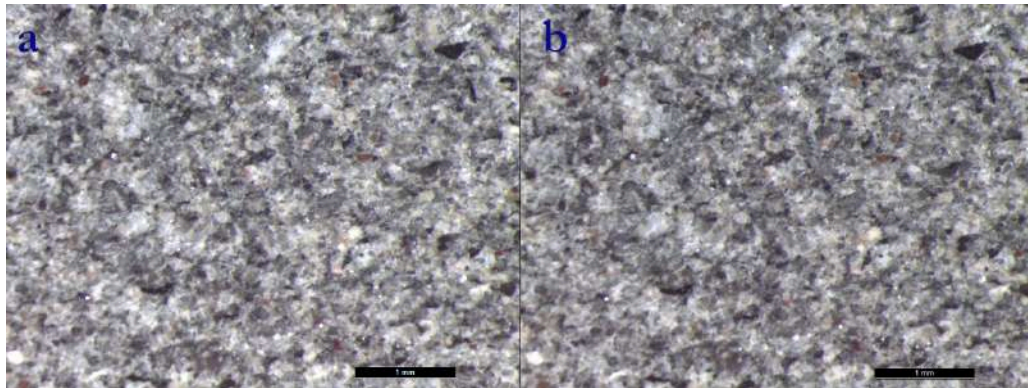


Figure 50. Microscopic investigation of specimen PF16 before (a) and after (b) the treatment.

Table 19. Values of colorimetric variations for *Pietra di Firenzuola* specimens treated with Evercrete Vetrofluid.

Evercrete Vetrofluid	
Specimen	ΔE
PF7	2,97
PF10	1,77
PF13	3,15
PF16	5,47
PF19	1,47

Ultrasound analysis (Figure 51) showed a reduction of ΔM and an increment of V for samples PF7, PF13, PF19. These results were probably related to a reduction of voids in the sample. PF16 showed a decrement of ΔM value and a meaningless decrement of ultrasound velocity (the value is in the range of error). PF10 sample was the only one which showed a significant increment of ΔM and decrement of ΔV .

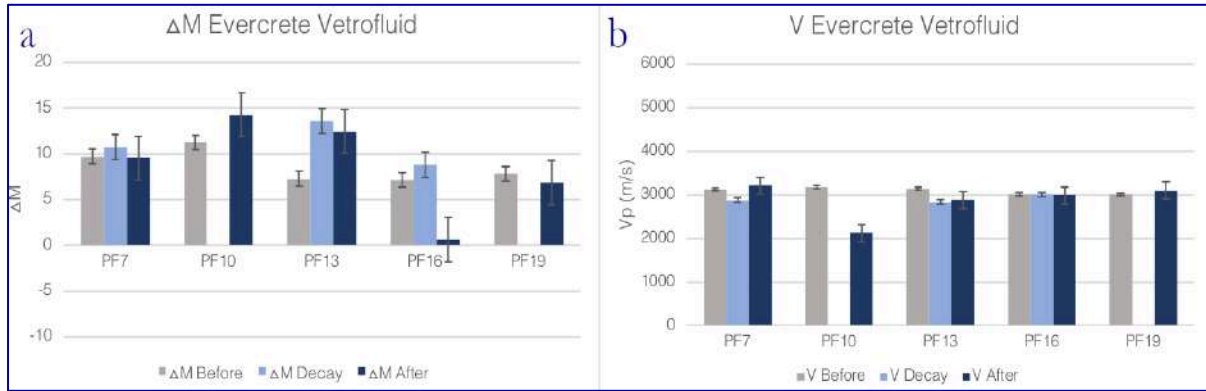


Figure 51. Graphs of changes of values of anisotropy (a) and velocities (b) for *Pietra di Firenzuola* samples treated with Evercrete Vetrofluid.

Figure 52 shows the water absorption variations obtained by sponge test. The sample decayed by thermal shock and, to a lesser extent, water lagoon slightly reduced, after treatment, the superficial water absorption capacity. PF13 (degraded by frost and thaw) and PF19 (not degraded) showed the increasing of WA coefficient after the application of Evercrete Vetrofluid. PF10 (salt crystallization) was almost unchanged.

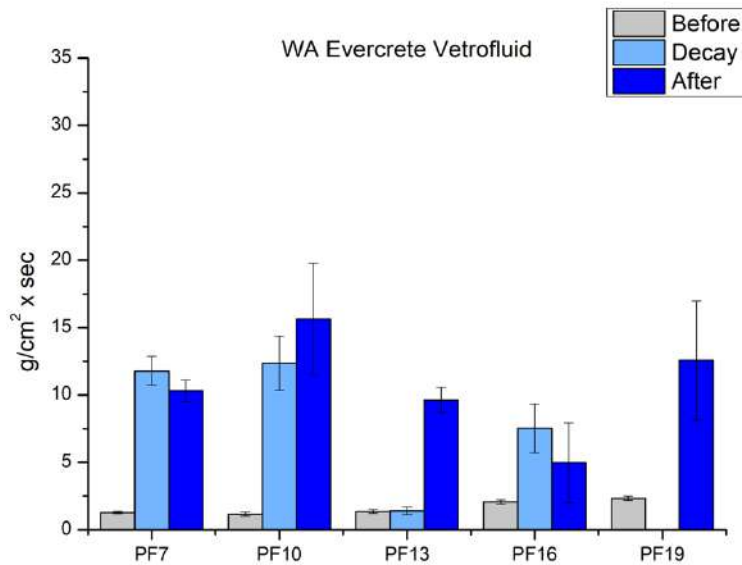


Figure 52. Graph of the evaluations of changes of water absorptions for *Pietra di Firenzuola* samples treated with Evercrete Vetrofluid.

Pietra di Muggia (PM)

Microscopic investigation revealed a particular change of the superficial aspect of sample PM7 (Figure 53). Effect of iridescence due to the reflection of light on the treated surface was visible. This effect was induced by the product and it was present moderately in all the other treated samples of *Pietra di Muggia*.

Colorimetric analysis confirmed the change induced by the presence of treatment on the surface. In Table 20 are reported values of ΔE .

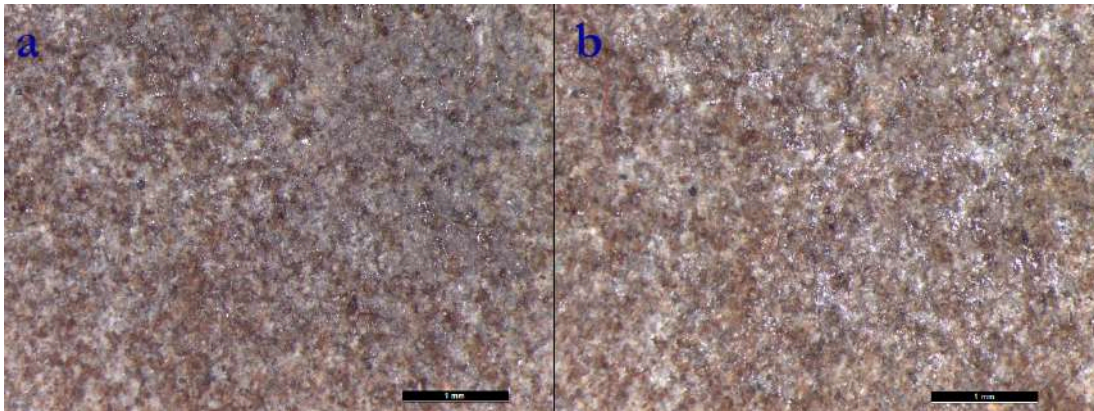


Figure 53. Microscopic investigation of specimen PM7 before (a) and after (b) the treatment.

Table 20. Values of colorimetric variations for *Pietra di Muggia* specimens treated with Evercrete Vetrofluid.

Evercrete	
Specimen	ΔE
PM7	4,11
PM10	1,51
PM13	2,15
PM16	4,04
PM19	5,67

Evaluation of ultrasound analysis (Figure 54) revealed that for sample PM7, PM13 and PM16 values of anisotropy were reduced after the application of Vetrofluid and those of ultrasound velocities increased for PM13 and PM16. These correspondences suggested the reduction of voids

in these specimens. Slight increment of values of ΔM (values fall in the range of error) were detected for samples PM10 and PM19 and for both of them also the velocity increased.

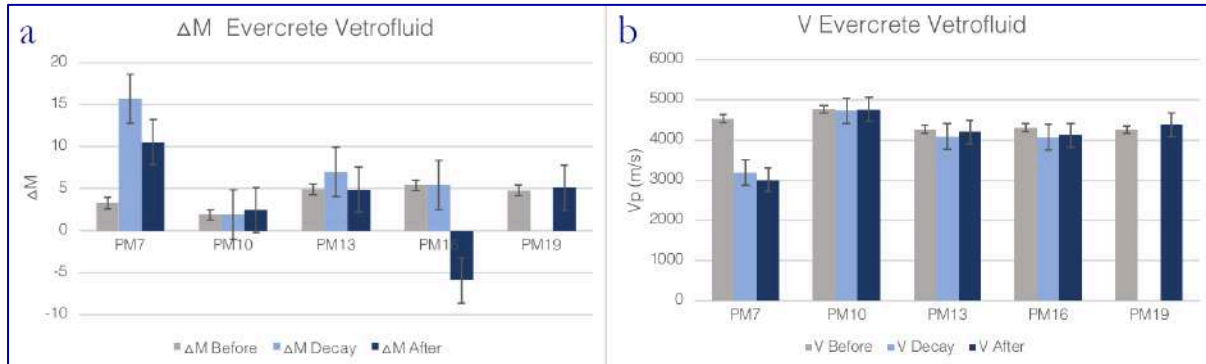


Figure 54. Graphs of changes of values of anisotropy (a) and velocities (b) for *Pietra di Muggia* samples treated with Evercrete Vetrofluid.

The amount of water absorbed by the treated surfaces decreased only for PM7 (thermal shock). WA showed a marked increment for PM10, PM13, PM19 (Figure 55). The treatment of PM16 degraded by water lagoon absorption did not show significant variation.

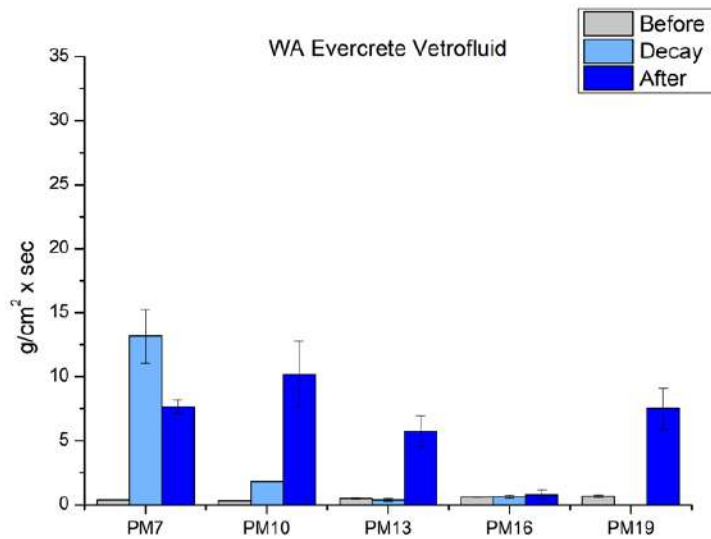


Figure 55. Graph of the evaluations of changes of water absorptions for *Pietra di Muggia* samples treated with Evercrete Vetrofluid.

Bianco Sardo (BS)

From a microscopic point of view, it was possible to observe a glowing effect diffused on the treated surfaces of granite specimens. This effect was particularly visible in sample BS7 (Figure 56), BS13 and BS16 (Figure 57). Colorimetric investigation confirmed this superficial variation for all the sample Table 21.

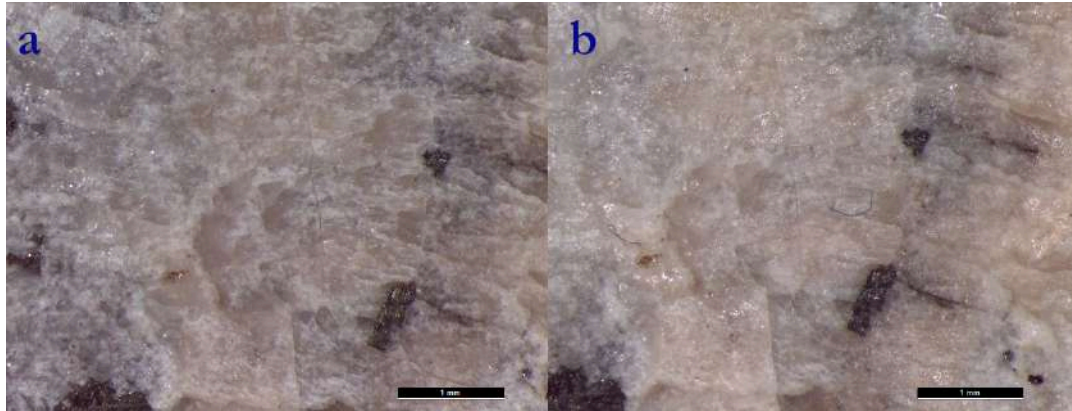


Figure 56. Microscopic investigation of specimen BS7 before (a) and after (b) the treatment.

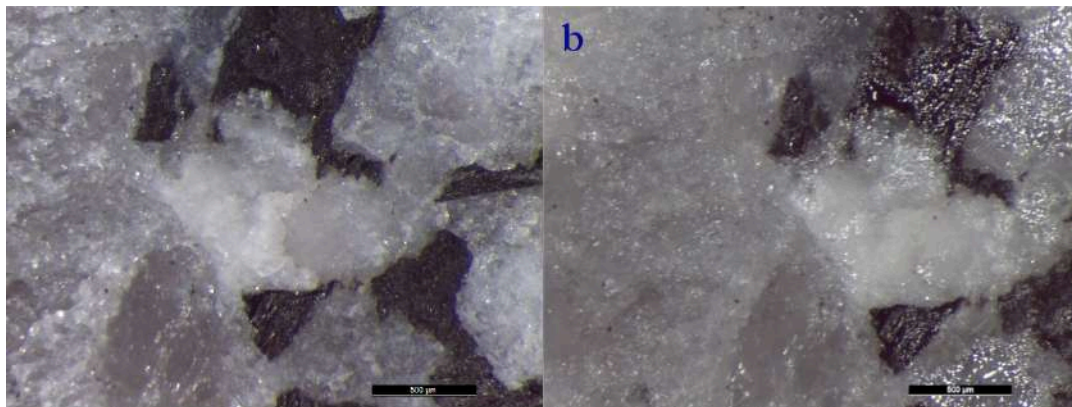


Figure 57. Microscopic investigation of specimen BS16 before (a) and after (b) the treatment.

Table 21. Values of colorimetric variations for *Bianco Sardo* specimens treated with Evercrete Vetrofluid.

Evercrete	
Specimen	ΔE
BS7	4,44
BS10	2,17
BS13	3,36

BS16	2,45
BS19	4,23

Evaluation of ultrasound analysis (Figure 58) confirmed the reduction of voids in all the samples. The values of ultrasound velocities increased for all the samples. Values of anisotropy clearly increased for three samples, while for two samples BS10 and BS16, the parameter increased only slightly (in the range of error).

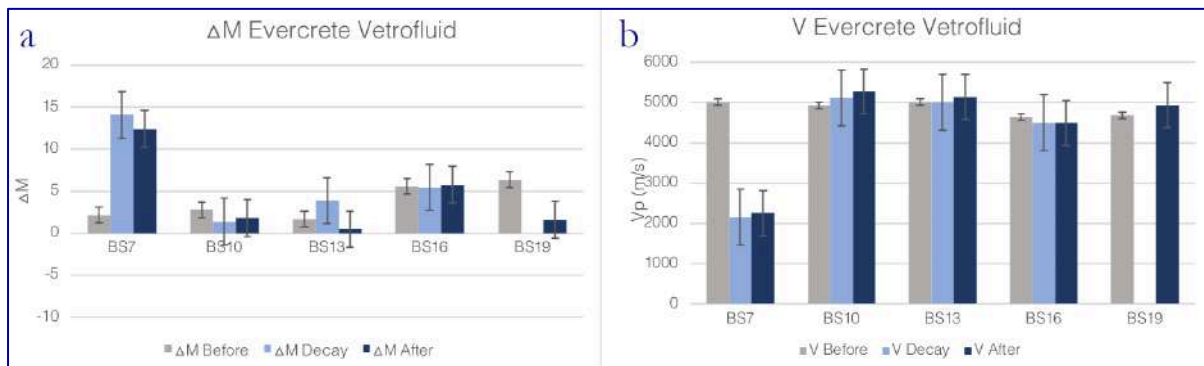


Figure 58. Graphs of changes of values of anisotropy (a) and velocities (b) for *Bianco Sardo* samples treated with Evercrete Vetrofluid.

Water absorption test (Figure 59) showed significant reduced value only for samples BS16 (water lagoon). BS13 remained almost unchanged, whereas BS7 (thermal shock), BS10 (salt crystallization) and BS19 (sound sample) increased greatly WA values.

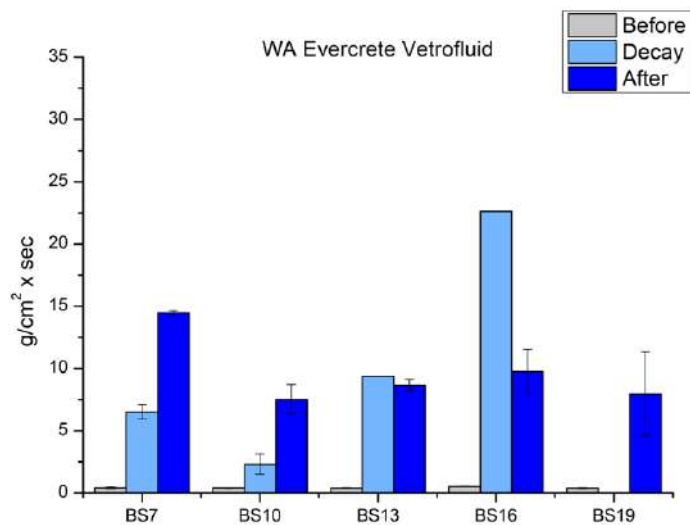


Figure 59. Graph of the evaluations of changes of water absorptions for *Bianco Sardo* samples treated with Evercrete Vetrofluid.

Portland Concrete (CSTP)

Variation of the superficial aspect after the application of Vetrofluid was visible on all the investigated Portland Concrete samples. On the surfaces it was possible to observe stains of the compound applied. The most significant examples are CSTP3, CSTP5 and CSTP9 reported in Figure 60, Figure 61, Figure 62 respectively. The variation of the aspect of CSTP3 and CSTP5 were confirmed also by the evaluation of ΔE values (Table 22). On the contrary, also if microscopic investigation showed a great change of sample CSTP9 it did not show a significant colorimetric variation. Sound sample CSTP11 as CSTP3 showed a change in the aspect because of the presence of stain of compound visible on the surface. Moreover, the two samples showed both the same colorimetric variation.

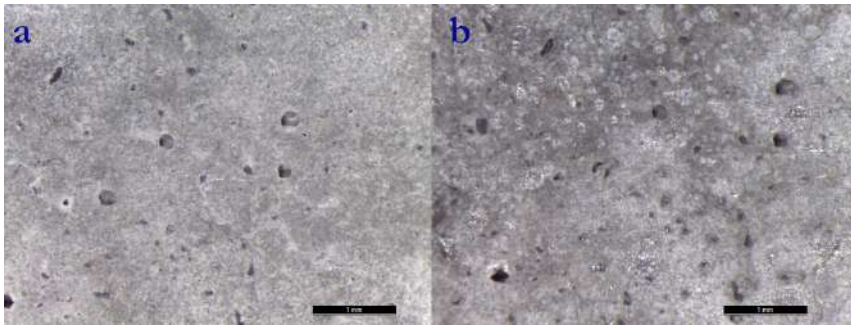


Figure 60. Microscopic investigation of specimen CSTP3 before (a) and after (b) the treatment.

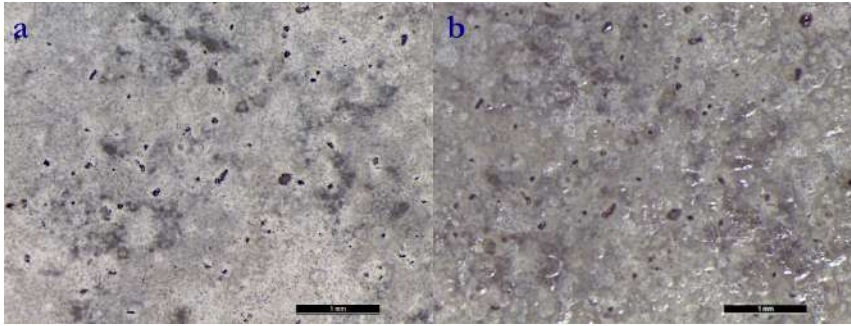


Figure 61. Microscopic investigation of specimen CSTP5 before (a) and after (b) the treatment.

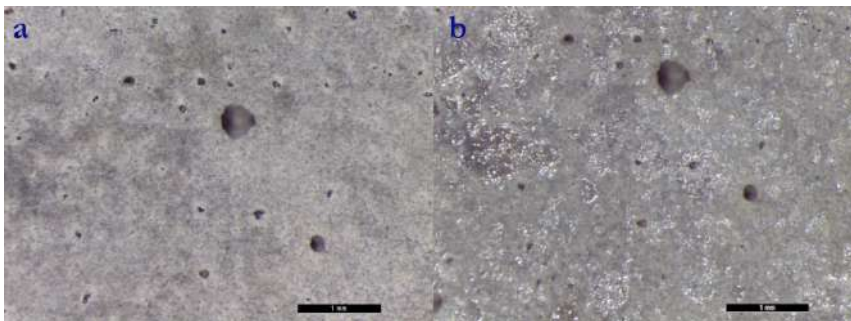


Figure 62. Microscopic investigation of specimen CSTP9 before (a) and after (b) the treatment.

Table 22. Values of colorimetric variations for Portland Concrete specimens treated with Evercrete Vetrofluid.

Evercrete	
Specimen	ΔE
CSTP3	4,19
CSTP5	3,36
CSTP7	0,86
CSTP9	0,76
CSTP11	4,09

Resulting graphs of ultrasound analysis are reported in Figure 63. CSTP3 was characterized by a greater value of anisotropy and a lower value of velocity. Decrement of ΔM values were recorded for all the other sample. Unlike what was expected, velocity decreased for samples CSTP7, CSTP9, CSTP11. Only sample CSTP5 respected the theory that to parity of decrement of ΔM , velocity should increase.

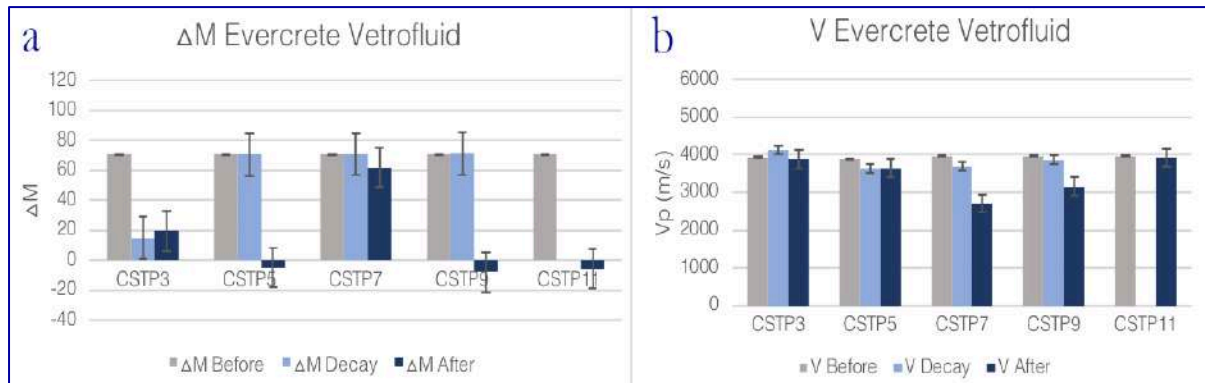


Figure 63. Graphs of changes of values of anisotropy (a) and velocities (b) for Portland Concrete samples treated with Evercrete Vetrofluid.

Figure 64 reports the results of sponge test. Since the degradation process were ineffective, the product seemed not to be absorbed from the substrate and the WA values increased for all the tested specimens. Only the sample, which did not suffer decay, reduced the amount of water absorbed after the application of Evercrete Vetrofluid.

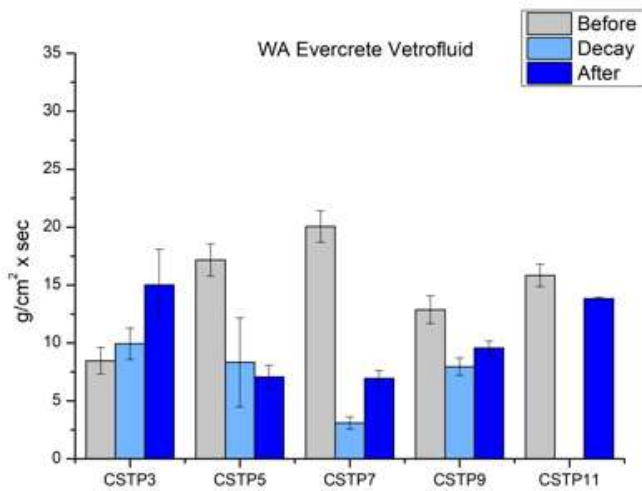


Figure 64. Graph of the evaluations of changes of water absorptions for Portland Concrete samples treated with Evercrete Vetrofluid.

Vicat Concrete (CSTV)

The presence of the treatment applied is visible on all the CSTV specimens with the naked eye. Sample CSTV7 and CSTV9 (Figure 65 and Figure 66) showed the greatest morphological variation, confirmed also by colorimetric evaluations (Table 23). The other concrete samples showed a lower change and a reduced colour variation ($1 < \Delta E < 3$).

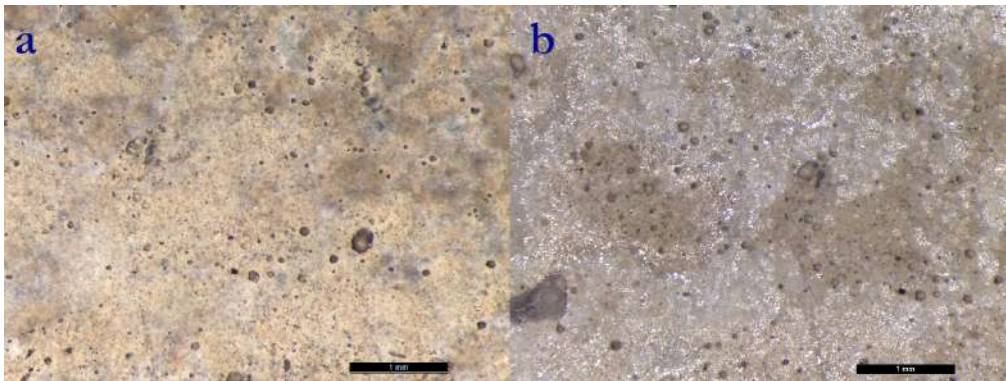


Figure 65. Microscopic investigation of specimen CSTV7 before (a) and after (b) the treatment.

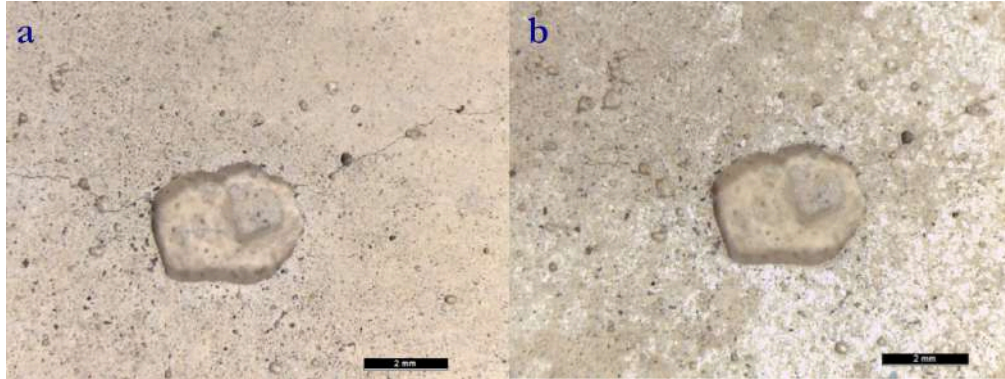


Figure 66. Microscopic investigation of specimen CSTV9 before (a) and after (b) the treatment.

Table 23. Values of colorimetric variations for Vicat Concrete specimens treated with Evercrete Vetrofluid.

Evercrete	
Specimen	ΔE
CSTV3	1,09
CSTV5	2,7
CSTV7	8,72
CSTV9	7,86
CSTV11	3,66

Because of the strong effect induced by degradation treatments of sample CSTV3 and CSTV9 degraded respectively with thermal shock and water lagoon processes, measurement of ultrasound analysis (Figure 67) failed. Measurements performed on CSTV5 and on CSTV11 revealed a decrement of anisotropy. CSTV7 showed a slight increment of anisotropy and a decrement of ultrasound velocity.

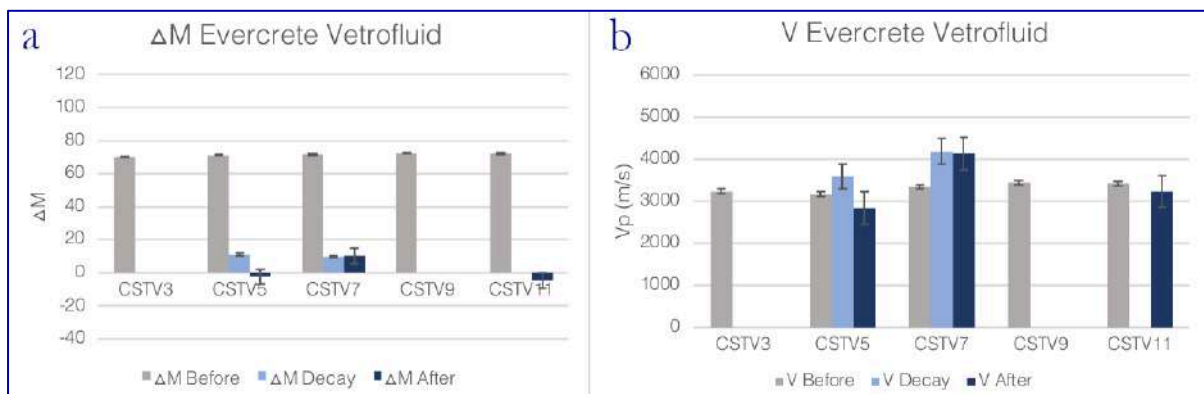


Figure 67. Graphs of changes of values of anisotropy (a) and velocities (b) for Vicat Concrete samples treated with Evercrete Vetrofluid.

Water absorption (Figure 68) values decreased for samples degraded by thermal shock (CSTV3) and salt crystallization (CSTV5) that were considered the most effective degradation process for this kind of concrete. Sample CSTV7, which showed after degradation (frost and thaw) a decrement of WA value, showed an increase of this parameter after the application of the treatment. Sound sample (CSTV11) was characterized by a lower mean value of WA, even if this is in the untreated error range.

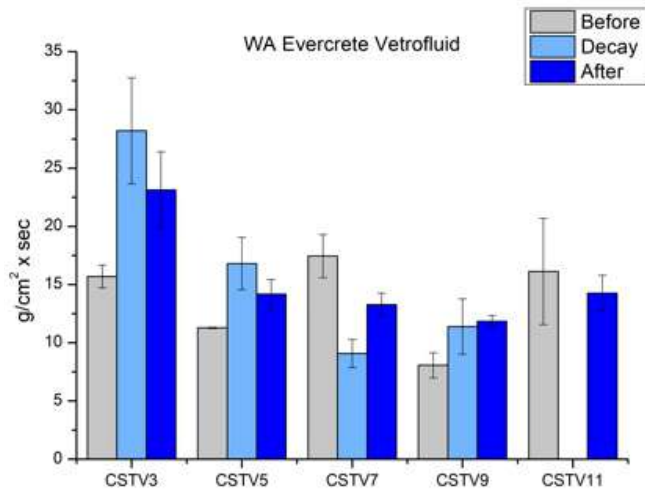


Figure 68. Graph of the evaluations of changes of water absorptions for Vicat Concrete samples treated with Evercrete Vetrofluid.

4.5 Comparison of different application methods

4.5.1 SNP100 applied using capillary absorption and spray methods.

Comparison of results achieved by the treatment of sandstone and granite through spray and capillary absorption methods is reported in this paragraph. In the preview research [1] one sound sample for each lithotypes was treated with SNP100 by capillary absorption method (samples PF1, PM1, BS1). Results of the application of this product (on sample PF6, PM6, BS6) by spray method are reported in §4.4.1.

Microscopic observations on Bianco Sardo, proved that capillary absorption method caused a chromatic variation, and the treated surface seemed to veer to clearer tonality. No visibile alteration was detected on *Pietra di Muggia* e *Pietra di Firenzuola* by optical microscope. The use of spray method did not cause aesthetical changes of the surfaces.

Colorimetric analysis did not show particular color variations of the samples after the application of SNP100 by capillary absorption and ΔE value was for all the specimens lower than 3. The absence of colour alteration was confirmed and improved by spray method, which guaranteed ΔE values less than 1.

The analysis of the changes of anisotropy and velocities let to make some assumptions. Among samples treated by capillary absorption PF1 and PM1, the values change suggesting a reduction of voids. While for BS1 an increment of voids could be defined. Ultrasound analysis showed a slight increment of ΔM (in the range of error) for all the three samples and it can be considered as unchanged. A decrement of voids for all the samples can be considered comparing these values with the values of velocity which increased (PM6, BS6) or stay unchanged (PF6).

Values of water absorption decreased for PF1 and slightly increased for PM1 and BS1. WA increased greatly for all the sample treated by spray method.

Comparing the results of the analysis of application methods it is possible to state that spray methods results the best treatment procedure. SNP100, applied by both capillary absorption and brushing, gave no change from an aesthetical point of view for all the samples. Results of ultrasound analysis gave cheering results for all the sample, while water absorption showed better results for sample treated by capillary absorption method.

4.5.2 Evercrete Vetrofluid applied using brush and spray methods

The effects induced by Evercrete Vetrofluid applied by capillary absorption and brushing methods on concrete samples are summarized in Table 24 and showed acceptable value of ΔE , except for Vicat specimen treated by brushing method.

Table 24. Values of colorimetric variations for Portland and Vicat Concrete specimens treated with Evercrete Vetrofluid via spray and brush method.

Evercrete			
Material	Specimen	Application method	ΔE
Portland	CSTP11	Spray	4,087077
Portland	PC/3	Brush	2,7
Vicat	CSTV11	Spray	3,658634
Vicat	890/3	Brush	7,86

From ultrasound analysis (Figure 69), the decrement of both ultrasound velocity and anisotropy values were recorded only for samples treated by spray method (CSTP11, CSTV11). On the contrary, application of the product by brushing induced an increment of both the values on Vicat concrete (890/3), while on Portland concrete (PC/3) it showed a decrement of both the values.

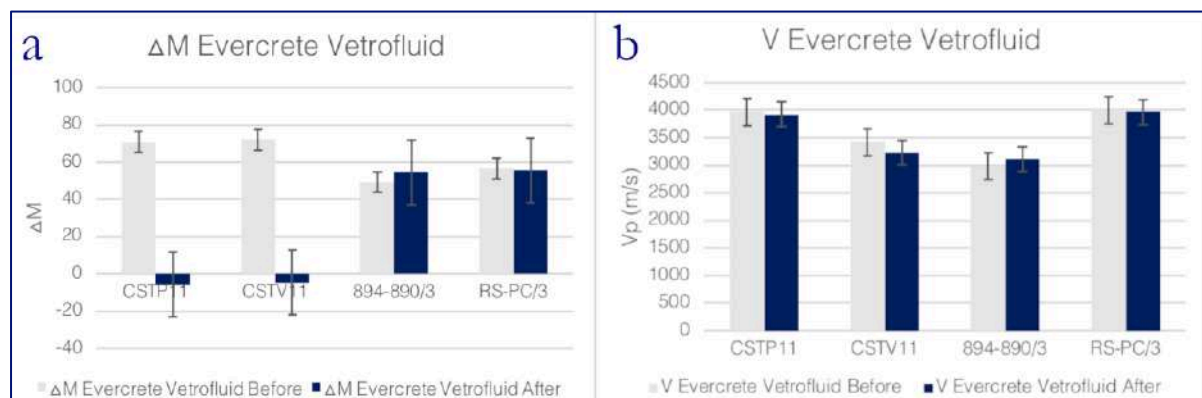


Figure 69. Graphs of changes of values of anisotropy (a) and velocities (b) for Vicat and Portland Concrete specimens treated with Evercrete Vetrofluid.

Vicat concrete specimens showed a very low reduction of the quantity of water absorbed after the treatment applied by spray method, while Portland showed a low increment. These changes are so derisory that are considerable null. Both the materials showed a marked reduction of the absorption of water when the product was applied using brush method (Figure 70).

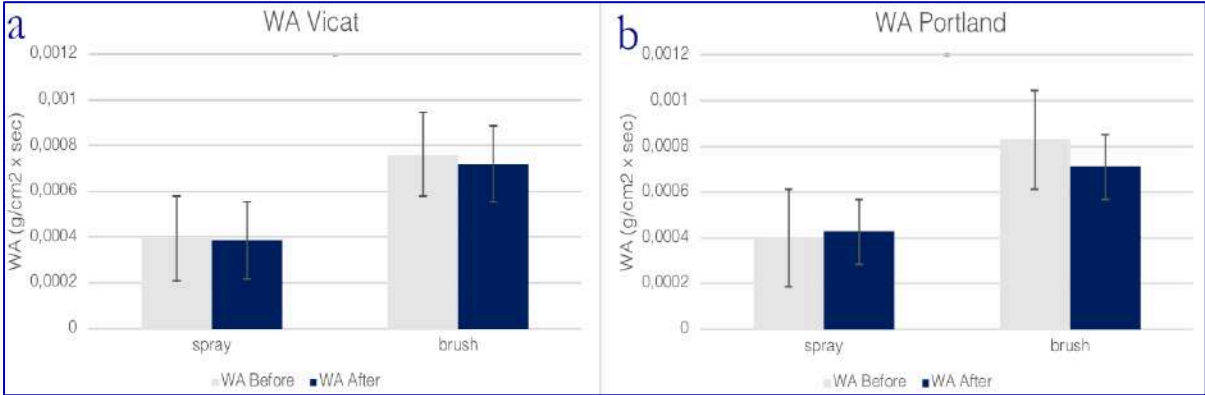


Figure 70. Graph of the evaluations of changes of water absorptions for Vicat Concrete samples treated with Evercrete Vetrofluid.

5 Discussion

5.1 Preliminary analysis of functionalised particles

5.1.1 Functionalisation with Calcium Nitrates

Achievement of the functionalisation of the particles made by the use of calcium nitrates was assessed thanks to SEM-EDS analysis. Dimensional evaluations of the particles showed that the functionalisation did not increase the dimensions of the particles and the average dimension was equal to that of not functionalised particles (100 nm). Presence of Ca was assessed thanks to EDS, mapping part of the particles. It was clearly visible that the presence of different amount of Ca, at the end of the functionalisation, it was related to the initial amount of SiO_2 : $\text{Ca}(\text{NO}_3)_2$. Evaluation of the achieved SEM images allowed to assess the effect of agglomeration and fusion of the particles related to different proportion of reagents and different temperature of calcination. For this reasons proportion of SiO_2 : $\text{Ca}(\text{NO}_3)_2$ reagents was set as best at 70:30 in concentration and temperature of calcination at 500°C . The relation between effect of aggregation and quantity of reagents is confirmed also by the use of Dispersion Analyser. From the results it was possible to see how to parity of higher concentration of $\text{Ca}(\text{NO}_3)_2$ corresponds a decrement of sedimentation velocity, confirming the increment of aggregates. FTIR analysis of the particles confirmed the composition of the compound based on Ca and Si. From the analysis of the particles the process of functionalisation confirmed the results expected and showed to be promising.

In order to evaluate the quality of the compound synthesised as consolidant, some tests of application were made. Functionalised SNP dispersed in an ethanol-water solution were applied. Treatments did not show promising results. The compound deposited on the surface of the treated specimens created a visible white patina. Colorimetric analysis confirmed the variation of L^* value, which veered to clearer tonality. The ineffective achievement of the treatment brought to the decision to not apply the consolidant on concrete and lithotypes specimens chosen for the purpose of the research. Anyway, the good results achieved by the analysis of the functionalisation were promising and became a good starting point for further development.

5.1.2 Functionalisation with Polymeric compound

The first synthetic process of functionalisation was made using the siloxane polymer PMHS. The achieved compound S2a was a solid gel substance. The synthesis was changed and TEOS was removed as reagent of the process obtaining a liquid dense compound named S2b. In order to unify the process of synthesis and functionalisation a one pot reaction was realised producing S2c. S2c was separated in sol (S2c1) and gel (S2c2) phases and the two part were investigated separately. In order to test the capability of S2a to be dispersed in the solvent, the gel compound was dissolved in solvent producing S2d compound.

Tests of application were fundamental in order to evaluate previously how to change the functionalisation and to investigate new synthetic routes. S2a was difficult to apply and, for this reason, no further analyses were made. Comparison of the applications made by the use of S2b, S2c1 and S2d allowed to assess S2b as the best. The application of the compound showed an increment of the water repellence property of the surface and an acceptable change of the aspect of the surface. In order to reduce the aesthetic variations seen by the application of S2b, dilution of the compound in ethanol were made.

For investigating different polymeric compounds PMHS was substitute by PDMS-OH, using the same process of synthesis of S2b. The achieved compound S2e was compared to S2b and both the substances were diluted with concentration of 10% and 20% in solvent. Comparing the results of application, S2e also with a concentration of 10% was evaluated as the best. The surfaces treated with this compound showed an acceptable increment of the contact angle and a low change of the aesthetic properties of the materials.

FTIR analysis of sol and gel phases of the synthesised polymeric compound, allowed to assess the presence of polymers used for the aim of the functionalisation. The synthesised compound showed similar spectral patterns and were characterised by the same peaks, underlining the similar composition of the compounds even if the process of synthesis was different.

From these results the final compound synthesised in order to be applied on the surface was the functionalised SNP by the use of PDMS-OH and dispersed in EtOH. The effectiveness of the functionalisation of SNP by the use of the polymer was assessed by NMR analysis. In NMR spectra of the functionalised compound S2e characteristic peak of the polymer was shifted and presented a secondary peak related to the presence of Si. Thus, the analysis underlined the difference in composition between functionalised and not functionalised SNP.

5.2 Characterisation of concrete materials and the effect of deterioration

Concrete materials taken into account for the purpose of the research were investigated by porosimetric analysis in order to evaluate the matrix quality of the specimens. Comparing porosimetric results of natural and artificial materials it was possible to assess the highest value of open porosity of Vicat concrete equal to 22,47% while Portland Concrete had a reduced value equal to 13,66%.

Evaluation of the strength of concrete were made considering the results achieved by the deterioration processes applied. From the results was possible to state that thermal shock was the process that more than other induced a marked degradation of concrete specimens. Increment of fractures and holes was visible on all Portland and Vicat specimens. This increment was also recorded by the use of ultrasound analysis. Strong effects of deterioration brought some ultrasound measurements to fail because the instrumentation recorded unstable values. Absence of record of measurements symbolized that the material was completely damaged by deterioration, thus we can assess the good achievement of the effect induced by the process. The ultrasound measurement failed for Portland concrete specimen altered by thermal shock (CSTP4) and Vicat concrete specimen decayed by salt crystallization (CSTV6). Probably both the decay procedures induced a strong alteration of the quantity of voids inside the specimen. If thermal shock increased breaks and voids into the materials, on the contrary salt crystallization induced closing of the voids because of the crystallization of salts in the cavity which clog the pores. Moreover, colour of Portland concrete changed showing an increment of ΔE value. From an aesthetical point of view, also specimens degraded by salt crystallisation showed marked change of colour and of the aspect of the surface. Indeed, the deterioration process induced the loss of the edges of the sample and the increment of holes on the surface, recording increment of vacuum in the specimens only for Portland sample n. 5 by ultrasound analysis. Frost and thaw process induced a marked colorimetric variation on samples, particularly for Vicat specimens. The change was probably due to the visible increment of the roughness of the surface.

Water lagoon process was the innovative decay applied in this research. Surfaces of concrete specimens, but also of the natural lithotypes treated with this process, did not show any particular change. Colorimetric investigation of samples demonstrated a change of colour more or less marked. ΔE parameters were lower than 5 for sandstones and granite materials, demonstrating an acceptable colorimetric variation. Differently, concrete materials showed greater values of ΔE . Concrete materials did not show a marked change in their capability of water absorption. *Pietra di Firenzuola* and *Bianco Sardo* increased greatly the absorption, while *Pietra di Muggia* decreased the

value. The majority of the concrete samples analysed showed unchanged value of ultrasound parameters, differently from natural lithotypes characterised by an increment of anisotropy and a general increment of voids. All the treated materials showed a high heterogeneity in their behaviour to the process of degradation. This can be due to the high and different amount of elements and species dispersed in water pollutant, heavy metals, salts and biological elements and to their different interaction with each single element.

5.3 SNP100

A preface must be made before reading the consideration about the results of the analysis. Values achieved by ultrasound investigation were considered a confirmation of the reduction of voids inside the material only when anisotropy decreases and also velocity increases. Moreover, in general when values fall inside the range of error the change of parameters was considered not acceptable.

From the aesthetical point of view, SNP100 could be considered a good consolidant for all the specimens because it did not induce chromatic or morphological variations to the treated surfaces. Variations of ultrasound parameters assessed the decrement of voids inside the samples for four out of five samples: CSTV2, PF6, PM6, BS6. The variation of water absorption is consistent with the porosity of the materials. In fact, Vicat Concrete is the most porous substrate, and it absorbs the most quantity of water when untreated. Its open porosity allowed the penetration of SNP100 that caused a reduction of the amount of water absorbed. All the other tested materials showed a greater amount of water absorbed after the application of the treatment, since their porosity is not sufficient for the penetration of the conservative product. Consequently, SNP100 remained on the surfaces absorbing water itself.

Capillary absorption method induced a greater aesthetic variation of the surface, even if it reduced water absorption if compared to spray method. The direct contact of the surfaces of the specimens with the compound, during the capillary absorption process, brought to a greater absorption of the consolidant inducing the deposition of the particles on the surface. For these reasons a greater change of the aspect was achieved. On the contrary, spray method application resulted better because the amount of compound applied can be more controlled.

5.4 SNP-PDMS

From the results obtained, this consolidant seems not induce particular change of the superficial aspect of the specimens. Indeed, none of the treated samples induced chromatic and morphological alteration.

On silicate stones the application of SNP-PDMS was attested through microscopic observation for those specimens deteriorated with salt crystallisation (n. 12). In case of granite samples, the evaluation of aesthetical changes resulted quite difficult because of the natural iridescence of crystals of the stone matrix.

Variation of water absorption revealed a decrement of WA on two samples of *Bianco Sardo* out of five: BS15 (degraded by frost and thaw) and BS18 (degraded by water lagoon). *Pietra di Firenzuola* showed a reduction of water absorbed only for specimens PF18 degraded by water lagoon, whereas *Pietra di Muggia* decreased WA values for PM12 (salt crystallization) and PM18 (water lagoon) samples.

Ultrasound analysis revealed a decrement of voids after the application of the compound for two samples of *Pietra di Firenzuola* and three samples for *Pietra di Muggia* and *Bianco Sardo*. It is interesting to assess that decrement of voids was recorded in all the materials that were previously degraded by frost and thaw (n. 15) process, samples degraded by water lagoon (PM18, BS18) and samples not degraded (PM21, BS21).

In general, sponge test and ultrasound measurements showed good performance of the treatment for those specimens degraded by water lagoon process (PF18, PM18, BS18). Moreover, these samples did not show any aesthetic change, probably because of the good penetration of the compound in the stone substrate.

The efficacy of the treatment is strictly related to the porosity of sound and degraded material.

The poor results achieved by sponge test analyses attested the not hydrorepellency of the surfaces. These results with the inconsistent chromatic change of the specimens and the not attested presence of the compound after the treatment, let to suppose the absence of the treatment, thus the inefficacy of spray application method.

On the other hand, on concrete the presence of the consolidant was visible only on two specimens: a Portland concrete, which showed a light glowing effect, and a Vicat concrete, where it was visible the compound deposited inside a fracture of the surface.

The greatest change of colour after the application of SNP-PDMS was recorded on those specimens deteriorated by frost and thaw process (n.8).

Both Portland and Vicat concrete showed a decrement of WA values for specimens n.10 degraded by water lagoon. Two other Vicat specimens showed the same trend: CSTV4 degraded by thermal shock and sound sample CSTV12.

For both concrete materials, decrement of voids after the application of consolidant was recorded for specimens degraded by frost and thaw process (n. 8). Portland concrete showed a decrement of voids after the application of the consolidants in samples CSTP6 and CSTP10 (respectively degraded by salt crystallisation and thermal shock), while Vicat concrete showed a decrement of void also for specimen CSTV4 (degraded by thermal shock) and that deteriorated by water lagoon.

No correlation between sponge test and ultrasound analyses was found. However, also in this case a major porosity of the material (Vicat concrete) guaranteed a greater penetration of the compound.

From these considerations, it is possible to assess that SNP-PDMS treatment is good to restore porous samples. Comparing stone and concrete materials, the product seems to be more effective in case of concrete samples, probably due to the highest porosity of the material, respect to that of natural lithotypes. These results and those obtained by the preliminary tests underlined the effectiveness of the functionalisation and the high performance of SNP-PDMS as consolidant. However, in order to guarantee a better performance, brushing method is strongly recommended for the application of the compound.

5.5 Evercrete

The presence of Evercrete Vetrofluid commercial product on sample surfaces was visible for about the totality of the treated specimens. The presence of consolidant induced a glowing effect to the surfaces, particularly marked on all the *Bianco Sardo* and concrete specimens, but limited in all the *Pietra di Muggia* samples and insubstantial on *Pietra di Firenzuola* specimens.

Generally, all the treated specimens showed a colorimetric variation higher than that achieved by the application of SNP-PDMS. In accordance to microscopic observations, all *Bianco Sardo* specimens showed ΔE values between 2 and 4,5, whereas samples deteriorated by salt crystallisation (PF13, PM13, BS13) showed the lowest values of ΔE .

Water absorption decreased in case of sample BS16 and PF16 both degraded by water lagoon and PM7, which suffered thermal shock.

Ultrasound analysis of samples showed satisfying results for sandstones and granite. For all sound and degraded materials (except for PF10 and PM10 degraded by salt crystallization) a reduction of voids after the treatment was detected.

From all the results obtained, it is possible to assess that the best performance of Evercrete Vetrofluid resulted in the specimens, which suffered decay induced by water lagoon process (PF16, PM16, BS16). Although a slight alteration of the aesthetic properties of the surfaces was visible, a decrement of WA coefficient and voids was found.

Comparing concrete samples, colour changes resulted particularly marked on Vicat specimens, especially on CSTV7 and CSTV9. A particular reflection of light, caused probably by the inhomogeneous application of Evercrete Vetrofluid, was visible on treated surfaces also to the naked eye and it altered the general aspect of the samples.

Regarding water absorption parameter, Vicat specimens showed a decrement of WA for those sample degraded by salt crystallization and thermal shock, whereas Portland concrete showed a reduction of WA only for sound specimens. The increasing of WA values after degradation processes, which involve the use of water, is probably due to the continuous of cement setting process, which induce the closure of material porosity.

Portland and Vicat specimens degraded by salt crystallisation (CSTP5, CSTV5) are the only concrete specimens, which showed decrement of void amount.

In general, the decrement of voids in the materials, the low colorimetric variation and no change of the aspect let to consider spray method the best way to apply the compound. However, the results of water absorption assessed brush method as the best.

6 Conclusions

The aim of the research was to synthesize and functionalize SNP in order to produce a consolidant for sandstone, granite and concrete. Siloxane polymers PMHS, PDMS-OH and calcium nitrate were individuated as promising reagents for the functionalization.

Evaluation of the synthesized compound by a physical chemical characterization and tests of application allowed to underline drawbacks and positive aspects of consolidants and to define some changes to improve qualities of the products.

Preliminary investigation of the particles functionalised with $\text{Ca}(\text{NO}_3)_2$, performed by SEM-EDX, FTIR and Dispersion Analyser, evidenced the presence of calcium on SNP surface. The main drawback concerned the low degree of separation of the particles and a marked effect of fusion. The effect was reduced for SNP prepared with a concentration of 70:30 SiO_2 : $\text{Ca}(\text{NO}_3)_2$ and treated at 500°C . The ratio 70:30 and $T=500^\circ\text{C}$ were selected as the best parameters to be used in the process of reaction. Analysis of the particles demonstrates the presence of Ca on SNP and the achievement of the functionalisation. Study of the concentration of the reagents in phase of synthesis allowed to confirm the relation between the proportion of reagents, the temperature of calcination and the degree of agglomeration of particles. Although the good results achieved by the analysis, tests of application did not show positive effect of consolidation of the tested surfaces and further development on the functionalisation have been made in order to investigate deeper the compound and improve its qualities.

The SNP functionalization with PDMS-OH was confirmed by FTIR analysis. The spectra showed the characteristic peaks related to the presence of polymeric substance and of silica. Moreover, the composition of the functionalised particles was also confirmed by NMR analysis. After several application tests, the best consolidant was composed of 10% of SNP functionalized with PDMS-OH (SNP-PDMS) dispersed in EtOH.

Three different consolidants, SNP100, SNP-PDMS and the commercial compound Evercrete Vetrofluid, were applied by spray method. Three natural lithotypes (*Pietra di Firenze*, *Pietra di Muggia*, Bianco Sardo) and two artificial lithotypes (Portland Concrete and Vicat concrete) were used as material to be consolidated.

Eight specimens of each material were degraded using four different processes (thermal shock, salt crystallization, frost and thaw and water lagoon) to simulate real conditions of conservation and to study the resistance of materials to degradation phenomena. Cements resulted to suffer

particularly the effect induced by thermal shock, while they showed to be less sensible to degradation caused by frost and thaw and salt crystallization. The necessity to study the effect of degradation of cements in lagoon environment, brought to the development of a new kind of test, and two samples of each material were immersed in water lagoon. This kind of degradation showed to affect differently each sample, also of the same material. Comparison with the effects induced by the immersion in salty solution, performed in the laboratory, underlined the difficulty to preserve material conserved in real lagoon conditions.

Investigation of different treatment methods to apply SNP100 demonstrated that the use of capillary absorption method increased the excess of compound on the surface inducing aesthetic variations that were not achieved by spray method. The compound applied by the use of spray method showed limited aesthetical variation and, for the majority of the specimens, a reduction of voids in the materials. Thus, application by the use of spray method could be considered the best.

The application of Evercrete Vetrofluid changed the general aspect of the treated surfaces. This effect was not recorded using SNP-PDMS and SNP100. From all the results obtained, it is possible to state that SNP-PDMS and Evercrete Vetrofluid can be considered good conservative treatments for improving qualities of specimens deteriorated by water lagoon process. The results obtained allowed to consider both the product as possible protectives with hydrophobic features but not as good strengthening agents. Nevertheless, comparing the two products it is possible to assess that SNP-PDMS showed the best results in terms of no morphological and chromatic alteration. No significant variation was achieved by ultrasound analyses using this nano-compound, probably due to its low or no penetration. In any case, an eventual low quantity of the product in the stone substrate resulted inefficient in order to influence ultrasound parameters.

Water absorption results showed significant variation only where the superficial porosity of the material allowed the penetration of the product. The increment of the quantity of water absorbed assessed an absence of product on the surfaces, also confirmed by microscopic investigations. This lack led to state that the application method used for testing SNP-PDMS on silicate stones and concrete was ineffective. The good results obtained by the preliminary test of SNP-PDMS on Carrara marble and Vicenza limestone suggest to use brushing method for the application of the compound. On the contrary, Evercrete Vetrofluid gave good results also when applied by spray method (as reported also in the technical sheet).

In conclusion, it is possible to state that SNP functionalized using PDMS-OH represents a promising nano system for the consolidation of sound and degraded silicate lithotypes and concretes.

7 Bibliography

- [1] Neva M. E. Stucchi, "Sintesi e analisi di nano-prodotti a base di silice per il consolidamento di materiali lapidei naturali", [Tesi di laurea Università Ca' Foscari Venezia, relatore Prof. Alvise Benedetti, a.a. 2018-2019]
- [2] E. Doehne et al., "Stone Conservation: an Overview of Current Research", second ed., Getty Publications, Los Angeles, 2010, pp. 35, 40
- [3] J. D. Rodrigues, "Stone consolidation: research and practice", Proceedings Int. Symp. on Works of Art and Conservation Science Today, Greece, 2010
- [4] G. Wheeler, "Alkoxysilanes and the Consolidation of Stone", 2005, pp. 2, 5, 63
- [5] A.P. Ferreira Pinto et al., "Impacts of consolidation procedures on colour and absorption kinetics of carbonate stones", *Stud. Conserv.* 59 (2), 2012, pp. 79–90
- [6] G. Borsoi et al., "Evaluation of the effectiveness and compatibility of nanolime consolidants with improved properties", *Construction and Building Materials* 142, 2017, pp. 385–394
- [7] E. Tesser et al., "Evaluation of silicone-based products used in the past as today for the consolidation of Venetian monumental stone surfaces", *Mediterranean Archaeology and Archaeometry* 18, 2018, pp. 159-170
- [8] B. Pigino et al., "Ethyl silicate for surface treatment of concrete - Part II: characteristics and performance", *Cement Concr. Compos.* 34, 2012, pp. 313–321.
- [9] A.M. Barberena-Fernández et al., "Interaction of TEOS with cementitious materials: chemical and physical effects", *Cement Concr. Compos.* 55, 2015, pp.145–152.
- [10] B. Stewart, "Analytical techniques Techniques in Materials Conservation", John Wiley & Sons, 2007, pp. 23,37, 91-95, 110-112
- [11] K. Hempel et al., "Summary of work on marble conservation at the Victoria and Albert Museum Conservation Department", Proceedings In The Treatment of Stone, ed. R. Rossi-Manaresi and G. Torraca, Bologna: Centro per la Conservazione delle Sculture all'Aperto, 1972, pp. 165-181
- [12] G. W. Scherer et al., "Silicate Consolidants for Stone", *Key Engineering Materials* Vol. 391, 2009, pp. 1-25
- [13] G.G. Amoroso et al., "Stone decay and conservation", Elsevier, New York, 1983
- [14] F. Iucolano, et al., "Suitability of silica nanoparticles for tuff consolidation", *Construction and Building Materials* 202, 2019, pp. 73-81
- [15] M.F. La Russa et al., "Cappadocian ignimbrite cave churches: stone degradation and conservation strategies", *Period. Mineral.* 8, 2014, pp. 187-206
- [16] M.F. La Russa et al., "The behaviour of consolidated Neapolitan yellow Tuff against salt weathering", *Bull. Eng. Geol. Environ.*, 2017, pp. 115-124
- [17] C. Miliani et al., "Particle-modified consolidants: a study on the effect of particles on sol–gel properties and consolidation effectiveness", *J. Cult. Herit.* 8, 2007, pp. 1–6.
- [18] A.M. Barberena-Fernández et al., "Use of nanosilica- or nanolime-added TEOS to consolidate cementitious materials in heritage structures: Physical and mechanical properties of mortars", *Cement and Concrete Composites* 95, 2019, pp. 271–276

- [19] E. Tesser et al., "The decay of the polysiloxane resin Sogesil XR893 applied in the past century for consolidating monumental marble surfaces", *Journal of Cultural Heritage* 27, 2017, pp. 107-115
- [20] J.S. Pozo-Antonio et al., "Nanolime- and nanosilica-based consolidants applied on heated granite and limestone: Effectiveness and durability", *Construction and Building Materials*, 2019, pp. 852-87
- [21] P. Hou et al., "Characteristics of surface- treatment of nano-SiO₂ on the transport properties of hardened cement pastes with different water-to-cement ratios", *Cement Concr. Compos.* 55, 2015, pp. 26–33.
- [22] UNI EN 12370, "Determinazione della resistenza alla cristallizzazione dei sali", 1999, pp. 1-8
- [23] UNI EN 1237, "Determinazione della resistenza al gelo", 2003, pp. 1-8
- [24] A. Zornoza-Indart et al., "Silica nanoparticles (SiO₂): Influence of relative humidity in stone consolidation", *Journal of Cultural Heritage* 18, 2016, pp. 258-270
- [25] T. Jesionowski et al., "Preparation of the hydrophilic/hydrophobic silica particles", *Colloids and Surfaces: Physicochemical and Engineering Aspects* 207, 2002, pp.49–58
- [26] K. Yu et al., "Coupling of synthesis and modification to produce hydrophobic or functionalized nano-silica particles", *Colloids and Surfaces A* 574, 2019, pp. 122–130
- [27] A. Del Tedesco et al., "Functionalization of Mesoporous Silica Nanoparticles with Organosilanes: Experimental Evidence of the Interaction Between Organic Groups and Silica Surface", *Current Organic Chemistry* (21), 2017, pp. 1-11
- [28] R. P. Bagwe, et al., "Surface Modification of Silica Nanoparticles to Reduce Aggregation and Nonspecific Binding", *Langmuir*, 2006, pp. 4357-4362
- [29] A. Idris et al., "Investigation on particle properties and extent of functionalization of silica nanoparticles", *Applied Surface Science* 506, 2020
- [30] B. G. Trewyn, et al., "Synthesis and Functionalization of a Mesoporous Silica Nanoparticle Based on the Sol–Gel Process and Applications in Controlled Release", *Acc. Chem. Res.* 40, 2007, pp. 846–853
- [31] V. V. Gorbachuk et al., "Silica Nanoparticles with Proton Donor and Proton Acceptor Groups: Synthesis and Aggregation", Springer Science+Business Media, 2011
- [32] B. Yu et al., "Synthesis and modification of monodisperse silica microspheres for UPLC separation of C60 and C70", *Analytical Methods*, 2016, pp. 919-924
- [33] X. Hue et al., "Super-hydrophobicity of silica nanoparticles modified with vinyl groups", *Colloids and Surfaces Physicochem. Eng. Aspects* 338, 2009
- [34] J. Haas, et al., "From C–S–H to C–A–S–H: experimental study and thermodynamic modelling", *Cem. Concr. Res.* (68), 2015, pp.124–138
- [35] V. Daniele et al., "Synthesis of Ca(OH)₂ Nanoparticles Aqueous Suspensions and Interaction with Silica Fume", *Advanced Materials Research* Vol 629, 2013, pp. 482-487
- [36] R. Camerini et al., "Hybrid nano-composites for the consolidation of earthen masonry", *Journal of Colloid and Interface Science*, 2019
- [37] D.R.G. Mitchell, et al., "Interaction of silica fume with calcium hydroxide solutions and hydrated cement pastes", *Cem. Concr. Res.* 28,1998, pp. 1571–1584,

- [38] B. Lothenbach et al., "Supplementary cementitious materials", *Cem. Concr. Res.* 41, 2011, pp.1244–1256.
- [39] E. Bernard et al., "Effective cation exchange capacity of calcium silicate hydrates (C-S-H)", *Cement and Concrete Research* 143, 2021
- [40] S. L. Greasley et al., "Controlling particle size in the Stöber process and incorporation of calcium", *Journal of Colloid and Interface Science* 469, 2016, pp. 213–223
- [41] O. Tsigkou et al., "Monodispersed bioactive glass submicron particles and their effect on bone marrow and adipose tissue-derived stem cells", *Adv. Healthc. Mater.* 3, 2014, pp.115–125.
- [42] S. Lin et al., "Nanostructure evolution and calcium distribution in sol–gel derived bioactive glass", *J. Mater. Chem.* 19, 2009, pp. 1276–1282.
- [43] C. Rodriguez-Navarro et al., "Alcohol Dispersions of Calcium Hydroxide Nanoparticles for Stone Conservation", *Langmuir*, 2013, pp. 11457–11470
- [44] P. Candiano et al., "Epoxy-Silica Polymers as stone conservation materials", *Polymer* (46), 2005
- [45] V. M. Gun'ko et al., "Polymethylsiloxane alone and in composition with nanosilica under various conditions", *Journal of Colloid and Interface Science* 541, 2019, pp. 213- 225
- [46] F. Juan, "Surfactant-Synthesized PDMS/Silica Nanomaterials Improve Robustness and Stain Resistance of Carbonate Stone", *Phys. Chem. C* (115), 2011, pp. 14624–14634
- [47] F. Xu et al., "Effects of addition of colloidal silica particles on TEOS-based stone protection using n-octylamine as a catalyst", *Progress in Organic Coatings* 75, 2012
- [48] Y. Luo et al., "Characterization of TEOS/PDMS/HA nanocomposites for application as consolidant/hydrophobic products on sandstones", *Journal of Cultural Heritage*, 2015, pp. 470-478
- [49] Z. Sun et al., "A reactive compatibilizer for polydimethylsiloxane-polyurethane composite coating", *Progress in Organic Coatings* 152, 2021, pp.106-118
- [50] Y. Zhan et al., "Tunable wettability of monodisperse core-shell nano-SiO₂ modified with poly(methylhydrosiloxane) and allyl-poly(ethylene glycol) ", *Colloids and Surfaces A: Physicochem. Eng. Aspects* 441, 2014, pp. 16-24
- [51] Information about PMHS : <https://www2.chemistry.msu.edu/faculty/maleczka/pdfs/EROS1.pdf>
- [52] J. Lin et al., "Mechanochemically conjugated PMHS/nano-SiO₂ hybrid and subsequent optimum grafting density study", *Applied Surface Science* 257, 2011, pp. 9024–9032
- [53] J. Wen et al., "Sol-Gel Preparation of Composites of Poly(dimethylsiloxane) with SiO₂ and SiO₂/TiO₂, and Their Mechanical Properties ", *Polymer Journal*, Vol. 27, No. 5, 2005, pp. 492-502
- [54] M. Pretelli et al., "From the artificial stone to the reinforced concrete: data system project for diagnostic", *Scientific research and safeguarding of Venice. Research Programme 2004-2006*, Vol. IV, 2005
- [55] P. Faccio et al., "From artificial stone to reinforced concrete II: project for experimental investigation protocol for the characterisation of decay phenomena", *Scientific research and safeguarding of Venice. Research Programme 2004-2006*, Vol. V, 2005
- [56] M. Pretelli et al., "La pietra artificiale. Un patrimonio da salvaguardare", *Università IUAV, Venezia*
- [57] G. Bruschi et al., "Materiali cementizi in ambiente lagunare veneziano: linee guida di una sperimentazione volta alla valutazione dello stato di conservazione del materiale", *Università IUAV, Venezia, DCA*

- [58] N. M. E. Stucchi et al., "Synthesis and characterization of nanosilica products for the consolidation of stones. ", 2019 IMEKO TC-4 International Conference on Metrology for Archaeology and Cultural Heritage Florence, Italy, 2019, pp. 299-304
- [59] D. S. de Toledo Pereira et al., "Comparative analysis between properties and microstructures of geopolymeric concrete and portland concrete", *j mater res technol.*, 2018, pp. 606–611
- [60] A. P. Ferreira Pinto et al., "Consolidation of carbonate stones: Influence of treatment procedures on the strengthening action of consolidants", *Journal of Cultural Heritage* 13, 2012, pp.154–166
- [61] Technical sheet: https://www.sigmaaldrich.com/specification-sheets/420/781/176206-BULK_ALDRICH.pdf
- [62] Technical sheet: <https://www.sigmaaldrich.com/specification-sheets/162/763/481939-BULK.pdf>
- [63] Ecobeton website: <https://www.ecobeton.it/products/evercrete-vetrofluid>
- [64] G. Blanco, "Manuale di progettazione marmi e pietre", Gruppo Mancosu Editore, 2008.
- [65] S. Furlani, F. Cucchi, "Short-term surface changes on sanstone rocks", *Annales, Ser. hist. nat.* 17, 2007, pp. 241-248.
- [66] S. Volpin et al. "Le analisi di laboratorio applicate ai beni artistici e policromi", Collana Talenti, Il prato, 2002, pp. 38-43
- [67] McGraw-Hill, "McGraw-Hill Dictionary of Chemistry", 27 January 2003, pp. 31
- [68] D. A. Skoog, D. M. West, "Fondamenti di chimica analitica", Edises, 2019, pp. 715- 719
- [69] T. Detloff et al., "Particle size distribution by space or time dependent extinction profiles obtained by analytical centrifugation (concentrated systems)", *Powder Technology* 174(1), 2007, pp. 50-55
- [70] S. L. Sedinkin et al., "An organogel library for solution NMR analysis of nanoparticle suspensions in non-aqueous samples", *Journal of Magnetic Resonance* 321, 2020
- [71] NORMAL 4/80, "Distribuzione del volume dei pori in funzione del loro diametro", *Porosimetria a mercurio*, Ediz. n° 1, 1980, pp. 1-10
- [72] UNI EN 11432: 2011, "Misura della capacità di assorbimento di acqua mediante spugna di contatto", 2011, pp. 1-12
- [73] UNI EN 14579: 2009, "Metodi di prova per le pietre naturali. Determinazione della velocità di propagazione del suono", 2009, pp. 2-11
- [74] M. R. Darrick et al., "Infrared Spectroscopy in Conservation Science", The Getty Conservation Institute, Los Angeles, 1999, pp. 117
- [75] A. Beganskiene et al., "FTIR, TEM and NMR investigations of Stöber Silica Nanoparticles", *Materials Science* Vol. 10 No. 4, 2004, pp. 287-290
- [76] P. Maravelaki et al., "A Hybrid Consolidant of Nano- Hydroxyapatite and Silica Inspired from Patinas for Stone Conservation" in *Advanced Materials for the Conservation of Stone*, Springer, 2018, pp. 83-93
- [77] I. Protsak et al, "A New Route for Preparation of Hydrophobic Silica Nanoparticles Using a Mixture of Poly(dimethylsiloxane) and Diethyl Carbonate",
- [78] J. Gonzalez-Rivera et al., "Structural and Thermoanalytical Characterization of 3D Porous PDMS Foam Materials: The Effect of Impurities Derived from a Sugar Templating Process.", *Polymers*, 2018, pp. 616
- [79] S. WookHan et al., "Polydimethylsiloxane thin-film coating on silica nanoparticles and its influence on the properties of SiO₂-polyethylene composite materials", *Polymer*, Volume 138, 2018, pp. 24-32

- [80] T. Rattanaumpa et al, "Polydimethylsiloxane Sponges Incorporated with Mesoporous Silica Nanoparticles (PDMS/H-MSNs) and Their Selective Solvent Absorptions
- [81] G.R. Fulmer et al., "NMR Chemical Shifts of Trace Impurities: Common Laboratory Solvents, Organics, and Gases in Deuterated Solvents Relevant to the Organometallic Chemist", *Organometallics* 2010, pp. 2176–2179
- [82] C. Coletti, et al., "Use of industrial ceramic sludge in brick production: Effect on aesthetic quality and physical properties", *Construction and Building Materials*, 2016, pp. 219-227
- [83] C. Coletti, et al., "How to face the new industrial challenge of compatible, sustainable brick production: Study of various types of commercially available bricks", *Applied Clay Science*, 2016, pp. 0-8

8 Technical sheets

A. TEOS

SIGMA-ALDRICH[®]

sigma-aldrich.com

3050 Spruce Street, Saint Louis, MO 63103, USA

Website: www.sigmaaldrich.com

Email USA: techserv@sial.com

Outside USA: eurtechserv@sial.com

Product Specification

Product Name:

Tetraethyl orthosilicate reagent grade, 98%

Product Number:

131903

CAS Number:

78-10-4

MDL:

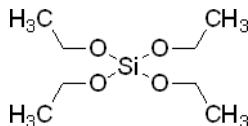
MFC00009062

Formula:

C₈H₂₀O₄Si

Formula Weight:

208.33 g/mol



TEST	Specification
Appearance (Color)	Colorless
Appearance (Form)	Liquid
Infrared spectrum	Conforms to Structure
Purity (GC)	≥97.5 %

Remarks:

Specification Date : 06/21/2010

Sigma-Aldrich warrants, that at the time of the quality release or subsequent retest date this product conformed to the information contained in this publication. The current Specification sheet may be available at Sigma-Aldrich.com. For further inquiries, please contact Technical Service. Purchaser must determine the suitability of the product for its particular use. See reverse side of invoice or packing slip for additional terms and conditions of sale.

B. Calcium Nitrate

SIGMA-ALDRICH[®]

sigma-aldrich.com

3050 Spruce Street, Saint Louis, MO 63103, USA

Website: www.sigmaaldrich.com

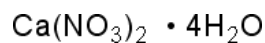
Email USA: techserv@sial.com

Outside USA: eurtechserv@sial.com

Product Specification

Product Name:
Calcium nitrate tetrahydrate - $\geq 99.0\%$

Product Number: C1396
CAS Number: 13477-34-4
MDL: MFCD00149604
Formula: CaN₂O₆ · 4H₂O
Formula Weight: 236.15 g/mol



TEST	Specification
Appearance (Color)	White
Appearance (Form)	Powder or Crystals
Solubility (Turbidity)	Clear
At 20g plus 100ml of Water	
Solubility (Color)	Colorless
Complexometric EDTA	$\geq 99.0\%$
Recommended Retest Period	-----
3 Years	

Specification: PRD.0.ZQ5.10000028031

Sigma-Aldrich warrants, that at the time of the quality release or subsequent retest date this product conformed to the information contained in this publication. The current Specification sheet may be available at Sigma-Aldrich.com. For further inquiries, please contact Technical Service. Purchaser must determine the suitability of the product for its particular use. See reverse side of invoice or packing slip for additional terms and conditions of sale.

C. Polymethylhydrosiloxane

SIGMA-ALDRICH[®]

sigma-aldrich.com

3050 Spruce Street, Saint Louis, MO 63103, USA

Website: www.sigmaaldrich.com

Email USA: techserv@sial.com

Outside USA: eurtechserv@sial.com

Product Specification

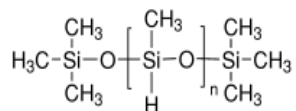
Product Name:

Poly(methylhydrosiloxane) average Mn 1,700-3,200

Product Number: 176206

CAS Number: 63148-57-2

MDL: MFCD00084478



TEST	Specification
Appearance (Color)	Colorless
Appearance (Form)	Liquid
Infrared spectrum	Conforms to Structure
Viscosity at 25 degrees Celsius	12- 45 cps

Remarks:

Specification Date : 12/28/2010

Sigma-Aldrich warrants, that at the time of the quality release or subsequent retest date this product conformed to the information contained in this publication. The current Specification sheet may be available at Sigma-Aldrich.com. For further inquiries, please contact Technical Service. Purchaser must determine the suitability of the product for its particular use. See reverse side of invoice or packing slip for additional terms and conditions of sale.

D. Poly(dimethylsiloxane) hydroxy terminated

SIGMA-ALDRICH[®]

sigma-aldrich.com

3050 Spruce Street, Saint Louis, MO 63103, USA

Website: www.sigmaaldrich.com

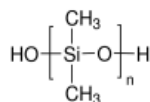
Email USA: techserv@sial.com

Outside USA: eurtechserv@sial.com

Product Specification

Product Name:
Poly(dimethylsiloxane), hydroxy terminated - viscosity ~65 cSt

Product Number: 481955
CAS Number: 70131-67-8
MDL: MFCD01325010
Formula: C₂H₆O_{Si}



TEST	Specification
Appearance (Color)	Colorless
Appearance (Form)	Liquid
Infrared spectrum	Conforms to Structure
Hydroxyl Value	1.0 - 1.7 %
Volatiles	≤ 4.0 %
Viscosity (cst) at 25 Degrees Celsius	55 - 90

Specification: PRD.1.ZQ5.1000051702

Sigma-Aldrich warrants, that at the time of the quality release or subsequent retest date this product conformed to the information contained in this publication. The current Specification sheet may be available at Sigma-Aldrich.com. For further inquiries, please contact Technical Service. Purchaser must determine the suitability of the product for its particular use. See reverse side of invoice or packing slip for additional terms and conditions of sale.

E. Hexylamine

Specification Sheet

Product Name	Hexylamine 99%
Product Number	219703
Product Brand	ALDRICH
CAS Number	111-26-2
Molecular Weight	101.19

TEST	SPECIFICATION
APPEARANCE (COLOR)	Colorless
APPEARANCE (FORM)	Liquid
COLOR (IN APHA)	≤ 100 APHA
TITRATION (NT) HClO₄ 0.1M	98.5 - 101.5 %
PURITY (GC AREA %)	≥ 98.5 %
INFRARED SPECTRUM	CONFORMS TO STRUCTURE

F. Evercrete Vetrolfluid

Evercrete Vetrolfluid®

IMPERMEABILIZZANTE PER CALCESTRUZZO



PRODOTTO DESTINATO AD USO PROFESSIONALE - REVISIONE: 3 DICEMBRE 2018

Evercrete Vetrolfluid® è uno speciale impermeabilizzante antidegrado per calcestruzzo. La sua formulazione, a base di vetro liquido e speciale additivo modificatore, permette al prodotto di penetrare autonomamente da un minimo di 10 mm fino a 40 mm nel calcestruzzo sigillandone le porosità e diventando una barriera definitiva e permanente nel tempo. Evercrete Vetrolfluid® viene applicato per impermeabilizzare, proteggere e consolidare qualsiasi tipo di calcestruzzo.

Proprietà

Evercrete Vetrolfluid® garantisce l'impermeabilizzazione permanente del calcestruzzo anche in spinta negativa fino a 10 atm (cento metri di colonna d'acqua).

Evercrete Vetrolfluid® conferisce al calcestruzzo una straordinaria resistenza ai cicli di gelo e disgelo, all'attacco di cloruri, solfati e sali disgelanti.

Evercrete Vetrolfluid® blocca completamente il fenomeno della carbonatazione e la penetrazione dei cloruri (UNI 9944). Mantiene nel tempo un ambiente alcalino stabile che protegge in modo totale il ferro d'armatura.

Evercrete Vetrolfluid® è certificato per l'uso a contatto con acqua potabile ed è adatto ad impermeabilizzare e proteggere vasche in calcestruzzo e superfici ad uso alimentare.

Evercrete Vetrolfluid® conferisce al calcestruzzo un'ottima resistenza agli attacchi chimici.

Evercrete Vetrolfluid® contrasta efficacemente la formazione di muffe, alghe e muschio.

Evercrete Vetrolfluid® è carrabile e abbinabile ad altri rivestimenti.

Evercrete Vetrolfluid® aumenta la resistenza al fuoco, è totalmente incombustibile e mantiene le sue caratteristiche a qualsiasi temperatura, compatibilmente con i limiti fisici del calcestruzzo trattato.

Evercrete Vetrolfluid® applicato nelle platee e nei piedi di fondazione blocca l'umidità di risalita.

Evercrete Vetrolfluid® impedisce al calcestruzzo di rilasciare polveri di cemento nell'ambiente, ostacola efficacemente la penetrazione di inquinanti e rende gli ambienti più salubri.

Evercrete Vetrolfluid® è un prodotto inodore, incolore ed atossico.

Evercrete Vetrolfluid® è un trattamento permanente e definitivo.

Evercrete Vetrolfluid® è un prodotto marcato CE secondo UNI EN 1504-2 "Prodotto per la protezione del calcestruzzo per impiego in fabbricati ed in opere di ingegneria civile".

Utilizzi

- Su muri controterra per impermeabilizzare sia dall'esterno che dall'interno.
- Per impermeabilizzare e proteggere dal degrado e dalla corrosione il calcestruzzo di ponti, sottopassi, dighe e gallerie.

- In depuratori, pozzetti e vasche di raccolta a contatto con sostanze aggressive e idrocarburi.
- In tutte le strutture di calcestruzzo immerse, per fermare l'attacco di cloruri.
- Nelle cantine e nelle strutture agricole (stalle, grigliati, depositi di cereali e fieno, porcilaie, silos in calcestruzzo).
- Nelle vasche di biogas e nelle trincee per la difesa del calcestruzzo dall'attacco acido della biomassa, dai gas e dal percolato.
- Nelle vasche a contatto con acque nere e reflue.
- Nelle vasche di acqua potabile.
- Su calcestruzzo sottoposto a gravose condizioni climatiche.
- Nelle fondazioni continue e nei piedi di fondazione per bloccare l'umidità di risalita.
- Negli interrati che trasudano umidità.
- Su solai e solette, sia come impermeabilizzazione temporanea che definitiva.
- Su loculi cimiteriali.
- Su canalizzazioni e canali di irrigazione.
- Su calcestruzzo facciavista.
- Su calcestruzzo prefabbricato e new jersey.
- Dovunque si desideri aumentare la durabilità delle opere in calcestruzzo.

Caratteristiche

Composizione	Miscela proprietaria di waterglass in soluzione acquosa arricchita di speciale catalizzatore
Scadenza	36 mesi se conservato sigillato
Inflamabilità	Non applicabile
Rischio ambientale	Assente
Proprietà organolettiche	Liquido inodore e incolore
Stoccaggio	Conservare in luogo fresco e asciutto, lontano da vetro e alluminio
Contenuto di VOC	Assente
Maturazione	36 giorni. Pedonabile dopo poche ore
Confezioni	Ecobox da 20 kg e secchio da 6 kg

ECOBETON

Certificazioni

 <p style="text-align: center;">Ecobeton Italy Srl Via Galileo Galilei 47, 36030 Costabissara (VI) 08 Certificato n° GB08/76012 DOP n° 140107DOP-1504-2</p>	
<p>UNI EN 1504-2:2005 Evercrete® - Vetrolfluid®</p> <p>Prodotto per la protezione del calcestruzzo per impiego in fabbricati ed in opere di ingegneria civile Impregnazione</p>	
EN 1339 EN 1062-3	Resistenza all'abrasione: miglioramento > 30% Assorbimento capillare e permeabilità all'acqua: w < 0,1 kg/mq x h0,5
EN 2812-1 EN 13687-1 EN ISO 6272-1 EN 1542 EN 13501-1	Resistenza chimica (mezzo assorbente): nessun difetto Compatibilità termica: ≥ 1,5 N/mm ² Resistenza all'urto: Classe III: ≥ 20 Nm Aderenza per trazione diretta: ≥ 1,5 N/mm ² Reazione al fuoco: euroclasse A1 Resistenza allo strisciamento: NPD Profondità di penetrazione: > 10 mm Sostanze pericolose: assenti

I dati tecnici soprariocati sono ottenuti con un dosaggio di 400g/m².
La Declaration of Performance (DOP) è scaricabile dal sito www.ecobeton.it.

<p>Test secondo la normativa ASTM (American Society for Testing and Materials International) Prodotti per l'impermeabilizzazione e la protezione del calcestruzzo</p>	
MTO LS-412	Resistenza alle efflorescenze saline: 0,123 kg/m ² (std < 0,8 kg/m ²)
MTO LS-417 ASTM C1202 ASTM E96 ASTM C1585 ASTM C666-A	Contenuto di cloruri: 0,231% su massa (< 16%*) Penetrazione ioni cloruro: 448 C (< 61%*) Trasmissione di vapore: < 26%* Tasso di assorbimento: < 52%* Resistenza al gelo-disgelo: nessuna perdita in peso Assorbimento soluzione 15% NaCl ¹⁾ : < 59%* Trasmissione di vapore soluzione 15% NaCl: < 26%*

¹⁾ Variazione del peso secco dopo immersione per 1, 3, 7, 14, 21 giorni.
* Rispetto a campione non trattato.

Prestazioni

Proprietà	Risultato	Normativa di riferimento
Carbonatazione	Resistenza totale	UNI 9944
Contatto con acqua potabile	Idoneo	D.M. 21.03.73
Resistenza in spinta negativa	1MPa - ca 10 atm	Sintef - Norvegia
Resistenza al gelo disgelo	300 cicli	UNI 7087/72

Applicazione

Prendere visione della scheda di sicurezza disponibile al sito www.ecobeton.it.

Il prodotto va applicato in almeno due mani, su superfici perfettamente pulite e prive di residui di olio e grasso. Può essere applicato a spruzzo, con pompe a bassa pressione (max 5 bar) normalmente disponibili per il giardinaggio (sia manuali che elettriche).

Su calcestruzzo gettato in casseri, assicurarsi di rimuovere bene eventuali residui di disarmante.

Su calcestruzzo vecchio, bagnare con acqua fino a saturazione il giorno prima dell'applicazione.

Per maggiori approfondimenti visitate il sito:

www.ecobeton.it

o contattate il nostro servizio tecnico via email:

tecnica@ecobeton.it

Evercrete Vetrolfluid® può essere applicato anche in presenza di umidità; in caso di venute d'acqua, è necessario procedere alla loro riparazione prima del trattamento.

Applicare la prima mano a saturazione senza fare colare il prodotto, aspettare che asciughi prima di applicare la seconda. Su superfici verticali applicare dal basso verso l'alto.

La maturazione del prodotto avviene in 36 giorni, tuttavia la superficie è disponibile già dopo poche ore; eventuali rivestimenti che non temono l'umidità (intonaci, getti di calcestruzzo) possono essere applicati dopo qualche ora mentre è opportuno attendere almeno 2-3 settimane per i trattamenti che richiedono un fondo completamente asciutto (vernici, resine, ecc.).

Applicazione su interrati:

Sigillare e stuccare bene i fori dei pannelli e le lame di cassero. Riparare ogni imperfezione del getto (inchi di ghiaia). **Evercrete Vetrolfluid®** è inefficace nelle riprese di getto, che devono essere rese impermeabili con altri materiali (esempio waterstop). È possibile interrare le superfici trattate dopo 12 ore, non sono necessari particolari accorgimenti di protezione.

Riparazioni:

Seguire le indicazioni fornite nella guida apposita disponibile al sito www.ecobeton.it.

Strutture già esistenti:

Per eliminare l'umidità e le infiltrazioni d'acqua su vecchi interrati o strutture già esistenti, è possibile operare anche dall'interno, previa rimozione di tutti gli strati superficiali (tinte, intonaci, ecc.).

1. Inumidire il supporto.
2. Spruzzare **Evercrete Vetrolfluid®** a saturazione.
3. Attendere qualche giorno.
4. Ripetere il trattamento.

Se si osserva la comparsa di efflorescenze nei giorni successivi all'applicazione è necessario rimuoverle meccanicamente evitando l'utilizzo di acqua in pressione. Su superfici particolarmente umide a volte è necessario ripetere la procedura per ottenere il risultato desiderato.

Altre applicazioni:

Il servizio tecnico Ecobeton è a completa disposizione per qualsiasi chiarimento o istruzione (e-mail: tecnica@ecobeton.it).

Avvertenze

Temperatura: **Evercrete Vetrolfluid®** è un prodotto a base d'acqua, teme perciò i climi rigidi. Non applicare sotto i 5° C.

Vetro e alluminio: proteggere vetro e alluminio durante l'applicazione (orologi, occhiali, ecc.). Essi vengono danneggiati dal prodotto.

Resa del prodotto

La resa del prodotto per metro quadro varia in funzione della capacità di assorbimento del supporto trattato. In generale è buona norma trattare il calcestruzzo fino a saturazione. Dalla nostra esperienza il dosaggio tipico varia tra i 250 e i 500 g/m² complessivi nelle due applicazioni previste.

Nota:

Le informazioni contenute in questa scheda sono vere al meglio delle nostre conoscenze attuali. I prodotti sono della più alta qualità e standard nelle tolleranze di produzione. Dal momento che nessun controllo è possibile sulla messa in opera del prodotto, nessuna garanzia, espressa o esplicita è fornita sul risultato finale e nessuna responsabilità è assunta direttamente o indirettamente dall'utilizzo dei prodotti. Gli utenti sono incoraggiati a fare dei test prima dell'applicazione.

Ecobeton Italy s.r.l. unipersonale è azienda certificata ISO 14001 con sistema di gestione ambientale.

ECOBETON

Ecobeton Italy® s.r.l. unipersonale
via G. Galilei, 47
36030 Costabissara (VI) Italy

T (+39) 0444 971893
E info@ecobeton.it
I www.ecobeton.it

Scheda di sicurezza

Evercrete Vetrolfluid

Revisione:

26 marzo 2021

Sostituisce la versione: 5 giugno 2017

SEZIONE 1: identificazione della sostanza/miscela e della società/impresa**1.1 Identificatore del prodotto:**

Evercrete Vetrolfluid

1.2 Usi identificati pertinenti della sostanza o della miscela e usi sconsigliati:

Trattamento impermeabilizzante, antidegrado per calcestruzzo

1.3 Informazioni sul fornitore della scheda di dati di sicurezza:Ecobeton Europe Srl
Via G. Galilei, 47
36030 Costabissara Vicenza
Italy**1.4 Numero telefonico di emergenza:**

Contattare Ecobeton: +39 0444 971893 - Lun - Ven 9:00 - 18:00

SEZIONE 2: identificazione dei pericoli**2.1 Classificazione della sostanza o della miscela:****Criteri regolamento CE 1272/2008 (CLP):**

Non è una sostanza o una miscela pericolosa.

2.2. Elementi dell'etichetta:

Non è richiesta l'etichettatura GHS.

2.3. Altri pericoli:

PVT: nessuno

vPvB: nessuno

Altri pericoli: nessuno

SEZIONE 3: composizione/informazioni sugli ingredienti**Identità chimica:**

Silicato di sodio in soluzione acquosa

3.1 Sostanze:

Non applicabile.

3.2 Miscela:

Questa miscela non è soggetta a classificazione secondo i criteri del Regolamento (CE) N. 1272/2008.

SEZIONE 4: misure di primo soccorso**4.1 Descrizione delle misure di primo soccorso****Consigli generali:** In condizioni ordinarie di lavoro: non sono necessarie misure speciali.**Inalazione:** Spostare la persona all'aria aperta. In caso di sintomi, consultare un medico.**Contatto con la pelle:** Togliere gli indumenti contaminati. Lavare con abbondante acqua o acqua e sapone. Rivolgersi al medico se si verificano sintomi o l'irritazione persiste.**Contatto con gli occhi:** Sciacquare immediatamente con abbondante acqua. Rimuovere le lenti a contatto qualora siano presenti e facili da togliere. Consultare un medico in caso di irritazione prolungata.**Ingestione:** Sciacquare la bocca con acqua. Non indurre vomito. In caso di sintomi, consultare un medico.**4.2 Principali sintomi ed effetti, sia acuti che ritardati:**

Informazioni specifiche sui sintomi e gli effetti causati dal prodotto sono sconosciute.

9 Index of figures

Figure 1. Monomers of the two polymers used respectively PMHS and PDMS-OH (from left to right).	11
Figure 2. Schematic presentation of main reagents and final functionalized compound.	11
Figure 3. Decorative elements visible in facade.	12
Figure 4. The three lithotypes studied in the present work: a) <i>Pietra di Firenzuola</i> , b) <i>Pietra di Muggia</i> , c) Bianco Sardo.	21
Figure 5. Artificial lithotypes (concrete) used in the research: a) Grey Portland concrete, b) Vicat concrete.	21
Figure 6. Application method used to apply the compounds.	29
Figure 7. SEM analysis: a) S1a, b) S1b, c)S1b.	30
Figure 8. Results of the analysis of the sizes of the functionalized particles: a) S1a, b) S1b, c)S1c.	30
Figure 9. SEM-EDS analysis of S1A: a) SEM images of the particles, b) EDS analysis of the composition, c) overlap of previews images.	31
Figure 10. SEM analysis of functionalised particles: a)S1a, b)S1e.	32
Figure 11. Spectra of SNP and of SNP functionalized with $\text{Ca}(\text{NO}_3)_2$: a) SNP; b) S1a; c) S1b; d) S1c.	35
Figure 12. Spectra of SNP functionalized with PMHS (sol phase): a) S2a; b) S2b; c) S2c; d) S2d.	37
Figure 13. Spectra of SNP functionalized with PMHS (gel phase): a) S2a; b) S2b; c) S2c; d) S2d.	39
Figure 14. Spectra of S2b1 (a) and S2e (b) synthesis.	40
Figure 15. Structure of the compounds analyzed (from left to right) S2e and PDMS-OH.	41
Figure 16. NMR spectra of: a) S2e; b) PDMS.OH; c) comparison of the main peaks blue line PDMS-OH, red line S2e.	41
Figure 17. Microscopic images of specimens after the treatment of S2A compound: a) Vicenza, b) Carrara.	45
Figure 18. Microscopic observation of the surface of specimen CSTP4 before (a) and after (b) the degradation process.	55
Figure 19. Microscopic observation of the surface of specimen CSTV4 before (a) and after (b) the degradation process.	55
Figure 20. Change of the aspect of sample CSTV5 induced by salt crystallisation degradation.	57
Figure 21. Microscopic observation of the surface of specimen CSTP5 before (a) and after (b) salt crystallization.	57
Figure 22. Microscopic observation of the surface of specimen CSTV6 before (a) and after (b) salt crystallization.	57
Figure 23. Change of the aspect of sample CSTP8 induced by frost and thaw degradation.	59
Figure 24. Change of the aspect of sample CSTV8 induced by frost and thaw degradation.	59
Figure 25. Microscopic observation of the surface of specimen CSTP8 before (a) and after (b) the degradation process.	59
Figure 26. Microscopic observation of the surface of specimen CSTV7 before (a) and after (b) the degradation process (enlargement 2x).	60
Figure 27. Change of the aspect of sample CSTP10 induced by water lagoon degradation.	61

Figure 28. Microscopic observation of the surface of specimen CSTP9 before (a) and after (b) the degradation process.	61
Figure 29. Microscopic observation of the surface of specimen CSTV9 before (a) and after (b) the degradation process.	62
Figure 30. Graphs of changes of values of anisotropy (a) and velocities for samples treated with SNP100.	65
Figure 31. Graph of the evaluations of changes of water absorption for samples treated with SNP100.	66
Figure 32. Production of SNP-PDMS: a) after the functionalization, b) after the dilution.	66
Figure 33. Microscopic investigation of the specimen PF12 before (a) and after (b) the treatment (enlargement 2x).	67
Figure 34. Graphs of changes of values of anisotropy (a) and velocities (b) for <i>Pietra di Firenzuola</i> samples treated with SNP-PDMS.	68
Figure 35. Graph of the evaluations of changes of water absorption for <i>Pietra di Firenzuola</i> samples treated with SNP-PDMS.	69
Figure 36. Microscopic investigation of the specimen PM12 before (a) and after (b) the treatment (enlargement 2x).	70
Figure 37. Graphs of changes of values of anisotropy (a) and velocities (b) for <i>Pietra di Muggia</i> samples treated with SNP-PDMS.	70
Figure 38. Graph of the evaluations of changes of water absorption for <i>Pietra di Muggia</i> samples treated with SNP-PDMS.	71
Figure 39. Microscopic investigation of the specimen BS12 before (a) and after (b) the treatment.	71
Figure 40. Graphs of changes of values of anisotropy (a) and velocities (b) for <i>Bianco Sardo</i> samples treated with SNP-PDMS.	72
Figure 41. Graph of the evaluations of changes of water absorption for <i>Bianco Sardo</i> samples treated with SNP-PDMS.	73
Figure 42. Microscopic investigation of the specimen CSTP8 before (a) and after (b) the treatment.	74
Figure 43. Graphs of changes of values of anisotropy (a) and velocities (b) for Portland Concrete samples treated with SNP-PDMS.	75
Figure 44. Graph of the evaluations of changes of water absorption for Portland Concrete samples treated with SNP-PDMS.	75
Figure 45. Microscopic investigation of specimen CSTV4 before (a) and after (b) the treatment (enlargement 2x), (c) detail of the crack (enlargment 4x).	76
Figure 46. Microscopic investigation of specimen CSTV8 before (a) and after (b) the treatment.	76
Figure 47. Microscopic investigation of specimen CSTV10 before (a) and after (b) the treatment.	77
Figure 48. Graphs of changes of values of anisotropy (a) and velocities (b) for Vicat Concrete samples treated with SNP-PDMS.	77
Figure 49. Graph of the evaluations of changes of water absorption for Vicat Concrete samples treated with SNP-PDMS.	78
Figure 50. Microscopic investigation of specimen PF16 before (a) and after (b) the treatment.	79
Figure 51. Graphs of changes of values of anisotropy (a) and velocities (b) for <i>Pietra di Firenzuola</i> samples treated with Evercrete Vetrofluid.	80

Figure 52. Graph of the evaluations of changes of water absorptions for <i>Pietra di Firenzuola</i> samples treated with Evercrete Vetrofluid.	80
Figure 53. Microscopic investigation of specimen PM7 before (a) and after (b) the treatment.	81
Figure 54. Graphs of changes of values of anisotropy (a) and velocities (b) for <i>Pietra di Muggia</i> samples treated with Evercrete Vetrofluid.	82
Figure 55. Graph of the evaluations of changes of water absorptions for <i>Pietra di Muggia</i> samples treated with Evercrete Vetrofluid.	82
Figure 56. Microscopic investigation of specimen BS7 before (a) and after (b) the treatment.	83
Figure 57. Microscopic investigation of specimen BS16 before (a) and after (b) the treatment.	83
Figure 58. Graphs of changes of values of anisotropy (a) and velocities (b) for <i>Bianco Sardo</i> samples treated with Evercrete Vetrofluid.	84
Figure 59. Graph of the evaluations of changes of water absorptions for <i>Bianco Sardo</i> samples treated with Evercrete Vetrofluid.	84
Figure 60. Microscopic investigation of specimen CSTP3 before (a) and after (b) the treatment.	85
Figure 61. Microscopic investigation of specimen CSTP5 before (a) and after (b) the treatment.	85
Figure 62. Microscopic investigation of specimen CSTP9 before (a) and after (b) the treatment.	85
Figure 63. Graphs of changes of values of anisotropy (a) and velocities (b) for Portland Concrete samples treated with Evercrete Vetrofluid.	86
Figure 64. Graph of the evaluations of changes of water absorptions for Portland Concrete samples treated with Evercrete Vetrofluid.	87
Figure 65. Microscopic investigation of specimen CSTV7 before (a) and after (b) the treatment.	87
Figure 66. Microscopic investigation of specimen CSTV9 before (a) and after (b) the treatment.	88
Figure 67. Graphs of changes of values of anisotropy (a) and velocities (b) for Vicat Concrete samples treated with Evercrete Vetrofluid.	88
Figure 68. Graph of the evaluations of changes of water absorptions for Vicat Concrete samples treated with Evercrete Vetrofluid.	89
Figure 69. Graphs of changes of values of anisotropy (a) and velocities (b) for Vicat and Portland Concrete specimens treated with Evercrete Vetrofluid.	91
Figure 70. Graph of the evaluations of changes of water absorptions for Vicat Concrete samples treated with Evercrete Vetrofluid.	92

10 Acknowledgments

Ho pensato spesso al momento in cui mi sarei adoperata a scrivere i ringraziamenti per questa tesi e ogni volta mi rendevo conto di quanto numerose fossero le persone a cui dovevo dire il mio grazie.

La prima persona a cui devo rivolgere la mia gratitudine è il Professor Alvisè Benedetti, non dimenticherò mai la fiducia che ha riposto in me, dandomi l'opportunità di continuare la ricerca che avevo iniziato sotto la sua guida tre anni fa. Questa fiducia, con il tempo, mi ha permesso di poter fare ricerca indirizzando le scelte sulla base del mio interesse. Il mio augurio, oggi, è che possa dire che la sua fiducia è stata ben riposta.

In seconda battuta ringrazio la Dott.ssa Elena Tesser, dal nostro primo incontro di ormai tre anni fa sono cresciuta e posso dire che buona parte della mia crescita professionale è merito suo. A lei la mia gratitudine per avermi insegnato un modo di lavorare, per avermi fatto questo preziosissimo dono che porterò sempre con me.

La realizzazione del progetto è stata possibile per la collaborazione di molti enti e professionisti altamente qualificati che hanno coordinato, fornito informazioni e materiali. Ringrazio il Prof. Paolo Faccio dell'Università IUAV di Venezia; Stefano Buratti consulente tecnico sui materiali e servizi per il restauro. Ringrazio le ditte Sgubbi Italiana srl e Vicat Group per la fornitura dei provini a base di cemento. Alberto Carollo di Ecobeton Italy srl per la fornitura del prodotto Evercrete Vetrofluid. Con grande riconoscenza la ditta Lythos srl per la fornitura di tutti i campioni di pietra e di granito. Infine, Greta Bruschi per l'assistenza e le informazioni fornite.

Ringrazio il Direttore Antonelli del laboratorio LAMA per avermi aperto le porte del laboratorio e tutti i collaboratori in particolare Alberto Conventi e Floriana Majerle per avermi aiutata nell'esecuzione di analisi risultate fondamentali ai fini della ricerca. Rivolgo un affettuoso ringraziamento alla Dott.ssa Rebecca Piovesan e alla Dott.ssa Francesca Visone, vicine di scrivania sempre pronte ad intervenire per risolvere ogni problema.

Al Dott. Vincenzo Lombardi e al Dott. Lorenzo Branzi dottorandi dell'Università Ca' Foscari devo il mio grazie per avermi aiutata nell'esecuzione di analisi SEM e NMR, per essersi calati nei panni di tutor a cui rivolgersi quando necessitavo di risposte. Nelle ricercatrici e nei ricercatori, dottorande e dottorandi, tesiste e tesisti incontrati in Università, nei quali ho sempre trovato disponibilità, aiuto e soprattutto comprensione. Grazie a loro ho imparato l'importanza del confronto, strumento imprescindibile nella ricerca.

Più che a qualsiasi altra persona devo il mio ringraziamento a mio papà Enrico, a lui che mi ha insegnato il significato del duro lavoro, che con il tempo viene ripagato. È solo grazie alla possibilità che mi hai dato se oggi mi trovo qui. Tu che ogni giorno non mi fai mai dubitare del fatto di avere qualcuno che crede in me. Ti sono infinitamente grata.

Un grazie leggero come il vento, che lo spingerà fin lassù, alla mia mamma il cui sguardo protettivo sento poggiato sulle mie spalle.

Grazie a Daniele, Elia e Letizia fratelli e sorella maggiori, è una fortuna immensa avervi come esempio costante a cui guardare, siete il metro con cui misuro le mie scelte. Grazie a Francesca dolcissima cognata, sempre disponibile a darmi consigli su come indirizzare la mia carriera. Grazie alla mia nipotina perché, dall'annuncio del tuo arrivo, tu sei diventata il pensiero felice che alleggerisce ogni preoccupazione.

A mia zia Betty, guida costante, che mi ha condotta lungo la strada aiutandomi sempre a guardare al passo successivo da compiere, è grazie a te se ho trovato il ritmo per stare al tempo di ogni passaggio.

Alle mie nonne e ai miei nonni, grazie per il vostro infinto e incondizionato amore, perché le vostre case sono il luogo in cui tornare per fare il pieno di affetto e di dolcezza.

Grazie a Laura, migliore amica, presenza certa, sempre pazientemente in attesa del mio ritorno, pronta a riaccogliermi e a supportarmi a distanza.

Grazie a Margherita, perché sei la luce accesa in casa che mi ricorda che anche qui ho qualcuno di famiglia da cui tornare.

Grazie alle amiche e agli amici che, sebbene i miei ritorni siano pochi, mi aspettano sempre in patria bergamasca. Siete la certezza che i rapporti non si misurano nella quantità del tempo trascorso insieme, ma piuttosto nella sua qualità.

Grazie a tutte le amiche e gli amici con cui ho condiviso l'Università e Venezia, è grazie ai momenti trascorsi con voi se ho trovato ristoro dalle difficoltà degli esami e dalla pesantezza dello studio.

Infine, grazie a Venezia, questa città che mi ha accolto e che *“ogni giorno, con i suoi canali, mi abbraccia”*.